THE PHYSICAL AND MECHANICAL PROPERTIES OF OXIDE FILMS.

A Thesis Presented

for the Degree of Ph. D.

in the

University of London

by

Douglas Hardie Bradhurst

1963

ABSTRACT

The physical and mechanical properties of the thin oxide films, which form on many metals, determine the rate at which metallic oxidation and corrosion may proceed. A survey of the literature showed that very few measurements, particularly of the mechanical properties of films, had previously been made. In this work, measurements were made of the deformability of oxide films, their electrical conductivity, and the stresses due to growth, as these should enable a clearer understanding to be obtained of the mechanism of oxidation and corrosion processes.

The measurements of stresses showed that both tensile and compressive stresses could occur, and in the case of oxide films on aluminium, the origin of the two types is discussed in terms of the growth rates, and the influence of ionic diffusion.

Measurements of the mechanical properties showed that the elastic deformation which may be tolerated by the thin oxide films on aluminium and several other metals and alloys, was considerably greater than that observed for the corresponding bulk oxides. In the absence of an ionic diffusion flux, the Young's Modulus of separated aluminium oxide films was found to be an order of mag-

nitude less than that for bulk alumina. In addition, some evidence was obtained that at room temperature, oxide films on aluminium could deform plastically if the ionic diffusion flux was sufficient.

Studies of the electrical properties showed that hydrogen could increase the electrical conductivity of thin oxide films, and a similar effect was observed in single crystals of rutile. Possible relations between the electrical and mechanical properties of oxide films are discussed.

CONTENTS

Contents Continued: Page

Contents Continued: Page

SECTION I

INTRODUCTION

INTRODUCTION

Almost all metals with the exception of gold, will react with oxygen in a gaseous or aqueous environment. In many cases, the reaction product takes the form of a thin film of oxide on the metal surface, which controls the rate of the subsequent oxidation reaction, by isolating the reactants. The usefulness of metals such as iron, titanium, and many others depends upon the existence of this type of oxide film, without which rapid oxidation could proceed. The investigation of those factors which can affect the protective nature of oxide films has therefore been an important aspect of research into corrosion and oxidation, with the two fold aim of obtaining further understanding of the detailed reaction mechanisms involved and from the more practical point of view of minimising damage to metallic materials in everyday use.

The effectiveness of an oxide film in minimising corrosion depends upon the extent to which it prevents access of the corrosion medium to the metal surface. If the film is impervious to the liquid, and is unbroken, the corrosion rate will depend upon the ease with which metal or oxygen can pass through it, and the rate

will decrease as the film thickens. Improved resistance to corrosion will result if either the diffusion constants of the film can be reduced, or if the total protective thickness of the film can be increased.

The application of the Wagner - Hauffe theory[1] of oxidation has led to the development of alloys which have improved corrosion resistance, by virtue of a reduction in the diffusion constants of the oxide film. However, attempts to alter the natural protective thickness of oxide have been limited by a lack of knowledge of the factors involved.

The ultimate thickness to which an oxide film may grow depends upon its ability to withstand the stresses which may arise during growth, from a variety of causes. In many cases, a point is reached when the accumulated stress exceeds the strength of the film, resulting in cracking or detachment, and a consequent increase in corrosion rate. In order to improve corrosion resistance by increasing the protective thickness of the oxide film, data are required both on the stresses which are produced during film growth, and the mechanical properties of oxide films.

Some recent corrosion studies[2] suggested that alloying

could increase the protective oxide thickness, and a tentative explanation was put forward in terms of a change in the mechanical and electrical properties of the film. An attempt to justify this approach showed that no data was available in the literature concerning the mechanical properties of the films in this case. Moreover it emerged that previous references to the influence of mechanical properties of films upon corrosion had seldom been based on measurements either of the stresses existing in the oxide films, or the strain which they will tolerate before mechanical breakdown occurs.

It was therefore decided that an attempt to measure properties such as the elasticity, and plasticity of oxide films, and the stresses in growing films would be rewarding from at least two points of view. Firstly, new data would be obtained, and secondly, by correlating the results with observed corrosion behaviour a better understanding might be gained of the role of the mechanical properties of oxide films in oxidation.

In addition to these measurements, a simultaneous study was made of the electrical conductivity of oxide films, and the effect of hydrogen, which is a reaction product in aqueous

corrosion, upon this. This aspect of the work arose from the suggestion [2] that the ability of oxide films to deform plastically might be connected with their electronic conductivity.

The results of this work are most conveniently presented under three headings, describing

(a) the measurements of stress in growing films,

(b) measurement of the mechanical properties, and

(c) the electrical conductivity of oxide films, and the

following sections are subdivided accordingly.

SECTION II

PREVIOUS WORK

PREVIOUS WORK

(a) Stresses in Oxide Films.

The importance of stresses in the oxidation process was first mentioned by Pilling and Bedworth in their classical paper [3] of 1923. They found that many metals oxidised according to the so-called parabolic law, in which oxide thickness increases as the square root of time. Pilling and Bedworth's paper also contained evidence to show that the tendency of the oxide film to reduce the oxidation rate depended upon a certain relation between the densities of the metal and the oxide, provided that the film was produced by the inward diffusion of oxygen. This relation, known as the volume ratio, may be conveniently expressed in the form:-

$$R_V = \frac{\text{molecular volume of metal oxide } MeX_x}{\text{atomic volume of metal}}$$

If this value is unity there should be no tendency for the oxide to form under stress. However, this is rarely true in practice. The light metals such as potassium, sodium, calcium, and magnesium all have volume ratios of less than unity, and

are usually found to oxidise according to a linear, or non-protective growth law [4], as would be expected if the film provided inadequate coverage of the metal surface, or formed pores, through which the oxidising medium could penetrate. Most other metals have volume ratios greater than unity, and should according to this principle, form in a state of compressive stress, thereby tending to retain the protective oxide film as a barrier to diffusion, and further oxidation.

The existence of stresses in oxide films was demonstrated by Evans [5] in experiments in which he observed that wrinkling and curling of nickel oxide films occurred when they were chemically separated from the metal substrate. These experiments also showed that any stresses existing in the metal were transferred to the film during growth, resulting in a different stress distribution from that expected from simple volume ratio considerations. The films grown on annealed metal specimens were observed to curl away from the metal surface confirming that the stress was compressive, and further that a stress gradient existed with the stress decreasing with thickness.

Further confirmation of the volume-ratio principle was provided by Dankov and Churaev's experiments [6] on nickel, iron, and magnesium, in which a thin mica strip coated on one side with metal was observed to bend when the metal was oxidised. For iron, and nickel the curvature indicated a compressive stress in the oxide, while for magnesium, which has a volume ratio of 0.82, tensile stress was found. This experiment is one of the very few attempts which have been made to study the stresses in oxide films on a quantitative rather than qualitative basis. Frequent reference has been made in the literature to the role of stresses in oxidation, and there seems little doubt that the build-up of stress, during growth, followed by stress relief by cracking of the film, is responsible for the sudden change in oxidation kinetics from protective to non-protective which occurs for many metals. For example in the high temperature oxidation of titanium [7] the dense grey protective film initially formed is replaced at the transition point by layers of oxide which are non-adherent and cracked when seen under the microscope. Moreover, x-ray examination shows that oxygen in solution in the metal expands the hexagonal titanium lattice

during the initial stages of oxidation.

Stresses can also arise in a growing oxide film as a result of the epitaxial relationship between the crystal structure of the metal substrate and the oxide forming on its surface. It was shown by Gwathmey and Lawless [8] that the oxidation of a copper single crystal resulted in the formation of different thicknesses of oxide on the different crystal faces. The fastest rate was on the crystal face which had the smallest degree of misfit between the metal and oxide lattices. This was explained in terms of the inhibiting effect of stresses upon the rate of oxidation, which has been theoretically justified by Dankov [9]. Lisgarten [10] found that thin films of silver iodide produced on the surface of single crystals of silver by exposing the metal surface to iodine vapour, usually crystallised with the 111 planes of the iodide parallel to the metal 111 planes. From the orientation of the iodide layer it seemed that epitaxial growth most readily occurred where the least lattice misfit, and therefore the least stress existed.

The theoretical work of Frank and van der Merwe [11] attempted to calculate the maximum amount of lattice mismatch

which could be tolerated between a monolayer of a superimposed crystalline material, and a crystalline substrate before the formation of a dislocation became energetically favourable. A value of between 9 and 14% was calculated as a critical misfit between the lattice parameter of the substrate and superimposed lattices, below which presumably the oxide would assume the parameter of the substrate. However, the application of this work is limited to extremely thin films, because mathematical difficulties prevented their simple model being used for films of thickness greater than a few atom layers.

For polycrystalline metals, any differential effect due to epitaxial growth is evened out by the random occurrence of grains of different orientation at the metal surface, but it has been observed on specimens of large grain size, by several workers. Misch [12] demonstrated that oxide films on polycrystalline zirconium grow to different thicknesses on the different grains, and more recently Wilkins [13] showed that anodically formed films also showed this behaviour, but that the differential effect due to grain orientation disappeared as the rate of film formation was increased.

Another important factor which determines the stress existing in an oxide film is the nature of the diffusing species.

Pilling and Bedworth specified that the volume ratio was only observed to be important in determining stress in those cases where growth proceeded by the inward diffusion of oxygen. If the metal ions also move there is no longer any reason to suppose that stress will arise, since, as growth proceeds, the migrating cations are free to move to the positions of lowest free energy, which will be those at which the least stress exists. This argument should also apply to the case where the metal ions are the only diffusion species, as is thought to be the case in the anodic oxidation of Tantalum.[14] The nature of the diffusing species in growing oxide films has been determined in a number of instances by radiotracer methods[15, 16, 17,] and marker experiments[18], and also by conductivity measurements on oxides in bulk. Nevertheless in many cases it is still not clear whether one, or both ions move, or whether, as is the case for the anodic oxidation of aluminium and zirconium, different rates of growth affect the balance of anionic and cationic currents passing through the oxide films.[13, 19.]

These considerations led to the conclusion that the measurement of stresses in growing oxide films should ideally

be confined to systems for which information concerning the nature of the diffusing species was known. Such a study would then not only produce new data, but might enable a clearer interpretation to be obtained of the role of stresses in oxidation. In this connection, the various methods of measuring stresses in thin films were investigated, and it was found that the variety of techniques which were applied in the past to electrodeposited metal films could be successfully adapted to measure stresses in oxide films. A review of these techniques has been published by Hammond [20]. The simplest method which involves the measurement of the bending of a metal strip oxidised on one side only, has been previously used by Reather [21], and Bradshaw and Clarke [22], and is superior to Dankov and Churaev's method in that continuous measurements of stress may be made as the oxide film thickens. The method in a refined form is capable of great sensitivity as has been recently shown by Campbell [23] in a study of the stresses developed in metal films. Stresses of 0.1 Kg/cm^2 were detected in films as thin as 100Å.

It was therefore decided to adopt this technique for the measurement of stresses developed during the formation of oxide films on metals in aqueous environment.

(b) Mechanical Properties of Oxides and Oxide Films.

If it is true, as has been discussed in the preceding section, that the sudden change in oxidation behaviour from protective to non-protective is due to mechanical breakdown of the oxide film, it should be possible to predict when this change will occur from a knowledge of the stresses existing in the film at a given time, and the tensile, or compressive strength of the film. Although a great deal of work has been done on the mechanical properties of single crystals of oxides [24, 25] and sintered compacts [26], no measurements have previously been made to the author's knowledge, directly on oxide films, even though techniques for their separation and observation have been in existence for many years [27].

It might be argued that the properties of oxide films could be determined from the properties of the bulk material with due regard to the effect of size on the mechanical properties. For example, the strength of crystalline alumina was studied by Ryshkewitch [24], and Schusterius [28], and it was shown that at ordinary temperatures a marked increase occurred in tensile strength as the diameter of the test specimen decreased.

Similar effects have been observed for thin metal films by Beames [29], and co-workers. This behaviour can be satisfactorily explained for brittle materials in terms of a reduction in the size of Griffiths cracks [30], and stress raisers which can exist in small specimens. The stress-raising ability of such defects is proportional to the square root of their length, so that below a certain thickness a significant gain in strength is achieved. A tensile test under these conditions will tend to measure more nearly the interatomic forces existing in the material, rather than the weakening effect due to imperfections in a particular test specimen. The size and number of grain boundaries in polycrystalline oxides also has an effect on the mechanical properties measured. Kingery [31] describes this effect as causing an apparent increase in modulus of rupture of the material, the smaller the grain size, again due to the restriction of the possible size of imperfections which can exist within a single grain.

Determination of the properties of oxide films by extrapolation of data on bulk materials, might be practicable if it were not for further uncertainties regarding the structure of

many of the films formed by oxidation. Using aluminium oxide films as an example it is found that the existing methods of structural analysis are insufficiently sensitive to enable a clear identification of crystal structure to be made. Recent work by Hart [32] on the morphology of oxide films formed on aluminium is an example of this. Many of the oxides formed under different conditions, gave no electron diffraction pattern at all, and it is usually assumed in such cases that the oxide is "amorphous". Even in those cases where diffraction patterns were identified as "gamma-alumina", the distinction between lattice dimensions does not allow a clear separation to be made between the five crystalline forms known by this name. It should be added that the study of mechanical properties previously mentioned has been confined almost exclusively to the hexagonal alpha - form, commonly known as corundum.

It seemed reasonable that although the data obtained for bulk oxides could be of some use in determining the type of mechanical properties expected of oxide films, such as high strength, high elasticity modulus, and low ductility, the uncertainty regarding structure particularly in the so-called

amorphous case, required that measurements should be made directly on oxide films before any attempt could be made to correlate the mechanical properties of oxide films with observed corrosion behaviour. Previous work at Imperial College by Leach and Nehru [2, 33], on the aqueous corrosion of uranium and uranium-zirconium alloys, had shown that the thickness of protective oxide which could be formed on the 5 and 10 wt. per cent zirconium alloys was greater than that formed on pure uranium, and it seemed possible that the addition of zirconium brought about a change in the mechanical properties of the oxide, or in the manner in which growth stresses were relieved.

An obvious extension of this work was the measurement of the mechanical properties of oxide films formed on uranium and uranium-zirconium alloys, in order to determine whether alloying affected the deformability of the oxide in the crystallographic sense, or by means of a capacity to deform by diffusion during growth. Consideration was therefore given to methods of determining these properties.

The experimental difficulties of measuring the mechanical properties of oxide films are formidable, due to the fragile nature

of films once separated from the basis metal, and this is undoubtedly the main reason for the scarcity of data in the literature. It seemed a reasonable approach to make initial measurements on anodically produced oxide films on aluminium. By anodising in inert electrolytes, compact "barrier type" films of known thickness may be readily produced, and chemically separated by methods which result in negligible chemical attack of the oxide [34]. In addition to measurements on the separated oxide films, it was decided to attempt to measure film properties by the deformation of oxide covered metal specimens, using electrical and other methods to detect failure of the oxide film. This second method of approach was clearly of wider application than the first, the object being to establish its validity in the case of aluminium, where confirmatory tests could be made on films separated from the metal, before applying it to a study of other metals.

(c) Electrical Properties of Oxide Films.

Previous corrosion rate studies, and conductivity measurements made on uranium and other metals showed that a simple relation existed [33] between the parabolic corrosion rate constant for uranium and the hydrogen activity at the metal surface, the rate increasing as a function of the applied cathodic potential. Conductivity measurements by Leach, and Isaacs [47] showed that hydrogen electrolytically evolved at the surface of the oxide films on uranium and titanium resulted in an apparent increase in oxide conductivity. It was suggested in this work that the increased corrosion rates observed at negative potentials might be due to hydrogen entering the oxide film and increasing its electrical conductivity. The increased conductivity might explain the increased corrosion rate by analogy with Wagner's observations [36] on the diffusion of silver in non-stoichiometric silver sulphide.

However, some doubt existed regarding this interpretation since it was possible that the apparent conductivity change measured for thin films was due to their mechanical breakdown following hydrogen evolution, or that the increase in conductivity resulted from changes in the behaviour of the metal-oxide, or oxide-liquid

interfaces rather than in the bulk of the film. It was felt that an experiment in which the conductivity was measured by a four-terminal method would resolve the problem.

It is well known that the electrical conductivity of oxides may be changed by the addition of ions of different valence. In the corrosion studies on uranium, and uranium-zirconium alloys already described in the preceding section, it was found that the ionic and electronic conductivity of the oxide films formed on the alloys were higher than for the oxide film on pure uranium. Furthermore, the protective thickness of the oxide film on the alloys was also greater than that of the film on uranium. One interpretation [2] of this behaviour was that the plasticity of the oxide film was increased by the alloying addition, possibly in a similar manner to that observed for ionic solids by Eshelby, Pratt, Newey, and Lidiard [37]. They showed that the addition of alter-valent ions to sodium chloride which increased its electronic conductivity also reduced the charge associated with dislocations within a critical temperature range and lowered the yield point of the material.

Further evidence of a possible connection between electronic

conductivity and deformability was obtained by Westbrook and Gilman [38], who performed hardness tests on a range of semiconductors. They found an "electromechanical" effect in which it was shown that the depth of penetration of the indentor used in the hardness tests could be considerably increased by the passage of an electronic current through the test specimen.

It was not known whether either of these effects could explain the apparent change in the mechanical properties of uranium oxide films, but in view of these possible connections between the electrical and mechanical properties of ionic crystals and semiconductors, it was felt that an investigation of the deformation of oxide films and the stresses developed in them due to growth, should also include a study of their electrical conductivity.

(d) Conclusions:

As a result of this study of previous work it was decided that the experimental program should include measurements of the stresses in growing oxide films, their deformability, and electrical conductivity.

It was considered that measurements of stress in oxide films, should ideally be confined to systems where some of the many important variables which can affect the stress were either known, or controlled. For example, stresses in the film arising from residual stresses in the metal, and epitaxy, are minimised by using annealed, polycrystalline metal specimens, and producing relatively fine-grained oxide films on the surface by anodising. The results might then be interpreted in terms of the nature of the diffusing species, and volume ratio considerations. Stress measurements could conveniently be made by observing the deflection of a metal strip anodised on one side only.

Anodic films were also especially suited to a study of the mechanical properties of oxide films, due to the ease with which well-characterised films may be formed, and separated

from the metal. It was considered essential to make measurements directly on oxide films in view of the lack of previous data, and the difficulties involved in determining the mechanical properties of films by extrapolation of the mechanical properties of oxides in bulk. Such measurements could be made on films separated from the metal, or by deformation of oxide covered metal specimens, detecting failure of the film by electrical and other means.

In order to obtain evidence of a possible correlation between the electrical and mechanical properties of oxide films, conductivity measurements made on the anodic films by conventional a.c. bridge techniques were also necessary. However, some ambiguity arises in the interpretation of conductivity measurements made by this method as, for example in the previous study [35] of the effect of hydrogen upon conductivity. It was considered that experiments in which conductivity measurements were made on a single crystal of oxide following evolution of hydrogen from the surface would have a relatively clear interpretation, and would add to the understanding of the effect of hydrogen on oxide films formed during corrosion.

The scope of the investigation was further influenced by

the need to choose metal-oxide systems upon which experimental work was possible, and for which previous corrosion data were available. The metals chosen on this basis were aluminium, zirconium, titanium, and alloys of the uranium-zirconium, and aluminium-magnesium systems.

SECTION III

EXPERIMENTAL METHODS

EXPERIMENTAL METHODS

(1) PREPARATION OF OXIDE FILMS.

(a) Preparation of Metal Surfaces.

Test specimens were prepared from metal sheet or foil to form strips, or in the case of tensile tests, shaped pieces of known gauge length. The metals used had the following composition in wt. % :

Aluminium (super pure) 99.99.

" 2S 0.1 Cu : 0.5 Fe : 0.2 Si : 0.1 Mn : 0.1 Zn

" M57S 2.0 Mg " " " " "

" B54S 4.5 Mg " " " " "

Zirconium 0.12 Fe : 2.0 Hf : 0.1 C : 0.05 N

Titanium 0.1 Na : 0.15 Cl : Others < 0.1

Uranium (99.95)

Surface treatment was confined to chemical deoxidation or etching, using chromium trioxide - phosphoric acid and sodium hydroxide for aluminium, hydrofluoric acid - nitric acid - water mixture (1 : 2 : 4 by volume) for zirconium, and hydrofluoric acid - hydrogen peroxide (1 : 1) for titanium. Chemical

polishing was more difficult for uranium and its alloys, and mechanical wet polishing to 600 grade on silicon carbide paper was used.

(b) Anodic Oxidation:-

Oxide films were formed on one or both sides of the specimens by anodising in one of several different electrolytes. Porous films on aluminium were grown in 20 per cent sulphuric acid solution, while films of the non-porous "barrier" type were produced in 3 per cent solutions of ammonium borate, and ammonium citrate. Ammonium borate solution was also used for the growth of barrier films on zirconium and titanium. Concentrated ammonia solution was found to be suitable for the production of barrier films on uranium and its alloys.

A circuit diagram of the anodising apparatus is shown in Figure 1. A variable D.C. power supply capable of a steady current of 40 mA, and voltages up to 600 V, was used in conjunction with a series resistance to supply a constant current to the cell. Current and voltage were measured continuously during anodising using precision resistors and a potentiometric recorder. For the growth of barrier type films, the current

during anodising was held constant until the applied voltage required for a film of given thickness was reached. This voltage was then held constant until the current had fallen to a steady "leakage" value (approximately five minutes) after which it was assumed that the film had reached a characteristic thickness. The porous films on aluminium were formed at constant applied voltage, as the oxide thickness increases as a function of time in this case [39].

(c) Determination of Film Thickness.

The thickness of oxide films on metals may be measured by a number of methods, such as weight gain, coulometry, optical absorption or interference, capacitance, and dielectric loss measurement. After consideration of the methods available, measurements of capacitance, and optical interference seemed best suited to the determination of the thickness of oxide films formed in aqueous media, particularly in the case where a series of measurements was required without disturbing the growth mechanism.

(i) Capacitance Technique.

The capacitance of an oxide film which behaves as a

dielectric, is given by the expression:

$$C = \frac{kA}{4\pi d}, \qquad \text{(i)}$$

where k = dielectric constant of the oxide

d = oxide thickness

and A = area measured.

This method was used for all the metals studied, but was found to give best results for films on aluminium and zirconium. Good correlation was obtained between measured capacitance, and the anodic formation voltage which was also used as a measure of oxide thickness when the anodising conditions were standardised. The apparatus used for the capacitance measurement is described in more detail in the following section.

(ii) Optical Technique.

The optical properties of the anodised films on uranium-zirconium alloys, were studied using an apparatus which compared the intensity of light reflected from a polished metal surface with that obtained during the formation of the oxide film. A diagram of this apparatus is shown in Figure 2. A mercury-arc light source S. was used in conjunction with a condenser lens, L_1

and Kodak "808" yellow filter, F to provide a converging monochromatic beam of wave length 5780 Å. This beam was reflected by a small mirror at M as a divergent beam, which after passing through lens L_2 and being reflected by the specimen at X, emerged as a parallel beam to fall on the photoelectric cell P_2. In practice alignment of the specimen was achieved by rotating it in the horizontal plane until P_2 gave a maximum voltage output. A second tube contained a filter, iris diaphragm, D and photocell, P_1 which was used in opposition to P_2. The diaphragm was adjusted to back off any photocurrent caused by extraneous light entering the main tube.

The output of P_2 was then coupled to a recorder enabling a continuous record of relative intensity to be obtained as a function of time. Using values for refractive index previously determined [40] oxide thicknesses at interference maxima and minima were calculated from the relations:-

$$2nd + \phi = p\lambda \qquad \text{(maximum)} \qquad (2)$$

and

$$2nd + \phi = (P + \tfrac{1}{2})\lambda \qquad \text{(minimum)} \qquad (3)$$

where d = film thickness

λ = wave length

ϕ = phase angle change at the metal-oxide interface.

n = refractive index.

p = an integer, the order of the interference.

A rough estimate of the relative absorption coefficients of the oxide films formed on a metal and its alloys, could also be made by comparing the number of interference cycles which occurred before the amplitude of the interference maxima and minima decreased to zero.

Thickness measurements made in this way were used as a calibration for the subsequent growth of films in which the anodising voltage alone was used as the criterion of thickness.

(2) MEASUREMENT OF GROWTH STRESSES IN ANODISED FILMS.

Stresses present in anodised films due to the growth process were measured by the following technique. Thin metal foil was anodised on one side, and the resultant bending was measured by a travelling microscope focussed on the tip of the foil.

Specimens were cut to form parallel sided strips, which were cold-rolled using light pressure to remove the burred edge, annealed, and then etched or chemically polished. An electrical contact was made to one end of the strip which was then mounted in a glass tube using N.H.P. quick setting resin. Finally one side of the specimen was coated with Lacomit, or Ebonide, and allowed to dry. The strip was then calibrated for deflection in milligrams per centimetre by means of the torsion balance, before commencing the anodic oxidation. High sensitivity was obtained by using very thin metal foils, which are generally not adaptable to some of the more elaborate techniques which have been developed [20] for measuring stresses in electrodeposits.

The stress within the oxide film can be calculated from the expression [41]:

$$S = \frac{E_b t^2 x}{3 l^2 d} \qquad (4)$$

where x = deflection of the tip of a metal strip of length l

E_b = Young's modulus of basis metal.

t = thickness of basis metal.

d = thickness of oxide film.

or alternatively, each strip could be calibrated in terms of force per unit deflection by means of a sensitive torsion balance, and the stress calculated from the relation:

$$S = \frac{2 F.l}{A(t-d)} \qquad (5)$$

where F = Force required to bend the strip a given distance (obtained from calibration curve),

and A = cross sectional area of film.

This second method had the advantage that small irregularities in an individual specimen which might affect its elastic modulus were taken into account in the calibration. The first method assumes that the specimen is uniformly flat and has an

elastic modulus equal to that of a pure single crystal.

Stresses were measured in porous films on aluminium, and in barrier type films on aluminium, zirconium, and titanium. A study was made of the effect of different conditions of pH, and current density upon the stress in the barrier films.

In many cases the impedance of the film was recorded automatically during the course of an experiment, by means of the auxiliary measuring circuit shown as a part of the anodising circuit in figure 1. Sine waves of frequencies 1K c/s, and 14 Kc/s were alternately applied to the cell, and the voltage developed between the specimen and a potential probe P, adjacent to the oxide surface, was amplified, rectified and fed to a recorder. The oxide film may be represented by an analogue circuit consisting of a capacitance, C_f and resistance R_f in parallel (see figure 3B) having an impedance Z which may be expressed in the form:

$$Z = \sqrt{\frac{R_f^2}{1 + w^2 C_f^2 R_f^2}} \qquad (6)$$

where w = frequency of the applied signal.

By calibrating the apparatus at two frequencies, the voltage appearing at P for an actual experiment was used to determine both the capacitance and resistance of the oxide film on the anode A. With the exception of very thin films, the values of C_f and R_f were such that at high frequency (14 Kc/s), the resistive component could be neglected without significant error being introduced, since the second term in the denominator was much greater than one, and the expression for the impedance was reduced to :-

$$Z = \frac{1}{\omega W C_f} \qquad (7)$$

The recorder was direct reading in units of capacitance $^{-1}$ at the high frequency, since the voltage at P was equal to a constant $x \frac{1}{C}$.

At the low frequency substitution of these capacitance values in equation 6, enabled the resistive component of the impedance to be obtained. For calibration purposes, pure resistance was inserted into the circuit at X to replace the oxide film and two large area platinum electrodes were used in a high conductivity electrolyte such as IN Na_2SO_4 (0.1 ohm^{-1}.cm^{-1}.)

(3) THE MECHANICAL PROPERTIES OF OXIDE FILMS.

The mechanical properties were studied in experiments in which the deformation and fracture of the oxide film were detected by measurements of capacity or potential, and also by more conventional mechanical techniques. Measurements were made both on oxide films on the metal substrate and on films which had been separated from the metal.

(a) Methods of Straining Oxide covered Metal Specimens.

Two methods were used to strain the oxide-covered metal specimens. The first was by means of a Houndsfield tensometer equipped with insulated pin jaws. Zero strain was determined by extrapolating the elastic portion of the stress-strain curve.

The second method was to bend the anodised metal strip either by using Perspex formers milled to known radii of curvature, or by using a bending jig attached to the Houndsfield tensometer. Assuming that the thickness of the film was negligible compared with the metal strip, then from the diagram below, it may be seen that the strain imposed on the film is given by $\frac{k}{r}$, where k = half the thickness, t of the metal strip and r = radius of curvature.

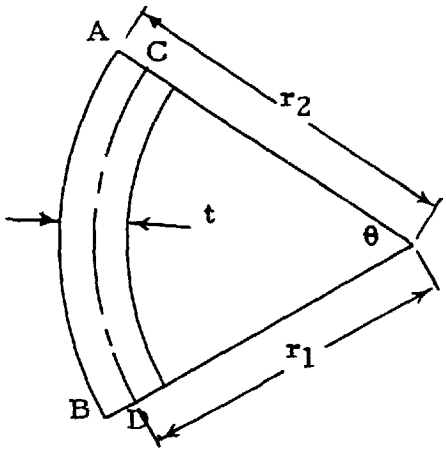

CD = neutral axis = const.

$AB = r_2\theta$

$CD = r_1\theta$ (8)

$$\text{Strain} = \frac{AB - CD}{CD}$$

$AB - CD = (r_2 - r_1)\theta$ (9)

Divide (9) by (8), then $$\frac{AB - CD}{CD} = \frac{r_2 - r_1}{r_1} = \frac{k}{r_1} \qquad (10)$$

where $k = t/2$.

(b) Methods of Detecting Failure of Oxide Films.

(i) Capacitance-Resistance Method:

The capacitance of an oxide covered aluminium surface gives a measure of the thickness of the oxide, provided the film is undamaged. If the oxide is cracked by deformation, the capacitance and resistance change to values more characteristic of "clean" aluminium, where the film thickness is 10 - 20 Å. This forms the basis of the capacitance-resistance method of measuring the ultimate tensile strain (U.T.S.) of oxide films.

A specific area was marked out on the oxide surface, using an easily deformable lacquer such as Lacomit or Ebonide. A cell was set up using a platinum disc as one electrode, the area of oxide-covered metal as the other, and one or two drops of the anodising solution as the electrolyte. Figure 3A shows the cell in section. It could be used in either the vertical or the horizontal position, surface tension being sufficient to hold the liquid in position.

The resistance and capacitance of the electrode were measured by means of the a.c. bridge shown in block diagram form in Figure 4. A square wave signal of 400 c/s frequency, was applied to the cell, and the voltage developed across it was compared with that obtained from an analogue circuit of a capacitance and resistance in parallel. The cell may be represented by the analogue circuit shown in Figure 3B, but in practice this was simplified to $R_f + C_f$ in parallel, since for all but the thinnest films the double layer capacitances were large compared with C_f, and R_e was small compared with R_f. The impedance of the unit $C_{d_1} + R_e + C_{d_2}$ was therefore negligible compared with $C_f + R_f$. The advantages of

using a square wave signal were that the resistive component R_e could also be resolved from the displacement of the two linear portions of the oscilloscope trace. In addition the high frequency component of the wave detected the presence of factors other than the capacitance of the film, such as double layer capacitance or faradaic processes which might be contributing to the total capacitance. The relative importance of these contributing components could be estimated from the shape of the oscilloscope trace obtained at the balance point.

(ii) Potential Method.

The open circuit potential of some metal electrodes changes according to the thickness of oxide present on the surface, being generally more negative for thinner films. If an oxide covered metal is deformed, a sudden fall in the electrode potential indicates the formation of cracks in the film.

The d.c. potential of the cell was measured using the bridge, or controlled potentiostatically. In some experiments the potential was measured directly by means of a valve voltmeter, and recorder. An automatic record was then obtained of potential

as a function of strain, by fitting a motor drive to the tensometer used to deform the specimen. A study was made by this means of the effect of different strain rates on the properties of the oxide.

(iii) "Leakage" Current Method.

The current which flows during the formation of a barrier-type anodic film is predominantly ionic. However, if the applied voltage is held constant this ionic current decays, and growth stops, but a small electronic "leakage" current remains. The magnitude of this current is determined by the electrical resistance of the film. If the film is deformed while maintaining a potential across it, the sudden surge in current which occurs when the film cracks may be used to indicate the ultimate tensile strain of the film.

(c) Measurements on Thin Foil and Separated Oxide Films.

(i) Deformation of Anodised Foils.

The differences between the stress-strain curves of thin metal foil, with and without an oxide film on the metal, were measured using a Houndsfield tensometer. The load which could be supported by the foil at low values of strain was increased in the presence of the film. As this increase was small, the mercury

capillary stress measuring device fitted to the tensometer was refined by following the movement of the meniscus with a travelling microscope. In later measurements, greater precision was obtained by using thin anodised wire specimens, and an "Instron" hard-beam tensometer.

(ii) Deformation of Separated Films.

A portion of anodised film was separated from the metal, and its stress-strain curve measured directly. The apparatus used for stripping the films from aluminium is shown in Figure 5. A 10% iodine-in-methanol solution was used at 55°C. Anodised specimens of .002" aluminium foil cut in the form of a tensile test specimen were cemented to a glass loop with Formvar. The whole was then immersed in the iodine methanol solution for 2-3 hours by which time all the aluminium had dissolved, leaving the film attached at each end to the glass. The film was then lifted clear of the solution using the windlass, washed in absolute methanol by immersion, and left to dry. The outer ends of the film were cemented with Araldite to the apparatus shown in Figure 6, which could strain the film by movement of the micrometer. The glass loop was melted near the apex by means of a small gas-oxygen

flame, before straining the film. Strain was measured directly with an eye-piece micrometer by measuring the relative movement of two points on the surface of the film within the field of view of the microscope.

After the film had broken, stress-strain curves were obtained using the remaining halves of the specimen, by cementing a light scale pan to the broken end, and adding weights. Strain was again measured using the eyepiece micrometer.

(4) MEASUREMENTS OF ELECTRICAL CONDUCTIVITY.

(a) Conductivity of Oxide Films.

The majority of these measurements were made by means of the a.c. bridge, which has been previously described. In addition to the measurements made on films in aqueous media, some measurements were attempted using a "Vibron" electrometer. In this method the time taken for a condenser to discharge through a resistance is measured. This process may be described by the equation:-

$$R = \frac{t}{C \log_e \frac{V_o}{V_t}} \qquad (11)$$

where R = resistance

C = capacitance

and V_o and V_t are the Voltages at zero time, and time t, respectively. If C is fixed, and V is measured as a function of time, R may be calculated. The conductivity, σ_s is then given by the relation:-

$$\sigma_s = \sigma \frac{l}{A} \qquad (12)$$

where σ = conductance

l = oxide thickness

and A = area.

Contacts were made to the oxide surface by means of "aquadag" colloidal graphite paint and pressure contacts as shown in figure 7. Conductivities of specimens prepared in this way were also measured by conventional a.c. bridge methods for comparison with the values obtained by measurements in aqueous solution.

(b) Effect of Hydrogen on Conductivity of Oxide Films.

In confirmation of previous work [35] measurements were made using the a.c. bridge, of the effect of cathodic polarisation on the conductivity of oxide films. Polarisation curves were obtained for aluminium, zirconium, and titanium for specimens which had been etched and then anodised. Measurements of resistance, capacitance, and current were made before and after the evolution of hydrogen at the oxide surface.

(c) Effect of Cathodically induced Hydrogen on the Conductivity of Rutile Single Crystals.

(i) Preliminary Experiments.

Single crystals of pure rutile* were cut from the boule with a diamond wheel, and ground to form parallel sided slices

* Supplied by the National Lead Co., South Amboy, New Jersey, U.S.A. Analysis in atomic per cent: Al, .001 : Si, .04 : Fe, .002 : others .001 individually.

measuring approximately 8 x 2 x 1 mm. The specimens were oxidised by heating in oxygen at 600°C for 16 hours, after which the conductivity was increased to the desired value by vacuum reduction in the temperature range 300° - 350°C. A number of specimens were prepared with resistivity in the range 10^3 to 10^7 ohm. cm., with the crystal c-axis perpendicular to the broad face.

One such sample, of 10^7 ohm. cm., was provided with four evaporated titanium strip contacts on one broad face, and mounted in Araldite so as to expose only the opposite broad face. Electrical contact to the titanium strips was made with indium soldered copper wires. The rutile electrode so formed (shown in figure 8A) was immersed in IN Na_2SO_4 solution, stirred by a stream of gaseous nitrogen, and a cathodic current of 0.1 mA/cm^2 was passed through the four contacts in parallel so as to evolve hydrogen from the exposed oxide surface. At intervals in this process, the rutile electrode was withdrawn, washed in distilled water, placed in a rough vacuum and the apparent resistance of the sample measured using the four back contacts. After a prolonged period of cathodic polarisation, the sample was left under vacuum, and its resistance monitored as a function of time.

Finally the specimen was returned to the electrolyte, and anodically polarised, oxygen being evolved at the surface.

From these experiments it was not possible to establish whether the changes in conductivity observed were due to changes in a thin surface layer, or in the bulk of the crystal. The following more refined series of experiments was undertaken to resolve this point.

(ii) Profile Experiments:

In these, the two broad faces of the specimens were ground optically flat and parallel using a hardened steel polishing jig, and a range of fine abrasives on plate glass, finishing with Linde "A". The amount removed after each period of grinding could be measured to within plus or minus one micron, using a precision comparator.

A gallium contact was made to the whole of one broad face of the specimen, which was then mounted in N.H.P. quick setting resin, with a copper wire making contact to the gallium, so as to leave only the opposite face exposed (see figure 8B). Cathodic treatment was carried out as before but in addition, the potential of the specimen was measured using a Luggin capillary

and calomel electrode, to ensure that the hydrogen evolution potential was exceeded. The current and potential were recorded for the duration of each experiment. After a given period of cathodic treatment, the electrode was removed from the solution, the resin dissolved in acetone with the assistance of an ultrasonic agitator, and the gallium contact removed in aqua-regia. The specimen was then washed in distilled water, dried, and remounted in quick setting resin on the polishing jig as shown in figure 8C, with the cathodically treated face exposed for subsequent measurements of resistance as a function of thickness.

The resistance measurements were made with a four probe technique, using "aquadag" current contacts covering the ends of the specimen, and point contacts of known separation for measurement of potential by a high impedance electrometer. The potential drop was taken as the mean of three readings in each direction and was reproducible to within $\pm$ 2%. After a measurement of resistance, the sample could be reduced in thickness in steps as small as one micron by polishing the exposed face. In this way a conductivity vs. thickness profile was obtained. To check the homogeneity of the starting material, a profile was

obtained on a specimen which had not been cathodically treated. No conductivity gradient was found, nor was there any significant change in conductivity of the vacuum reduced specimens with time, over periods up to two weeks. The effect of residual moisture on the resistance was small, the values obtained being the same whether the measurements were made in vacuum or in air.

SECTION IV

RESULTS

(1) MEASUREMENT OF GROWTH STRESSES IN OXIDE FILMS.

(a) Oxide Films on Aluminium.

Stresses were measured in the oxide films formed by anodising aluminium in the electrolytes, ammonium borate, ammonium citrate, and sulphuric acid under varying conditions of current density, and pH. The oxides formed in the first two electrolytes are compact, non-porous and amorphous in structure, whereas in sulphuric acid a thick porous oxide film is produced.

Preliminary experiments were done on porous films, in an attempt to reproduce the results of Bradshaw and Clarke [22], who were the first to report the existence of tensile stresses in anodic oxide films. The oxide film formed in sulphuric acid solution consists of a thin "barrier layer" adjacent to the metal over which the porous layer grows at constant voltage, and may reach a thickness of up to 100 microns. The data shown in figure 9 shows that the film thickness is initially proportional to time at an applied voltage of 15V. The results obtained from the stress measurement are shown in figure 10, in which the deflection of aluminium strips of different thicknesses is plotted as a function of the time of anodic oxidation, under conditions where the growth

rate was constant. It may be seen that initially the stress is tensile. However, as the film grows, a gradual change to compression occurs, the deflection at a given time being greater for the thinner metal strips, illustrating that the stress reversal effect is reproducible. Assuming from figure 9 that the growth rate under these conditions is approximately 0.5 micron per minute, the deflection minima occur at a thickness of approximately 15 microns. This would explain why Bradshaw and Clarke did not observe the stress reversal since their measurements were confined to thinner films, where the stress is tensile only.

Further experiments on the measurement of stresses in oxide films were done on the non-porous type of film, which, it was felt, bore a closer resemblance to the oxide films formed during aqueous corrosion than did the porous films. In these experiments, two main factors were found to influence the deflection of the metal strip during oxide growth. The primary factor was the stress inherent in the film itself, which may arise in a number of ways, but superimposed upon this was a voltage dependent deflection, which always acted upon the strip in such a way as to indicate an apparent compressive stress in the oxide film.

An example of this effect is shown in figure 11 in which the deflection of an aluminium strip, previously anodised to 300 volts, is shown as the voltage is raised slowly to the formation voltage. The reason for this movement is not clear, but it is possible that it is associated with the electrostatic compression of the film as has been suggested by Vermilyea [42]. If this is the case, the deflection would be expected to be proportional to V^2. The observed dependence of the deflection upon V^2 is therefore shown in figure 11.

In order to eliminate the influence of this "electrostatic" effect, measurements of deflection were always made at zero field, by allowing an arbitary time to elapse after switching off, during which the strip came to rest under the influence of the stresses within the oxide film.

Figure 12 shows the resultant deflection of an aluminium strip, due to the stresses in the oxide film on one side, as a function of the film thickness. The calculated values of stress existing within the oxide layer are plotted on the same axes, and it may be seen that reasonable agreement is obtained between the two methods used for calculation (see page 38). The dotted curve,

based on the direct calibration of the strip is probably the more reliable. The fact that similar values of stress were obtained by both methods shows that the Lacomit protective layer does not alter the elastic properties of the aluminium strip to any great extent for these small deflections.

The current density used for anodising was found to be important in determining the nature of the stress developed in the film. In general, the lower the current density, the greater was the tendency for a compressive stress to develop. This may be seen from figure 13, in which a number of curves of deflection vs. voltage are shown for aluminium oxide films anodically formed at current densities in the range 0.1 to 10 mA/cm^2 in ammonium borate solution. It is not clear why the initial compressive deflection observed for the film formed at the lowest current density of 0.1 mA/cm^2 is so much less than that found for the films formed at current densities in the range 0.2 - 0.4 mA/cm^2, but it might be associated with the much longer time required to form the film in this case.

The experiments were repeated using ammonium citrate as the anodising solution, to enable a more direct comparison to

be made between these experiments and recent diffusion experiments by Davies [19, 58], in which the nature of the mobile species was found to depend upon the current density used for anodising in ammonium citrate solution. The results obtained in pH9 ammonium citrate solution are also shown in figure 13, and are very similar to those obtained in borate solution of the same pH. At pH6, however, the results were slightly different, and although the tendency still remained for low current density to be associated with compressive stress in the oxide film, the value of current density at which the stress reversal occurred was increased from between 0.4 and 1.0 mA/cm^2 at pH9, to 1.0 - 2.0 mA/cm^2 at pH6. These results are shown in figure 14. The maximum values of stress calculated for films on aluminium are summarised in Table I. It will be seen that the compressive stresses developed are generally larger than the tensile stresses.

TABLE I.

Maximum Stresses in Anodic Films on Aluminium.

Electrolyte	Current Density mA/cm^2	Maximum Stress Kg/cm^2	Nature of Stress
Ammonium	0.2	1800	Compressive
borate	0.3	1100	"
pH9			

Table I continued:

Electrolyte	Current Density mA/cm^2	Maximum Stress Kg/cm^2	Nature of Stress
Ammonium	1.0	500	Tensile
borate	3.3	600	"
pH9			
Ammonium	1.0	1400	Compressive
Citrate	1.0	1000	"
pH6	2.0	400	Tensile
	5.0	600	"

(b) Oxide Films on Zirconium.

The stresses in anodic films on zirconium were measured using the same technique as for aluminium. However, in ammonium borate electrolyte, no basic difference was observed in the nature of the stress developed at different current densities in the range 1.0 to 10 mA/cm^2. The stress was predominantly compressive although tensile stress was observed for very thin films as can be seen from figure 15 in which three curves of deflection vs. voltage are shown. These measurements were of interest because the stresses in the anodic films were markedly greater than were found

for aluminium.

It may be seen from figure 16 that the calculated stress reaches a maximum value in all three cases near 4000 Kg/cm^2, at a thickness of approximately 3000 Å. This value of stress might be expected from the results of the tensile tests described in the following section, to cause mechanical failure of the film, and in fact there was some indication that this was occurring from observations made on specimens where the oxide film thickness was greater than 3000 Å. The steady motion of the strip due to the increasing compressive stress was replaced by an intermittent wavering motion after this thickness was reached, as if the stress in the film had been momentarily relieved. It should be added that this type of effect could also be explained in terms of a transient electrical breakdown of areas of the film, which would cause a drop in voltage and temporarily remove the voltage dependent compressive effect. However, there is no reason to expect that electrical breakdown would occur at such low voltages on zirconium, or that it would cause the "zero field" deflection to reach a steady value as observed.

(c) Oxide Films on Titanium.

The formation of anodic films on titanium is not as simple as on the "valve-metals" such as zirconium and tantalum, and it was found that films could not be formed at all on titanium in ammonium borate solution unless a fairly high current density was used. Other factors such as surface preparation, and the time of immersion before applying the anodic potential, were found to be critical, in determining the type of film growth which occurred. Two distinct types of film formation were observed.

The first, which will be called "normal" growth proceeded rapidly and with relatively little oxygen evolution, giving an approximately linear rise of voltage with time. The conditions required for this type of growth were high current density, a chemically polished surface, and minimum time of immersion before anodising.

The second, or "abnormal" type of growth often spontaneously followed the first type, and was characterised by a relatively slow rise in applied voltage, with time, together with vigorous evolution of oxygen. Abnormal growth could also be initiated if the titanium specimens were left in solution for several minutes before applying the anodising voltage, or if the anodising was

commenced at low current density. Values of approximately 1 mA/cm^2 seemed critical, in this respect.

Figure 17 illustrates this behaviour by showing the fluctuation of voltage obtained for a chemically polished specimen anodised at a constant current of 5 mA/cm^2 . Initially, the voltage rises smoothly to 100 V after which a spontaneous fall occurs. This is followed by the typically cyclic abnormal growth, with a steady decrease in the voltage at which spontaneous breakdown occurs. After the initial breakdown, the lower limit of voltage appears to be approximately equal to the IR drop in solution, as might be expected if the film had suddenly become porous or partly detached.

The reciprocal of the film capacitance, which was recorded automatically during anodising, is also shown in figure 17. The fact that this follows the same pattern as the voltage suggests that extensive breakdown of the film occurs at each step in the cyclic growth process, possibly allowing the solution to penetrate through to the metal surface, where a new film can again commence to grow. Direct observation of the metal surface during this cyclic process reveals a progressive change in interference colour of the film which suggests that the overall thickness of the oxide increases with each cycle, probably in steps which are roughly proportional to the

intercepts of voltage and $(\text{capacitance})^{-1}$ shown in figure 17.

For this reason the results of the stress measurements are presented in the form of curves of deflection vs. ΣV, where ΣV is the sum of the separate voltage steps which have occurred in sequence. The stresses observed in both types of growth were found to be compressive as can be seen from figure 18. Two of the curves (A and B) show the deflection observed during "normal" growth succeeded by abnormal growth, while in curve C, abnormal growth was initiated by prolonged immersion before anodising. In curve A, breakdown is spontaneous, whereas in curve B, breakdown was initiated by slowly reducing the applied voltage.

The compressive stress for abnormal growth was generally found to be higher than for normal growth. This may be seen from the way in which the deflection increases in curves A and B after the first breakdown, and from the greater initial slope of curve C. It seems reasonable that this is due to the greater evolution of oxygen observed under abnormal growth conditions, which, if trapped under existing cracked or partially detached layers of oxide, could cause an apparent increase in the compressive stress observed by this method.

Calculation of stresses was therefore confined to the initial regions of oxide growth only. These values are presented in Table II for the points on the deflection time curves corresponding to the first sharp change in voltage and $(\text{capacitance})^{-1}$.

TABLE II.

Maximum Stresses in Anodic Films on Titanium.

Current density mA/cm^2	Compressive Stress Kg/cm^2	Type of Growth
5.0	890	Normal
5.0	703	"
5.0	3010	Abnormal

After film breakdown had occurred, irregular motion of the strip was observed, but was more marked than for zirconium, and may have been partly due to the vigorous evolution of oxygen which occurs during abnormal growth.

(2) MECHANICAL PROPERTIES OF OXIDE FILMS.

(a) Measurements on Oxide Covered Metals.

(i) Oxide Films on Aluminium and Aluminium-Magnesium Alloys.

Measurements of the ultimate tensile strain (U.T.S.) of oxide films were made by the capacitance, resistance, potential, and "leakage" current methods previously described.

Figure 19 is a graph of the reciprocal of oxide film capacitance before deformation, plotted against the anodising voltage. Curve A is for aluminium, and curve B for Aluminium + 2% Magnesium. Assuming that the dielectric constant of the film did not change with thickness, the thickness was proportional to the anodising voltage, and a value of 15 Å per volt was used as a conversion factor.[43] The slope of this line agrees well with that recently obtained by Bernhard [44].

When a film was deformed by extending the underlying metal, the value of $^1/_C$ remained constant for a time, then rapidly decreased to a value which approached that obtained for "clean" aluminium, where the oxide film is 10 - 20 Å thick. The value of strain at which the first significant decrease in $^1/_C$

occurred, was considered to be the ultimate tensile strain of the oxide. The extent of the change depended on the thickness of the film, i.e. $^{1}/_{C}$ changed by a greater amount for thick films than for thin films. This effect is clearly seen in figure 20 which shows the curves for three films of 3000, 1500, and 375 Å thickness. It may be seen that the U.T.S. values are in the region of one per cent strain, which is approximately twenty times greater than the corresponding strain which may be tolerated by crystalline alumina [24]. The limitation of this technique is apparent in that the initial change becomes less sharp, the thinner the film.

The function $^{1}/_{CV}$ where V = anodising voltage, was used in some cases in preference to $^{1}/_{C}$ because it may be considered to be a measure of the relative amount of cracking of a given film. It is similar to the function $^{1}/_{CW}$ used by Wanklyn [45] to characterise much thicker films formed on zirconium. The initial value of $^{1}/_{CV}$ should be the same for films of different thicknesses, and this provides a check on the initial condition of films before deformation. Figure 21 is a graph of $^{1}/_{CV}$ vs. strain for several oxide films. Similar results were obtained if the oxide-covered metal specimens were deformed by the bending technique.

Resistance measurements, using the a.c. bridge were in general less accurate than capacitance measurements, but similarly shaped curves were obtained for resistance vs. strain, and where possible, the first significant drop in resistance was used to measure the ultimate tensile strain. Figure 22 shows some typical resistance vs. strain curves. The capacitance-resistance technique was used in order to compare the ultimate tensile strains of oxide films on 2S aluminium, and the aluminium-magnesium alloys, M57S and B54S, which contain 2, and 4 wt. per cent of magnesium respectively. The results obtained by this technique are shown in figure 23.

The scatter obtained is only partly due to inaccuracies in the resolution of the change in slope of the C-R vs. strain curves, since this can be measured to within $\pm$ 5%, in most cases. The primary cause of variation in this type of measurement is generally thought to be the random occurrence in the test specimens of stress-raising flaws of different sizes, which will effect the propagation of cracks at a different stress for each specimen [30]. All such imperfections will have the effect of lowering the U.T.S. obtained, to values below the maximum strain which could other-

wise be tolerated by the specimen.

It may be seen from figure 23 that the effect of alloying is a small but significant decrease in the U.T.S. of the anodic film. This is further illustrated in Table III, which compares the average U.T.S. values for 100 V films on the three metals. In the case of the films on aluminium, there is a tendency for the values of U.T.S. to increase with decreasing thickness. It will be seen that this tendency is also apparent in the results obtained for these films by other methods.

TABLE III.

U.T.S. of Anodic Films on Aluminium, and Aluminium-Magnesium Alloys by Capacitance-Resistance Method

Film Thickness Å	Composition wt. per cent Magnesium	Average U.T.S. per cent Strain
1500	0	1.50 ± 0.35
1500	2	0.89 ± 0.19
1500	4	0.87 ± 0.15

The potential vs. strain method was not subject to the same decrease in precision for thinner films as was the case for the resistance and capacitance methods. Figure 24 shows some

typical potential vs. strain curves obtained using the valve voltmeter-continuous strain method previously described. The strain at which the first sharp change in potential occurred was taken to indicate the U.T.S. of the oxide. Figure 25 shows two sets of results obtained using the potential method for anodic films on aluminium. The higher values are for films formed on specimens which had been previously annealed in the usual manner at 350°C for 30 minutes, while the remainder are for films formed on cold-rolled aluminium. Other measurements made on films on cold-rolled aluminium by the "leakage current" method also gave slightly lower values than those for films on the annealed metal.

A summary of the U.T.S. values obtained by all methods for oxide films on annealed aluminium, is given in the section on separated films and foils, and is illustrated in figure 35.

(ii) Oxide Films on Zirconium.

Measurements of U.T.S. were made on oxide films anodically formedon zirconium, using the capacitance-resistance method. These oxide films were also found to be capable of tolerating greater strains than the corresponding crystalline oxide in

bulk. This effect was not so pronounced as in the case of alumina, however, as can be seen in figure 26. No significant difference was found between U.T.S. values for films of differing thicknesses, although some uncertainty arises from the fact that the values for films thinner than 2000 Å were obtained by the bending technique, whereas values for the thicker films were determined by tensometer. If it is assumed that these methods were equivalent, an overall average value of 0.49 ± 0.12 per cent is obtained for the U.T.S. of these films, compared with 0.087 per cent for crystalline zirconia [46].

(iii) Oxide Films on Titanium.

Measurements of U.T.S. on titanium oxide films were complicated by the unusual anodic growth behaviour, which has already been described in the section on stress measurement. The difficulty arises in the use of reciprocal capacitance as a measure of the thickness of an undeformed film. Although the reciprocal capacitance values vary in proportion to anodising voltage during "normal" growth, removal of the applied voltage causes a sudden drop in the apparent value of $^1/_C$, producing more scattered values. The reason for this behaviour is not clear. However, subsequent

measurements of U.T.S. were made by the capacitance technique, as if these values were characteristic of an uncracked film, since it was not possible to form the film and subsequently carry out a tensile test without removing the applied potential.

Further results which may possibly have a bearing on this point are shown in figure 27. The function $\frac{1}{CV}$ is a rough measure in the case of aluminium and zirconium oxide films, of the relative degree of cracking of a given oxide film. The sharp decrease in $\frac{1}{CV}$ illustrated in figure 27 suggests that all but the thinnest films were initially damaged. However, it does not necessarily follow that any mechanical breakdown has occurred in the titanium oxide films since the change in $\frac{1}{CV}$ might reflect a change only in their electrical resistance.

This is supported by the results of the tensile tests, which are shown in figure 28. If the thicker films were initially cracked as suggested by the $\frac{1}{CV}$ measurements, presumably an immediate decrease in resistance, and $1/C$ would have occurred on deformation, whereas, small but finite amounts of strain were tolerated by the films without change in these properties. However, these results might also be explained if it is assumed that cracks formed in the

oxide as a result of compressive stress, were not appreciably widened during the tensile tests, until the small amount of compressive stress in the surrounding oxide had been relieved. Films thinner than 1000 Å have the highest U.T.S. values, as was found for aluminium.

(iv) Oxide Films on Uranium and Uranium-Zirconium Alloys.

Oxide films of the "barrier" type were formed on uranium and uranium-zirconium alloys by anodising in concentrated ammonia solution. Oxide films on zirconium-rich alloys were also studied. The oxide thickness, which is proportional to the anodising voltage, was measured using the optical technique, and also by impedance measurements.

Figure 29 shows a typical curve of relative intensity vs. time obtained for uranium using monochromatic light, and a constant anodising current. The rise of anodic voltage is also shown, corrected for the voltage drop through the electrolyte. Similar curves were obtained for uranium-zirconium alloys containing 5, and 10 wt. per cent of zirconium respectively, suggesting that the optical properties of the oxide films formed by this method are not greatly affected by alloying. This is more obvious from figure 30 in which

the optical thickness of the anodic films formed on the three metals at constant current density is plotted as a function of time. Optical thicknesses were calculated assuming the same value of 1.92[40] for the refractive index in each case, and it may be seen that the three curves almost coincide. The ultimate thickness which may be reached by anodising, decreases as the zirconium content of the alloy increases.

The capacitance of an oxide covered uranium electrode may be used as a measure of the oxide thickness, provided the electrode is anodically polarised during the measurement. For potentials more anodic than + 1.0V (calomel) the capacitance is independent of potential. The reciprocal of this capacitance was found to change in proportion to oxide thickness, although it is probable that some contribution was being made to the total capacitance by other variables, such as double-layer capacitance, and faradaic processes occurring at the oxide surface, or in the oxide film[47]. This may be shown by calculation of the oxide thickness on the basis of capacitance measurements alone. Extraordinarily large values of the dielectric constant (from 40 to 120) must be assumed in order to obtain agreement between these apparent thicknesses

and the measured optical values. The reciprocal capacitance of anodic films on uranium-zirconium alloys, measured at + 1.5 V (calomel) is shown as a function of optical thickness in figure 31.

Tensile tests were carried out on anodised specimens, maintained potentiostatically at + 1.5V (calomel). The films were deformed by extension of the basis metal using a Hounds-field tensometer, and also by bending strips of known thickness, and measuring the radius of curvature with a travelling micro-scope. Measurements of resistance, and potentiostatic current were made simultaneously with the capacitance measurements so that any one experiment yielded three results for the U.T.S. of the film based on the values at which the first sudden change in these variables occurred. The results from a number of experiments were used to determine a mean value of U.T.S. for films on each alloy.

Table IV summarises the values obtained for films on uranium-zirconium alloys. Tensile tests were not possible on the U + 10% zirconium alloy due to the extremely brittle nature of the metal specimens, even after annealing.

The most obvious feature of the results is the relatively

TABLE IV

Metal Composition	Number of Measurements	Mean value of U.T.S. of oxide film per cent strain
U	10	$0.82 \pm .16$
U + 5% Zr.	20	0.51 ± 0.11
Zr	13	$0.49 \pm .12$
Zr + 5% U	9	$0.65 \pm .12$
Zr + 10% U	9	$0.61 \pm .12$

small range of U.T.S. values obtained for all alloys. As for the other films studied these values are higher than the corresponding values for urania or zirconia in bulk. The effect of alloying does not appear to be large in either the zirconium rich or uranium rich alloys. Addition of zirconium to uranium appears to cause a small decrease in U.T.S., whereas alloying up to 10% of uranium with zirconium causes a change in the U.T.S. of the oxide which, in view of the scatter of results, cannot be considered to be significant.

(b) Measurements on Foils and Separated Films.

(i) Films on Aluminium.

Figure 32 shows the stress-strain curves obtained for specimens of annealed aluminium foil prepared in the form of standard tensile test pieces having a gauge length of 5 cm. Curves A and B are for the "clean" metal. Curves C and D are for anodised specimens. The second "kink" II occurred only for the anodised specimens and was more pronounced for thicker films. It became indistinguishable from curves of type A and B when the thickness ratio, metal to oxide exceeded 150 : 1. The kink was thought to show the stress raising effect of the film possibly due to blocking of dislocations at the aluminium surface. The sudden change of slope at II may have been due to yielding along one or more slip planes, and this would imply that the oxide film had cracked at this point. This was assumed to be the case in determining the oxide U.T.S. by this technique.

The results obtained for aluminium suggest that this assumption was justified. Figure 33 shows the variation of U.T.S. as a function of oxide film thickness, and again, as found by the other methods, the values increase with decreasing thickness.

It is noticeable that the scatter is much less for this method, and this may be because the method only detects extensive failure of the film in these tests. The effect of individual cracks, easily detectable by electrical means might be expected to be additive in lowering the overall stress which the film could support, thus tending to give rise to an average value of critical strain, at which the greatest number of cracks occur in the film.

Figure 34 shows one of a series of stress-strain curves obtained by the direct loading technique, on separated 1500 Å films of alumina anodically formed in ammonium borate. The notable features are the large apparently elastic strain before fracture, and the low values of Young's Modulus $4.1 \pm 0.8 \times 10^5$ (average) compared with 3.8×10^6 Kg/cm^2 for bulk Al_2O_3. Table V summarises the data obtained for other films of the same thickness using this technique. Reasonable agreement exists between the average U.T.S. value obtained by this method, and the values determined by the other techniques for 1500 Å films on aluminium.

These are compared in Table VI.

TABLE V.

Mechanical Properties of Separated Aluminium Oxide Films.

Film Thickness Å	Ultimate Tensile Strain per cent	Ultimate Tensile Stress $Kg.cm^{-2}$	Young's Modulus $Kg.cm^{-2}$
1500	1.6	-	-
"	1.98	7,300	3.7×10^5
"	1.95	6,500	3.3×10^5
"	2.09	11,300	5.4×10^5
"	2.48	10,800	4.3×10^5
"	1.65	6,100	3.7×10^5

TABLE VI.

Comparison of U.T.S. values for 1500 Å films on Aluminium.

Method of Measurement	U.T.S. (average) per cent.
Separated Film	1.96 ± 0.32
"Kink" in stress-strain curve	1.52 ± 0.05
Capacitance-Resistance	1.50 ± 0.35
Potential Method.	2.0 ± 0.3

A summary of all the results obtained for films having

thicknesses in the range 300 to 3750 Å is shown in figure 35. The value for single crystal alumina in bulk is shown as a dotted line on this graph, and is approximately an order of magnitude below the values obtained for these thin films.

(ii) Films on Zirconium.

Several attempts were made to examine the mechanical properties of zirconium oxide films separated from the metal by Dalziel's methanol-bromine technique[48], and also using $HF-HNO_3$ etching solution. The second of these techniques was extremely rapid, and simple to use, although some solution of the oxide film probably occurred, during separation. This was inferred from the change in interference colour of the film which occurred if it was allowed to stand in the etching solution. Two of these films were separated successfully and mounted for testing, but no clear result was obtained. One of the films briefly supported a 700 mg load (corresponding to a stress of only 70 Kg/cm^2) before breaking, but it seems unlikely that this low value reflected the true strength of the film, in view of the large U.T.S. values (approximately 0.5%) obtained by the electrical methods. It is possible that the etching solution may have weakened the film.

(c) Deformation of Oxide Films during Growth.

Recent measurements by Davies [19] have shown that both anion and cation movement occurs during the anodic oxidation of aluminium at high current density, and the following experiments were designed to test the concept that oxide films may deform plastically during growth, under conditions where both ions are mobile. Thin wires of grade I (99.999%) aluminium were annealed, and mounted in tubular glass end pieces using N.H.P. quick setting resin. Stress-strain curves were obtained for both "clean" and anodised specimens using an "Instron" hard-beam recording tensometer. These curves are shown in figure 36. A duplicate specimen was anodised to 200 volts at 6.28 mA/cm^2 current density in ammonium borate solution. It was then mounted as for the tensile tests, but re-immersed in the anodising solution, and loaded by hanging a weight on the lower support so that the load corresponded to point X_1 on the stress-strain curve.

A steady anodic current of 7.00 mA/cm^2 was then passed through the oxide film for $2\frac{1}{2}$ minutes, and a small extension of the wire (to point X_2) occurred.

A higher load was then applied, (point Y_1) and an anodic

current of 7mA/cm^2 again passed through the oxide, for a similar period of time. This time a larger extension occurred (to point Y_2). This sequence of events is shown again in figure 37 in which the extension of the wire is shown as a function of time. It is clear that a current density of 7.00 mA/cm^2 is sufficient to allow the wire to extend to values of strain more characteristic of those for the "clean" aluminium wire, at the two different load values applied to the specimen.

It was not anticipated that any further extension of the wire would occur after point Y_2 was reached. However, a relatively slow increase in length was obtained, which coincided with dielectric breakdown of the film, when the current density was increased ~~above 2.0~~ from 2-3 mA/cm^2. Movement ceased when the current was reduced below a certain critical value which appeared to be in the region of 3.~~0~~ mA/cm^2. This additional extension may have been assisted by weakening of the aluminium core of the wire at those points where breakdown occurred.

A blank experiment was done on a freely suspended wire, by measuring whether any change in length occurred during anodising at a current density of 7 mA/cm^2.

Under these conditions, a slight tensile stress would have been expected to develop in the oxide by analogy with the results presented in section 2(a) on the deflection of anodised foils, but no significant change in length was observed.

(3) MEASUREMENTS OF ELECTRICAL CONDUCTIVITY.

(a) Conductivity of Oxide Films on Metal Alloys.

The results obtained for the conductivities of the anodic films on aluminium and aluminium-magnesium alloys are summarised in Table VII. The values quoted are average conductivities calculated from impedance measurements made at 400 c/s using the a.c. bridge technique, on films in the thickness range 300 - 4000 Å.

The conductivities calculated from the electrometer measurements, and the "leakage current" technique are also included in Table VII. The low values obtained by the electrometer technique are probably due to high contact resistance, since no estimate of this may be made in a two-contact method.

Each set of results clearly indicates an increase in conductivity of the oxide film as the magnesium content of the metal is increased. The a.c. bridge value for aluminium oxide films is in reasonably good agreement with Pryor's [49] value of 1.0×10^{-10} $Ohm^{-1} cm^{-1}$.

The conductivities of films on uranium-zirconium alloys are shown in Table VIII. These values were again calculated

TABLE VII.

Conductivities of Anodic Oxide Films on Aluminium-Magnesium Alloys.

Metal	Conductivity (a.c. bridge) $Ohm^{-1}.cm^{-1}$	Conductivity (electrometer) $Ohm^{-1}.cm^{-1}$	Conductivity (leakage current) $Ohm^{-1}.cm^{-1}$.
Al (2S)	1.45×10^{-10}	1.29×10^{-11}	4.0×10^{-11}
Al (2% Mg)	3.57×10^{-10}	4.67×10^{-11}	1.0×10^{-10}
Al (4% Mg)	5.55×10^{-10}	4.91×10^{-11}	1.59×10^{-10}

TABLE VIII.

Conductivities of Anodic Oxide Films on Uranium-Zirconium Alloys.

Metal	Conductivity A.c. bridge $Ohm^{-1}.cm^{-1}$	Conductivity (leakage current) $Ohm^{-1}.cm^{-1}$
U	3.26×10^{-9}	5.9×10^{-10}
U + 5% Zr	3.32×10^{-9}	2.1×10^{-9}
U + 10% Zr	4.98×10^{-9}	1.8×10^{-9}
Zr.	2.08×10^{-10}	-
Zr. + 5% U	3.0×10^{-9}	-
Zr. + 10% U	6.9×10^{-9}	-

from results obtained using the a.c. bridge technique and also from "leakage current" measurements. Thicknesses were determined optically in the case of the uranium-rich alloys. Although the conductivity obtained for zirconium oxide agrees roughly with previous results [50], the values obtained for uranium and its alloys are much too ~~high~~ low for the oxide to be uranium dioxide, which has a conductivity of the order of 10^{-3} $ohm^{-1}.cm^{-1}$. It is much more likely from thermodynamic considerations that the oxide produced under strongly anodic conditions is U_3O_8, or one of the higher oxides which can have conductivities in this range [51].

In all cases, the effect of the alloying addition is to increase the conductivity of the oxide film produced on the metal.

(b) Effect of Hydrogen on the Conductivity of Oxide Films.

The effect of a period of cathodic polarisation on the apparent conductivity of anodic oxide films on uranium and titanium is illustrated in figure 38, in which resistance is plotted as a function of potential (with respect to a saturated calomel electrode). It may be seen that for uranium, maintaining the potential at -1.8V for a period of approximately 10 minutes decreases the resistance

(at zero potential) by about 10 times. No change in oxide thickness occurred during this period, since the interference colour of the film was unchanged. The slow drift in resistance towards the original value which occurred over a period of one hour is shown. Similar effects were found for oxide films on zirconium, and titanium, when given similar cathodic treatment in agreement with previous work [35]. A possible explanation of this behaviour is that hydrogen diffuses into the oxide, and ionises, thereby changing the oxide conductivity. The results of the experiments on single crystals of rutile support this explanation in the case of titanium oxide films.

(c) Effect of Cathodically Induced Hydrogen on the Conductivity of Rutile Single Crystals.

The results of the preliminary experiments may be seen in figure 39, which shows the change in resistance of a rutile specimen, initially of 10^7 ohm. cm. resistivity, during the course of electrolytic treatment. The rutile structure is such that relatively large interstitial channels exist parallel to the c-axis of the crystal [52]. Experiments were therefore done on crystals with

the c-axis at right angles to the exposed surface, since the diffusion of hydrogen into rutile might be expected to occur with the least difficulty in this direction. The curve shown in figure 39 has three distinct sections, the first showing the decrease in resistance during the cathodic treatment, the second its recovery in vacuum, and finally, the much more rapid recovery obtained by subsequent anodic polarisation, evolving oxygen at the oxide surface.

The results of the profile experiments are presented in figures 40 and 41, in which the conductivity of the portion of the crystal removed by grinding, is plotted against the thickness removed. The profiles shown in figure 40 are for specimens of comparable initial conductivity, and only one profile was obtained in each case. In other experiments the samples were cathodically polarised more than once with a conductivity profile to a depth of about 10^{-2} cm. taken after each polarisation. The profiles in figure 41 are for one such sample. The effective time of treatment was taken to be the accumulated time of polarisation.

Resistivity-Temperature data for three rutile specimens are presented in figure 42. Specimen F was vacuum reduced only, while the other two had been cathodically treated in addition to the vacuum reduction.

The Infra-red spectrum of the crystals confirmed the presence of the O-H stretching vibration originally detected by Soffer[53]. The peak height was small, but the wave number of 3270 cm^{-1}. agreed well with Soffer's value. However, the absorption peak was observed both in the vacuum reduced, and cathodically treated samples, and it could not be said from the relative peak heights that any significant change in the number of O-H bonds had occurred as a result of the cathodic treatment.

SECTION V.

DISCUSSION

DISCUSSION

(a) Stresses in Oxide Films.

The origin of stresses in growing oxide films is often assumed to be determined by the volume change which occurs when a specific quantity of metal is converted into metal oxide. Experimental evidence shows that this is an over-simplification, and that in many instances, other factors may partly or wholly determine the nature and magnitude of the stress which develops in a growing oxide film. Some of these factors, which have already been considered in detail in the introduction, include the nature of the diffusing species, epitaxy, surface roughness, and residual stresses in the metal.

In this discussion, the evidence obtained from the experiments done on anodic films will be used to substantiate the suggestion[54] that the nature of the diffusing species is of primary importance in determining the stress in oxide films. and that under conditions where a sufficiently high diffusion flux of both ions exists in the oxide, stress relief may occur by deformation during growth.

Perhaps the best way to illustrate the inadequacy of the volume ratio concept is by means of a simple calculation of the stress which would be expected to develop in an oxide film on aluminium where the volume ratio is 1 : 1.28. If it is assumed that oxygen is the only diffusing species then the compressive strain which must be tolerated by the film in a direction parallel to the metal surface is 8.5 per cent, clearly greatly in excess of the maximum strain which may be tolerated either by bulk alumina or oxide films. If it is assumed that this strain is elastic then a crude estimate of the maximum permissible thickness may be made using Evans[55] model. In this, detachment or cracking of the film is assumed to occur when the stored elastic energy exceeds the work of adhesion between metal and metal oxide or the work of cohesion of the oxide film, depending on which is the higher value. Assuming that the work of cohesion of the film is approximately 2000 erg. cm^{-2},[56] and using the experimental value of 4.1×10^5 Kg. cm^{-2} for Young's modulus[57], the maximum permissible oxide thickness on aluminium is calculated to be of the order of 70 Å, before cracking becomes a favourable change. The theoretical compressive

stress at this thickness would be 35,000 Kg.cm^{-2}.

It is clear that neither the thickness nor the stress values agree with experimental observations. In the first place it is possible to form much thicker oxide films on aluminium than 70 Å, without the occurence of any detectable mechanical failure. Anodic films of the compact barrier type may be formed up to 6000 Å, and corrosion films of 2000 Å and more may be produced on aluminium in boiling water [42].

Furthermore, the stresses in these oxide films have been shown in some cases to be tensile both in this work, and by others [22, 42]. It may be seen from the results of the deflection experiments presented in figures 13 and 14, that the stresses are influenced by the rate of oxide growth, which is determined in anodic oxidation by the current density. For low current densities, the stress is compressive, whereas above a certain critical value, tensile stresses were found. Recent work by Davies [58] has provided evidence which may explain why this behaviour was observed. He showed that for low current densities, of the order of 0.1 mA/cm^2, oxygen was the predominant mobile ion, while

at higher current density (10 mA/cm^2) both ions move, with cationic movement accounting for approximately twenty per cent of the ionic current.

The observation of compressive stresses at low current density is consistent with the results of Davies experiments, since the volume ratio for aluminium oxide should at least determine the sign of the stress in the case where oxide growth proceeds only at the metal-metal oxide interface. However, it is interesting to note that the value of compressive stress observed is much lower than the calculated value in all cases where this type of growth occurs. Table IX illustrates this tendency for oxide films grown on aluminium at low current density, and for zirconium oxide films in which oxygen is thought to be the only diffusing species [59]. The results of Dankov and Churaev's experiment on iron, and nickel oxide films are compared with these values, as a further illustration of this effect.

The observation of tensile stresses, in the oxide films formed at high current density on aluminium, demonstrates that the volume ratio completely fails to indicate stress under conditions where both ions move. Furthermore it seems reasonable

TABLE IX

Comparison of Observed Stresses in Oxide Films with Stresses Calculated from the Volume Ratio

Metal	Maximum Compressive Stress in Oxide Film (observed) Kg/cm^2.	Volume Ratio	Theoretical† Stress in Oxide Film Kg/cm^2.
Al (anodised at low current density)	1800	1.28 (α-Al_2O_3)	340,000
Zr	4000	1.56 (ZrO_2)	270,000
Fe *	3850	2.14 (Fe_2O_3)	290,000
Ni *	2830	1.65 (NiO)	180,000

(* Dankov and Churaev's measurements (1953))[6].

(† The stress values shown were calculated using the elastic constants of the corresponding oxides in bulk.)

that the anomalously low compressive stresses in the other examples shown in Table IX, might also be explained in terms of a degree of cationic mobility occurring during growth.

The concept of more than one moving species in oxide films is becoming increasingly used in explaining some aspects of

aqueous corrosion even though such a picture is difficult to interpret in terms of thermally activated diffusion. Measurements of the relative diffusion coefficients of cationic and anionic species at elevated temperatures have been made in many cases on oxide specimens in bulk, and it is usually found that one ion dominates due to large differences in the relative number of defects, and/or their activation energies for diffusion. If the possibility exists for the two species to have comparable rates, it will usually be restricted to a narrow range of temperature.

A considerable amount of evidence exists in support of the simultaneous movement of anions and cations in oxide films formed in aqueous media, and at low temperatures. For example, Potter's model of magnetite film formation on iron [60] requires that approximately equal cationic and anionic currents pass through the growing oxide layer, over a wide range of temperatures. Evans has recently expressed the view [61] that this counter-current principle deserves to be applied to other film substances than these boiler films. Recent papers by Davies [19], Vermilyea [42] and Wilkins [13] also contain evidence which is best explained in terms of two moving species in oxide films at room temperature.

It is well known that the presence of water lowers the activation energy for metallic oxidation [62, 60], and this could have the effect in some cases of making the relative diffusion rates more nearly equal. However, it seems that the energy of activation for diffusion in the bulk material is not the only factor to be considered for thin films. Movement of both ions may occur because of free energy considerations, in order to maintain the stress in the film within "safe" limits.

The second possible explanation of the results in table IX, namely plastic deformation of the oxide film in the crystallographic sense, seems at first sight very unlikely at room temperature in view of the observed brittle behaviour of separated aluminium oxide films (see figure 34). However, as will be shown in the following section, deformation by a creep mechanism cannot be ruled out in the case where both ions are mobile, and a sufficiently high ionic flux exists in the oxide film.

Before discussing the possible origin of tensile stress in oxide films it is convenient to consider the nature of the "electrostatic" effect observed in the deflection experiments (see figure 11). A possible explanation for this was sought in terms of the slight thermal expansion which occurs when the anodic current passes

through the oxide. Young [14] estimated that the heat dissipated in anodic films on tantalum corresponds to a 1°C rise at 1 mA/cm^2 and 10°C at 10 mA/cm^2. Applying these values to aluminium the corresponding stresses resulting from thermal expansion are 4, and 40 Kg/cm^2 respectively which are clearly too low to explain the relatively large differences in stress (up to 400 Kg/cm^2) observed on removing the anodising current. Furthermore, the "electrostatic" effect is obtained for fully formed oxide films, where the ionic current has been allowed to decay to the leakage value. Figure 11 shows that the deflection is dependent on applied voltage. Compression of the film due to the high electrostatic field (approximately 5 x 10^6 V/cm) might be a possible explanation. The stress in the film due to this field may be calculated to be approximately 200 Kg/cm^2 normal to the metal surface, which is of the right order of magnitude but too small to account for the observed deflection, if Poisson's ratio is assumed to be between 0.2 - 0.3. The deflection should depend on the square of the field and although this seems to be the case for conditions of decreasing field, the hysteresis observed with increasing field suggests that a higher power than two is involved.

Another possible explanation arises from the mutual repulsion of charges on the surface of the film during anodic polarisation. Since there need not be any evolution of oxygen during anodic growth, the potential at the oxide surface is probably not greater than the overpotential for oxygen evolution. The effect of surface potential upon deflection was therefore tested by anodically polarising a gold foil specimen, laquered on one side. No deflection occurred in the range 0 - 2 Volts (anodic).

Tensile stresses in anodic films on aluminium were observed both by "zero field" measurements, and in experiments where the potential was continuously applied. Examples of this may be seen in figure 12 and for the highest current density curves in figures 13 and 14. In all experiments the effect of removing the field was to produce a more tensile, or less compressive value of stress in the oxide film. Tensile stresses were also found in the initial stages of growth for films on zirconium (figure 15) and porous films on aluminium grown at 16 mA/cm^2 in sulphuric acid (figure 10).

Although the possibility of cationic movement will explain the reduction or absence of compressive stress in oxide films expected from the volume ratio principle, it is difficult to see how

this can explain the existence of tensile stress. A possible explanation for the origin of tensile stresses in anodic films on aluminium and zirconium has been recently suggested by Vermilyea [42]. He assumed that each new layer of oxide formed is hydrated, but undergoes a subsequent dehydration by field-assisted proton migration, which might be expected to produce tension in the film. In confirmation of this, he found that a thick hydrated film produced on aluminium by immersion in boiling water developed tensile stress when subsequently anodised. It is not possible to determine from the data in Vermilyea's paper whether this effect is sufficiently large to account for the magnitude of the tensile stresses observed. The difficulty with this interpretation is that there is no evidence to support the premise that films are hydrated on formation, although it is well known [44] that hydration of barrier type anodic films does occur slowly after formation in most aqueous solutions. Recrystallised anodic films give electron diffraction patterns corresponding to the γ-alumina structure [32] with lattice dimensions of the dehydrated oxide.

Another possible explanation has been put forward [61, 63] namely, that there may be a near balance between the ionic currents

flowing through the film, which certainly appears to be the case for the growth of films on aluminium at high current density. If the migrating cations leave behind vacancies which do not coallesce, the oxide subsequently formed in this region by the inward diffusion of oxygen will have a lower density than the oxide in bulk, and might therefore be in tension.

(b) Mechanical Properties of Oxide Films.

It is clear from the data in figure 35, which summarises the ultimate tensile strain values obtained for anodic films on aluminium, that the films have substantially different properties from the bulk material. The films are about five times stronger (tensile strength of 10,000 Kg/cm^2 compared with 2000 Kg/cm^2 bulk) and are more easily deformed (0.5 to 2.0% strain before fracture compared with .07% bulk).

It must be emphasised that these figures apply to the properties of fully formed films under conditions of "static" test, where the ionic diffusion occurring in the films is confined to thermal motion at room temperature, and where the rate of deformation is relatively high. The high tensile strength observed under these conditions is not surprising since it is well established that the tensile strength of brittle materials increases with decreasing specimen size due to the necessarily smaller dimensions of Griffith cracks [30] and stress-raisers which can exist.

The large apparently elastic deformation is less easily explained. The high values of strain observed in measurements made directly on separated films might possibly be explained if

these films had been slightly wrinkled due to surface irregularities on the metal foil from which they were removed. However, it is difficult to visualise any similar mechanism which could also account for the equally high values observed with the films still attached to the metal (see table VI). As further confirmation, recent results by Edeleanu [64] are in agreement with these strain values, for anodic films formed on aluminium in dilute sulphuric acid. If the measured values represent the true tensile properties of the film then it must be assumed that the structure of anodised films is different in some fundamental way from that of the bulk crystalline material. This is supported to some extent by electron diffraction measurements, in which no crystal structure characteristic of the bulk can be resolved [32]. There is some evidence to suggest that crystallinity develops slightly at thicknesses greater than 2500 Å, but it seems probable that the majority of the films studied here may be considered "amorphous". If the structure consisted of a preponderance of grain boundaries, in which very small grains existed (possibly $(Al_2O_3)_2$) [65], a lower Young's Modulus than that of crystalline alumina might be expected. If the oxide had a glass-like structure, again a lower Young's Modulus might be expected than for crystalline alumina.

Plastic deformation of the oxide films under the conditions used for testing seems to be unlikely, for two reasons. The temperature was too low to permit thermally activated movement of dislocations (if dislocations could exist in an amorphous material) and the stress-strain relationship (figure 34) obtained by repeated loading and unloading of the oxide film is linear within experimental error. Tests at slower strain rates, and under conditions where the ionic diffusion flux is comparable to that during growth, might be expected to show whether plastic deformation by diffusion is a possibility during oxide formation.

The results of the experiments done on anodised aluminium wires suggest that this possibility must be considered in the case where a sufficiently high diffusion flux of both ions exists in the oxide film during growth. The effect which the presence of a thin oxide film has on the mechanical properties of aluminium has been studied by several workers including Barrett [66], and more recently by Holt [67]. Two types of effect can be distinguished. The first, which occurs for very thin films, operates by pinning surface dislocation sources, thereby increasing the elastic strain which the underlying metal can tolerate before yielding. In the

second type, of which this work is an example, the whole stress-strain curve is raised, as may be seen in figure 36. In this case the oxide film is thick enough to act not only in pinning surface sources in the above manner, but as a barrier preventing the escape of dislocations having internal sources.

The film may also contribute to the increased slope of the elastic region by supporting some of the load directly. The cross sectional area of the film, which is approximately one tenth of the total cross sectional area, is sufficient to enable the film to support the total applied load. However, the relative proportions of the load carried by the oxide film and the metal cannot be simply calculated in view of the complex manner in which they interact. At a value of strain corresponding to point Y_1 in figure 36 it may be shown that the stress in a separated film equal in area to that of the film surrounding the wire would correspond to approximately 0.2 of the applied load. It seems likely therefore that the major effect of the film upon the mechanical properties of the wire is a stiffening by means of one or both of the dislocation blocking mechanisms, with a smaller, but significant contribution due to the tensile strength of the oxide film itself.

The extension of the loaded anodised wire, represented in figure 36 as the distance $Y_1 - Y_2$ shows that the influence of the film is removed during the passage through it of an ionic current of 7 mA/cm^2, which is sufficiently large to cause movement of both cation and anion in the oxide film. Since the movement is apparently confined to the elastic regions of both stress strain curves, it might be assumed that no metallic slip was involved in this extension. However, recent work by Kramer [68] on the effect of electropolishing on the deformation of aluminium suggests that plastic deformation of the metal may be initiated by a sudden increase in anodic current density. He describes this phenomenon as dislocation "pop-out". If this effect applies to the present case, and only operates when the applied load is near the yield point of the metal, it would explain why the extension $X_1 - X_2$ (figure 36) at low load was so much smaller than $Y_1 - Y_2$, and furthermore, why additional current sensitive extension of the wire occurred after the commencement of dielectric breakdown.

Regardless of whether the extension of the wire was plastic or elastic, it is clear that extension of the oxide film must have occurred in both cases. A reasonable explanation, particu-

larly in the case of deformation before dielectric breakdown of the film, appears to be plastic deformation of the film by creep.

Normally, creep deformation of aluminium oxide does not become significant until the temperature is in excess of 1000°C [69]. However, during anodic oxidation, the current density may be sufficient for the ionic diffusion flux to equal that attained at a much higher temperature by thermal diffusion. For example, in the anodic oxidation of aluminium, a steady formation current of 7 mA/cm^2 produces an ionic diffusion flux through the oxide film equivalent to that achieved by thermal diffusion in alumina at 1700°C [70]. It is important to consider the fact that in thermal diffusion, the ionic motion is random, whereas in high-field activated diffusion, ionic movement is predominantly in the direction of the field. In this experiment the direction of the field is normal to that of the applied stress. However, there will be a component of ionic motion in the direction normal to the applied field due to the random distribution of vacancies in the oxide, and the action of the applied stress will be to assist this motion. If a value for the diffusion coefficient based on the anodic diffusion flux is substituted in Nabarro's equation for the

rate of creep[71], together with the observed rate of deformation (figure 37) of 4.0×10^{-5} sec.$^{-1}$, the resolved shear stress required to maintain this rate is found to be only 0.8 Kg.cm^{-2}. From this it seems that the theoretical creep rate under the conditions of this experiment would be more than adequate to explain the rate of oxide deformation observed, since the actual shear stress was undoubtedly higher than this, probably being in the region of 500 Kg/cm^{2}.

This observation of the ability of anodic films to deform at room temperature during the passage of an ionic current appears to be an important one, since it is possible that the mechanical properties of oxide films formed by other means might be affected under conditions of growth where both ions are mobile.

If this is assumed to be the case during the formation of oxide films on uranium and uranium-zirconium alloys under aqueous corrosion conditions, it provides a rational explanation of the apparent conflict between the results of tensile tests made on anodic oxide films on uranium-zirconium alloys, and the results of previous corrosion rate measurements. In this previous work it was shown that thicker protective, and therefore uncracked oxide

films could be formed on the alloys than on pure uranium, suggesting that the film formed on the alloys was either formed in a state of lower stress, or was capable of relieving growth stresses more effectively than was possible for the film on uranium.

However, as may be seen from the results of "static" tensile tests carried out on anodic oxide films formed on these metals (table IV) the reverse seems to be true. That is, the oxide film formed on the 5% zirconium alloy is less able to tolerate strain than the film on pure uranium. Furthermore, it seems likely that the deformation before fracture was elastic rather than plastic in this type of test. If this were the case, then the reduction in ultimate tensile strain obtained for the mixed oxide formed on the alloy would be in qualitative agreement with Armstrong's experiments [72] in which small additions of zirconia have been observed to cause a hardening of uranium dioxide, under conditions where the deformation rate was large compared to the strain rate expected from the Nabarro model. This trend was also found in the "static" test values of U.T.S. for anodic oxide films on aluminium-magnesium alloys (table III).

The fact that thicker protective films may be formed on

uranium-zirconium alloys than on pure uranium may not be incompatible with the data of the tensile tests if the mechanical properties of the oxide during growth were different from those measured in a "static" tensile test, where the ionic diffusion flux through the oxide is small.

At high temperatures, it has been shown[26] that the rate of creep of uranium dioxide is determined by the mobility of the slowest moving species, which is the uranium cation. Furthermore, the addition of zirconium oxide to uranium dioxide compacts considerably increases the diffusion coefficient of uranium in the mixed oxide[73]. Although these data cannot be meaningfully extrapolated to room temperature, it is likely that the addition of zirconium to uranium would increase the mobility of uranium in the oxide film if the activation energy for diffusion were important in the diffusion process of the film.

If the cation mobility in the oxide were increased as a result of the zirconium addition, the stress developed in the oxide film on the alloy resulting from volume ratio considerations would be less per unit thickness than that for the film on pure uranium. This would therefore allow a thicker protective film to form on

the alloy. An increase in cation mobility would also favour deformation by creep during growth, so that it is not possible to exclude this as an additional mechanism for stress relief.

A similar explanation might apply in the case of aluminium-magnesium alloys for which the same increased protective oxide thickness is observed. This case is more complex since the oxide film may be two-phase, whereas in the uranium oxide - zirconium oxide system, it seems more likely that a homogenous oxide film would be formed on the uranium-zirconium alloys[74, 75] under corrosion conditions.

This work emphasises the differences which exist between the properties of thin oxide films and the massive oxide. The tensile tests illustrate the differences in mechanical properties and suggest that they may be affected by the presence of an ionic flux through the film.

It seems important in view of these differences in fundamental properties, that any attempt to explain corrosion behaviour in terms of the physical properties of the oxide film should be based on measurements made on the film, and not on the bulk material.

(c) Measurements of Electrical Conductivity.

(i) Conductivity of Oxide Films on Metal Alloys.

It may be seen by referring to the data of tables VII and VIII, that the conductivities of the oxide films produced on aluminium, uranium, and zirconium, were increased by the alloying additions shown.

It seems that these results might reasonably be explained on a similar basis to that used by Hauffe [1] to account for the conductivities of tarnish films formed on a variety of metals and alloys. For example, if the addition of magnesium to aluminium resulted in a significant number of aluminium sites in the oxide lattice being occupied by magnesium ions, the resulting charge imbalance would favour the formation of additional positive holes. The electrical conductivity of the oxide would therefore be increased.

Similar arguments may be applied in the case of the uranium rich uranium-zirconium alloys. The composition ofthe anodic oxide film on uranium is probably U_3O_8, or possibly a mixture of U_3O_8 and U_2O_5. This seems reasonable from the electron diffraction measurements made by Hart [76] and also from

thermodynamic considerations[77]. The low conductivity values obtained for these films (see table VIII) are also more in agreement with values characteristic of the higher oxides[51] than with those for oxides of the type UO_{2+x}. In order to explain the increased conductivity obtained for oxide films on the alloys, it is necessary to assume that the film on the pure metal is a p-type semiconductor, since only then would small additions of zirconium be expected to increase the oxide conductivity as observed. It is well known that oxide films on uranium can assume either n - or p - type semiconductivity depending on their oxygen - uranium ratio[78]. Oxides of the composition UO_{2+x}, U_4O_{9+x}, U_3O_{7+x}, and U_3O_{8+x} are believed to be p-type semiconductors. Replacement of six-valent uranium ions in these oxides by four-valent zirconium might be expected to increase both the number of positive holes, and the electrical conductivity.

On the other hand, it is known that zirconium oxide is an n-type semiconductor. The conductivity results observed for oxide films on the zirconium rich alloys might be explained in terms of the addition of six-valent uranium ions to the oxide lattice as a result of alloying the metal with uranium. Such an addition

would favour the formation of additional free electrons in the oxide produced on the alloys, again increasing the electronic conductivity of the film.

This interpretation of the results is complicated by the possibility of two phases existing in the oxide films formed on the alloys at room temperature. The increased conductivity of a two phase oxide film might be partly due to increased conduction at phase boundaries. Uneven distribution of the alloying element at the metal surface might also give rise to areas of oxide of different composition, and therefore different conductivity from that of the oxide formed on the surface of an alloy which consisted of a homogeneous solid solution.

Having established that the effect of alloying in the cases studied, can be to increase the electronic conductivity of the oxide film formed on the metal, it is relevant to the present study to compare these results with the observed mechanical properties of the films, represented by the ultimate tensile strain data in tables III and IV. For convenience these data are presented together in table XI below.

At first sight, the results apparently contradict the

TABLE XI

Comparison of the Electrical Conductivity, and Ultimate Tensile Strain Data for Anodic Oxide Films.

Metal Composition	Conductivity (a.c. bridge) ($ohm^{-1}.cm^{-1}$)	U.T.S. per cent Strain
Al	1.45×10^{-10}	1.50 ± 0.35
Al + 2% Mg	3.57×10^{-10}	0.89 ± 0.19
Al + 4% Mg	5.55×10^{-10}	0.87 ± 0.15
U	3.26×10^{-9}	0.82 ± 0.16
U + 5% Zr	3.32×10^{-9}	0.51 ± 0.11
U + 10% Zr	4.98×10^{-9}	-
Zr	2.08×10^{-10}	0.49 ± 0.12
Zr + 5% U	3.0×10^{-9}	0.65 ± 0.12
Zr + 10% U	6.9×10^{-9}	0.61 ± 0.12

suggestion based on previous work, that increased oxide conductivity is related to increased deformability of the film. Alloying the metal decreased the U.T.S. value for the film in the case of aluminium-magnesium and the uranium rich alloys. It is con-

sidered that the apparent increase in U.T.S. of the films with alloying in the case of the zirconium rich alloys is not significant in view of the scatter of results.

It has been shown that in the case of aluminium oxide films, the deformation before fracture is entirely elastic. Moreover, it seems likely that the mechanical properties of the films on the other metals and alloys studied was also elastic under the conditions of the "static" tensile tests. If this is assumed then it follows that the limit of deformability of these oxide films will be determined by the conditions governing brittle fracture, such as the size of flaws and inclusions, and grain size. Consequently, there is no reason to suppose that the evidence relating increased conductivity with increased plasticity is applicable to these results.

However, if plastic deformation of oxide films occurs by the diffusion of point defects during growth, as suggested in the preceding section, then the increase in electrical conductivity of an oxide film resulting from an alloying addition to the metal might be expected to indicate the improved ability of the film to deform by diffusion. This follows from the known dependence of both the rate of creep, and the electrical conductivity upon the number

of defects in an oxide.

It is not possible from the present work to exclude the possibility of a causal relationship between the electrical conductivity and plasticity of oxide films. However, it has been shown that under the conditions of the tests made on anodic films, both the deformability, and conductivity results obtained for films on alloys can be independently accounted for.

It is possible that the electronic conductivity of some oxide films might be related to their deformation by diffusion assisted creep if the availability, and movement of free electrons could affect the mobility of ions in the oxide. It seems that this concept might therefore be limited in application to semiconductors of similar properties to Ag_2S, and Cu_2S, where such a relationship is thought to exist[36].

(ii) Effect of Hydrogen on the Conductivity of Oxide Films.

The results obtained in this work confirm previous observations by Leach [79] and Fawkes [35], in which it was shown that a short period of cathodic polarisation decreased the apparent resistance of oxide films on several different metals. The data in figure 38 illustrate the change in resistance obtained for anodic films on uranium and titanium following cathodic polarisation. It seems reasonable that this resistance change might be brought about by the inward diffusion and ionisation of some of the hydrogen which is evolved at the oxide surface during cathodic polarisation. However, it is not possible to determine whether the apparent change in resistance in this type of experiment is due to a change in the bulk resistance of the film, or a change in the properties of the metal-oxide, or oxide-liquid interfaces. This problem was resolved by making conductivity measurements by a four terminal method on single crystals of rutile, which had been subjected to electrolytic treatment.

(iii) Effect of Hydrogen on the Conductivity of Single Crystals of Rutile.

Although the preliminary experiments made on rutile crystals (figure 39) showed that their resistance could be decreased by several orders of magnitude following hydrogen evolution at the oxide surface, it was not possible to determine whether the effects observed were the result of chemical reduction of a thin surface layer of oxide, or a change in the bulk resistance of the crystal. This was because the geometrical arrangement of contacts used in the preliminary experiments (see figure 8(a)) exaggerated the contribution made to the apparent resistance of the crystal by changes in the surface resistance.

However, the improved technique used in subsequent experiments enables a clearer interpretation of the measurements to be made. The profiles in figures 40 and 41, show that the bulk of the crystals has undergone a fairly uniform increase in conductivity after cathodic treatment, while a surface layer of approximately a micron in thickness has undergone a much greater increase in conductivity than the bulk in each case. This latter

fact suggests fairly strong reduction of the surface by atomic hydrogen produced during the electrolysis.

Some support for this comes from the fact that in specimen A, which had been cathodically polarised for 14,000 minutes, a blue colouration was apparent which disappeared when the exposed surface was ground off. More direct evidence for a disordered layer with properties significantly different from the bulk has been obtained by means of grazing incidence electron diffraction.

This was carried out by Professor Blackman and Dr. Lisgarten of the Physics Department, Imperial College, on the exposed and unexposed faces of a specimen cathodically treated for 960 minutes. The expected spot pattern was observed from the unexposed face, while no such pattern could be discerned from the cathodically exposed face. This is consistent with the presence of a heavily reduced, disordered, surface layer at least 10 Å thick. An upper limit to the thickness of the layer can be set from figure 41 at approximately one micron. Using these limits, and the data of figures 40 and 41, limits for the conductivity of the surface layer have been calculated for different exposure times. These are shown together with the bulk conductivities in Table X.

TABLE X.

Sample	Time of Cathodic Exposure Minutes	Bulk Conductivity before Cathodic Treatment $Ohm^{-1}.cm^{-1} \times 10^5$	Increase in Bulk Conductivity after Cathodic Treatment $Ohm^{-1}.cm^{-1} \times 10^5$	Limits to Surface Conductivity $Ohm^{-1}.cm^{-1}$ Upper	Lower
B	10	1.3	0	25	.025
"	90	1.3	0.5	23	.023
"	830	1.8	6.5	124	.124
"	2820	8.3	4.7	240	.240
C	3840	2.4	10.6	1400	1.4
"	5280	13	32	1700	1.7

The increase in bulk conductivity shown in figures 40 and 41 is surprisingly uniform, particularly for the shorter times of polarisation. This implies that the electrically active centres diffuse rapidly in the bulk of the samples at room temperature. For this reason it is difficult to believe that they could be oxygen vacancies or interstitial titanium atoms produced by surface reduction. It

seems far more likely that some of the hydrogen atoms which are produced at the electrolyte - rutile interface during the evolution process, enter the rutile lattice, ionise, and diffuse into the interstitial channels under the combined influence of the concentration gradient and the applied electric field. The resulting increase in bulk conductivity may be seen from Table X to be roughly proportional to the time of electrolysis, which supports the model of hydrogen at a constant activity diffusing into the crystal across an essentially constant activity gradient. Diffusion probably plays a dominant role since it is difficult to see how the electric field alone could produce a uniform distribution increasing in density with time.

A rough estimate of the diffusion coefficient, D at room temperature was made from the data of figure 41 by putting $x^2/_{Dt}$ equal to one, where x is the thickness of the crystal, and t the time to reach uniformity. Taking t as 100 minutes, and x as 3×10^{-2} cm., a value for D was obtained of the order 10^{-7} $cm^2.sec^{-1}$.

No significant change in the rate of increase of bulk conductivity was observed on increasing the cathodic current

density from 0.1 mA/cm^2 to 1.0 mA/cm^2. This observation together with the data of figures 40 and 41 indicates that the rate determining step in the increase of bulk conductivity is the initial entry of hydrogen through the surface. This might be expected with a heavily reduced surface layer, particularly if the reduction gives rise to interstitial titanium atoms. In this connection, the surface conductivity limits shown in Table X are consistent with the room temperature conductivity of heavily reduced rutile which is known to be of the order of 1 - 10 $ohm^{-1}.cm^{-1}$.

It is implicit in the foregoing discussion that hydrogen in rutile is ionised at room temperature. This is supported by the data in figure 42, in which it may be seen that the resistance of samples A and E decreased by a factor of two between room temperature and 77°K. A theoretical estimate of the donor ionisation energy [80] gives a value of .02 e V which would also imply complete ionisation at room temperature.

Evidence of the mobility of the donor centres may be obtained by comparing the resistance-temperature profiles of specimens F and A in the region 0-200°C. The resistivity of specimen F which had been vacuum reduced only, falls sharply

in this region indicating the ionisation of those centres produced by vacuum reduction. In the same region, for specimen A, which had been cathodically treated in addition to the preliminary vacuum reduction, this ionisation is masked by a simultaneous rise in resistance which is consistent with the behaviour expected if hydrogen were diffusing out of the crystal.

The infra-red experiments demonstrated the existence of hydrogen in the rutile specimens both before and after the cathodic treatment. It is possible that the amount of hydrogen already present in the crystal as a result of the flame fusion growth process was large compared with the amount introduced by the cathodic treatment, but was present in a different less readily ionisable form. Previous measurements on the optical properties of rutile [52, 53] show clearly that at temperatures near 800°C, hydrogen can enter the lattice to form strong O-H bonds. Soffer [53] estimated that the concentration of O-H groups can be as high as 10^{17} cm.$^{-3}$ in some crystals. The presence of these O-H bonds is not directly related to electronic conduction, since the O-H absorption is observed in well oxidised and relatively insulating crystals. An approximate calculation of the relative

amounts of grown-in, and cathodically induced hydrogen was made for specimen E, which was the first specimen used for the infra red study. From the height of the O-H absorption peak at 3300 $cm.^{-1}$, it can be inferred that the amount of grown-in hydrogen present in the vacuum reduced state was within an order of magnitude of that calculated by Soffer. Assuming that the ratio of cathodically induced hydrogen atoms to electrons was approximately 1 : 1, the number of hydrogen atoms added by the cathodic treatment may be calculated from the change in conductivity of the rutile specimen. Taking Frederickse's data [81] for the electronic mobility of slightly reduced rutile at room temperature (0.1 - 1.0 $cm.^2$ $volt^{-1}$. $sec.^{-1}$) this number may be shown to be between 5×10^{14} and 5×10^{15} hydrogen atoms per $cm.^3$, clearly much less than the amount of hydrogen already present in the rutile specimens before the cathodic treatment.

VI. SUMMARY AND CONCLUSIONS

(a) Measurements have been made of the stresses which exist in anodic oxide films formed on a number of different metals. The results may be summarised as follows:

(1) The stresses in porous anodic oxide films formed on aluminium in sulphuric acid solution were initially tensile, but changed to compressive as the film thickened.

(2) The stresses in non-porous barrier-type films formed by anodising aluminium in ammonium borate, and ammonium citrate solutions, were tensile when formed at high current density, and compressive at low current density.

(3) Stresses in barrier-type films on zirconium were initially tensile but changed to compressive as the film thickened. No marked dependence was observed of the stress upon the current density of formation.

(4) Stresses in barrier-type films on titanium were found to be compressive under the conditions studied. Extensive breakdown of the film, probably of a mechanical nature, was observed to occur at regular intervals during growth.

(b) Tensile tests were successfully made on thin barrier type anodic oxide films on a number of metals and alloys, by methods which involved measurements both on oxide-covered metals, and separated oxide films. The following results were obtained:

(1) It was shown that films on aluminium were stronger than bulk alumina, and could tolerate a substantially greater amount of strain before failure than could the massive oxide. The deformation was elastic.

(2) Measurements made on oxide-covered metal specimens of zirconium, uranium, and uranium-zirconium, and aluminium-magnesium alloys, demonstrated that the films on these metals can also tolerate much greater strain than the corresponding oxides in bulk.

(3) It was shown in the experiments made on thin anodised aluminium wires that the influence of the oxide film which restricts extension of the wire under an applied load was apparently removed when a sufficiently large anodic current was caused to flow through the film. It is possible that the oxide film deforms plastically by creep under these conditions.

(4) Comparison of the results of the tensile tests on anodic oxide films on metal alloys with the properties of the films on the

pure metals shows that the alloying additions either reduce, or cause little change in the strain which may be tolerated by the oxide films before failure occurs. This is consistent with the behaviour expected if the deformation of the films under the test conditions were elastic, followed by brittle fracture.

(c) The results obtained for the electrical conductivity measurements were as follows:

(1) The electrical conductivity of the oxide films on aluminium, uranium, and zirconium was increased by alloying additions of magnesium, zirconium, and uranium respectively.

(2) The electrical conductivity of anodic oxide films was increased following electrolytic evolution of hydrogen from the oxide surface.

(3) It was shown that hydrogen may be electrolytically introduced into single crystals of rutile, that it diffuses rapidly in the bulk of the material, and increases the oxide conductivity by behaving as a fully ionised donor at room temperature.

Conclusions:

(1) From the results of the stress measurements made on anodic oxide films on aluminium and other metals, it is clear that the volume ratio concept, which has been used in the past to explain the origin of stresses in oxide films, is inadequate alone as a means of accounting for the magnitude, and in some cases the sign of the stresses developed. The results may be explained if it is assumed that the stress produced in an oxide film is a function both of the volume ratio, and the relative magnitude of the anionic and cationic currents which flow through the film during growth. It is reasonable to suppose that a near balance between the two currents might be favourable from free energy considerations, in order to maintain the stress in the film within tolerable limits, as has been observed in these anodic films. In the case of oxide film growth which occurs by the movement of both ionic species through the film, plastic deformation may be a possible means of stress relief. The observations made on thin anodised wires suggest that diffusion assisted creep may be a possible mechanism of deformation in this case.

(2) This work emphasises the differences which exist

between the mechanical properties of thin oxide films and those of the bulk oxide. It is clear from the results of the tensile tests made on oxide covered metals and on separated films, that the deformability of anodic oxide films at room temperature, and at relatively high rates of deformation is considerably greater than that of the corresponding oxide in bulk. This deformation has been shown to be entirely elastic in the case of aluminium oxide films, and it seems likely that the other films studied also have little ductility under these conditions. However, it seems likely that an oxide film may have completely different mechanical properties during growth, when an appreciable ionic diffusion flux exists in the film, from those determined in a tensile test. If the rate of deformation is large compared with that which might be expected from ionic diffusion in the film, brittle behaviour will be observed. On the other hand, if the rate of deformation is relatively low, the film might be expected to behave plastically. Tests carried out under conditions where the rate of deformation is related to the ionic diffusion in the film seem to be essential in any further investigation of the role of the mechanical properties of oxide films in determining the corrosion behaviour of metals and alloys.

(3) From the electrical measurements made on oxide films, it is clear that hydrogen electrolytically produced at the oxide surface can increase the electrical conductivity of the films. From the experiments on rutile it seems likely that this change is due to the ability of hydrogen to act as a mobile donor in the oxide lattice. Hydrogen produced during aqueous corrosion might also be expected to increase the electrical conductivity of a protective oxide film. However, no evidence was found to support the suggestion that a change in electrical conductivity can affect the mechanical properties of oxide films, although in some cases, the increased conductivity of films on metal alloys might indirectly indicate an improved ability of the oxide to deform plastically by a diffusional mechanism during growth.

VII. PROPOSALS FOR FURTHER WORK

There is a great deal of scope for further work to be done in this field in order to increase the understanding of the role of the mechanical properties of oxide films and the stresses in them, in aqueous corrosion.

(i) Further measurements of stress are desirable since there are still very little data available on the magnitude or sign of the stresses which exist in growing oxide films. In view of the important influence which the nature of the diffusing species has upon stress, it is felt that further stress measurements should be supplemented by experiments in which the relative rates of diffusion could be determined.

(ii) It would also be of interest to determine the effects of epitaxy, and surface roughness upon the stresses in oxide films. Such a study might be possible by means of Campbell's technique[23] of stress measurement applied to electropolished single crystal metal specimens.

(iii) The possibility of plastic deformation of oxide films during growth deserves further study. Experiments similar in

kind to those done on thin anodised wires seem suitable, provided that information is available concerning the nature of the diffusing species under the conditions of the experiments made.

(iv) It is considered that further measurements of the mechanical properties of oxide films should be confined to the type of experiment where the rate of deformation can be controlled so that possible deformation of the film due to the ionic diffusion flux through it is taken into consideration. Tests made at very slow rates of strain during aqueous corrosion might be an alternative approach to the experiments on anodised wires.

(v) It is felt that in order to resolve the problem of a possible relationship between electronic conductivity, and plastic deformation, of oxide films, a more fundamental approach is required than the one attempted in this work. Although it is necessary to make measurements directly on films in order to correlate the results directly with corrosion behaviour, it is considered that this problem would be more readily resolved by means of a series of experiments on single crystals and polycrystalline oxide specimens. Perhaps similar experiments to those of Williams,[26] and Armstrong[72] would enable the separate effects upon the conductivity of variables such as grain size and defect structure to be determined.

VIII. BIBLIOGRAPHY

1. K. Hauffe, Progress in Metal Physics 4, 71 (1961).
2. J.S.L. Leach, International Conference on Properties of Reactor Materials and the Effects of Radiation Damage, C.E.G.B. Nuclear Laboratories, Berkeley. Butterworths, London, (1962).
3. N.B. Pilling, and R.E. Bedworth, J. Inst. Metals, 29, 529 (1923).
4. S.J. Gregg, and W.B. Jepson, J. Inst. Metals, 87, 187 (1958-9).
5. U.R. Evans, Inst. Metals Symposium on Internal Stresses in Metals and Alloys, London (1947) p. 291.
6. P.D. Dankov, and P.V. Churaev, C.R. Acad. Sci. U.R.S.S. 73, 1221 (1950).
7. A.E. Jenkins, J. Inst. Metals, 82, 213 (1952).
8. A.T. Gwathmey, and K.R. Lawless, "The Surface Chemistry of Metals and Semi-Conductors", Symposium, Electrochem. Soc. John Wiley and Son, New York (1959) p. 483.
9. P.D. Dankov, C.R. Acad. Sci. U.R.S.S. 51, 453 (1946).

10. N.D. Lisgarten, Phil. Mag. 3, 1306 (1958).

11. F.C. Frank, and J.H. van der Merwe, Proc. Roy. Soc. A198, 205 (1949): A200, 125 (1950): A201, 261 (1950).

12. R.D. Misch, and E.S. Fischer, Acta Metallurgia 4, 222 (1956).

13. N.J.M. Wilkins, J. Electrochem. Soc. 109, 998 (1962).

14. L. Young, "Anodic Oxide Films" Academic Press, New York (1961) pp. 70-72.

15. B. Verkerk, P. Winkel, and D.G. de Groot, Phillips. Res. Repts. 13, 506 (1958).

16. G. Amsel, and D. Samuel, J. Phys. Chem. Solids, 23, 1707 (1962).

17. P.H.G. Draper, Acta. Met. 11 (1963) (in press).

18. R.F. Tylecote, J. Iron and Steel Inst. 196, 445 (1960).

19. J.A. Davies, J.P.S. Pringle, R.L. Graham, and F. Brown, J. Electrochem. Soc. 109, 999 (1962).

20. R.A.F. Hammond, Trans. Inst. Met. Finishing, 30, 140 (1954).

21. S. Reather, Z. Ang. Phys. 11, 456 (1959).

22. W.N. Bradshaw, and S. Clarke, J. Electrodep. Tech. Soc.

(continued over)

24, 147 (1949).

23. D.F. Campbell, and H. Blackburn, Phil. Mag. (1963) (in press).

24. E. Ryshkewitch, "Oxide Ceramics" Academic Press, London, (1960) p. 125.

25. K.H. Ashbee, and R.E. Smallman, Brit. Ceram. Soc. Conf. on Mechanical Properties of Non-Metallic Crystals, and Polycrystals, Hastings (1962).

26. R. Scott, A.R. Hall, and J. Williams, J. Nuclear Materials 1, 39 (1959).

27. W.H.J. Vernon, F. Wormwell, and T.J. Nurse, J. Chem. Soc. (1939) p. 621.

28. C. Schusterius, "Landolt - Börnstein Tabellen" 6th Ed. 4, 421 (1955).

29. J.W. Beames, W.E. Walker, and H.S. Morton, Phys. Rev. 87, 524 (1952).

30. A.A. Griffith, Phil. Trans. Roy. Soc. A221, 163 (1920).

31. W.D. Kingery, "Introduction to Ceramics" John Wiley & Son, New York, (1960), pp. 622-624.

32. R.K. Hart, and W.E. Ruther, J. Nuclear Materials, 4,

(continued over)

272 (1961).

33. J.S.L. Leach, and A.Y. Nehru, Int. Atomic Energy Agency Conf. on the Corrosion of Reactor Materials, Salzburg, 1, 59 (1962).

34. M.J. Pryor, and D.L. Keir, J. Electrochem. Soc. 102, 370 (1955).

35. G.D. Fawkes, M.Sc. Thesis, University of London, (1962).

36. C. Wagner, J. Chem. Phys. 21, 1819 (1953).

37. J.D. Eshelby, C.W.A. Newey, P.L. Pratt and A.B. Lidiard, Phil. Mag. 3, 75 (1958).

38. J.H. Westbrook, and J.J. Gilman, J. Appl. Phys. 33, 2360 (1962).

39. H.W.L. Phillips, "Properties of Metallic Surfaces", Inst. Metals Monograph No. 13, (1953) p. 240.

40. A.E. Stebbens, and L.L. Shreir, J. Electrochem. Soc. 108, 30 (1961).

41. A. Brenner, and S. Senderoff, J. Res. Nat. Bur. Standards 42, 89 (1949).

42. D.A. Vermilyea, J. Electrochem. Soc. 110, 345 (1963).

43. M.S. Hunter, and P. Fowle, J. Electrochem. Soc., 101, 481 (1954).

44. W.J. Bernhard, J. Electrochem. Soc. 109, 1082 (1962).

45. J.N. Wanklyn, and D.R. Sylvester, J. Electrochem. Soc. 105, 647 (1958).

46. E. Ryshkewitch, "Oxide Ceramics" Academic Press, London (1960) p. 380.

47. H.S. Isaacs, Ph. D. Thesis, University of London (1963).

48. J.A. Dalziel, and D. Kealey, Chem. and Ind. (1962) p. 302.

49. M.J. Pryor, and J.J. McMullen, 1st. Int. Cong. Metallic Corrosion, London (1961) p. 52.

50. R.D. Misch, U.S.A.E.C. Report, ANL-6259 (1961).

51. E. Rabinowitz and J.J. Katz, "The Chemistry of Uranium" Dover Publications, New York, (1951) pp. 250-280.

52. A. von Hippel, J. Kalnajs, and W.B. Westphal. J.Phys. Chem. Solids, 23, 779 (1962).

53. B.H. Soffer, J. Chem. Phys. 35, 940 (1961).

54. D.A. Vermilyea, Acta Metallurgia 5, 402 (1957).

55. U.R. Evans, "The Corrosion and Oxidation of Metals"

Arnold Ltd., London (1960) p. 855.

56. D.J. Livey, and P. Murray, Plansee Proc. (1955) pp. 375-404.

57. D.H. Bradhurst, and J.S.L. Leach, Trans. Brit. Ceram. Soc. (in press).

58. J.A. Davies, Private Communication (1962).

59. O. Flint, and J.H.O. Varley, Nature 179, 145 (1957).

60. E.C. Potter and G.M.W. Mann, 1st. Nat. Cong. Metallic Corrosion, Butterworths, London (1961) p. 417.

61. U.R. Evans, Private Communication, April (1963).

62. J.T. Waber, Conference on the Aqueous Corrosion of Reactor Materials, Brussels (1959).

63. D.R. Holmes, Private Communication, (1962).

64. C. Edeleanu and T.J. Law, Phil. Mag. 7, 573 (1962).

65. H.G. Wilsdorf, Nature 168, 600 (1951).

66. C.S. Barrett, P.M. Aziz, and I. Markson, J. Metals, 5, 1655 (1953).

67. D.B. Holt, Acta Metallurgia 11, 1021 (1962).

68. I.R. Kramer, and L.J. Demer, Trans. Amer. Inst. Min.

(Metall.) Engnrs. 221, 780 (1961).

69. M.L. Kronberg, J. Am. Ceram. Soc. 40, 561 (1960).

70. D. Hayes, D.W. Budworth, and J.P. Roberts, Trans. Brit. Ceram. Soc. 60, 494 (1961).

71. F.R.N. Nabarro, Phys. Soc. Conf. on Strength of Solids, London (1948) p. 75.

72. W.M. Armstrong, W.R. Irvine, and R.H. Martinson, J. Nuclear Materials 7, 133 (1962).

73. P. McNamara, Private Communication (1962).

74. E.M. Levin, H.F. McMurdie, and F.P. Hall, "Phase Diagrams for Ceramicists" Amer. Ceram. Soc. (1956) p. 71.

75. J.E. Antill, and K.A. Peakall, J. Less-Common Metals, 3, 239 (1961).

76. R.K. Hart, Trans. Farad. Soc. 49, 299 (1953).

77. J. Schmets, and M. Pourbaix, 6th Meeting C.I.T.C.E. Butterworth (1955) p. 167.

78. R.K. Willardson, J.W. Moody and H.L. Goering, J. Inorg. Nucl. Chem. 6, 19 (1958).

79. J.S.L. Leach, J. Inst. Metals, 88, 24 (1959).

80. D.H. Bradhurst and P.F. Chester, Central Electricity Generating Board Research Laboratory Note, Leatherhead, (1962).

81. H.P.R. Frederickse, J. Appl. Phys. 32, 2211 (1961).

IX. ACKNOWLEDGEMENTS

The assistance and encouragement provided by Dr. J.S.L. Leach throughout this work is gratefully acknowledged. The author is also indebted to Professor J.G. Ball, for the provision of a Research Assistantship in the Metallurgy Department, Imperial College where this work was done, and to Dr. P.F. Chester, of the Central Electricity Generating Board, for arranging for laboratory facilities at C.E.R.L., Leatherhead for the experiments on rutile single crystals. Financial support was provided by the Central Electricity Generating Board. The author is also thankful for assistance from his wife, Margaret, with the typing and final preparation of the manuscript.

X. DIAGRAMS

Figure 42. Resistivity vs. temperature profiles for rutile single crystals before and after cathodic treatment.

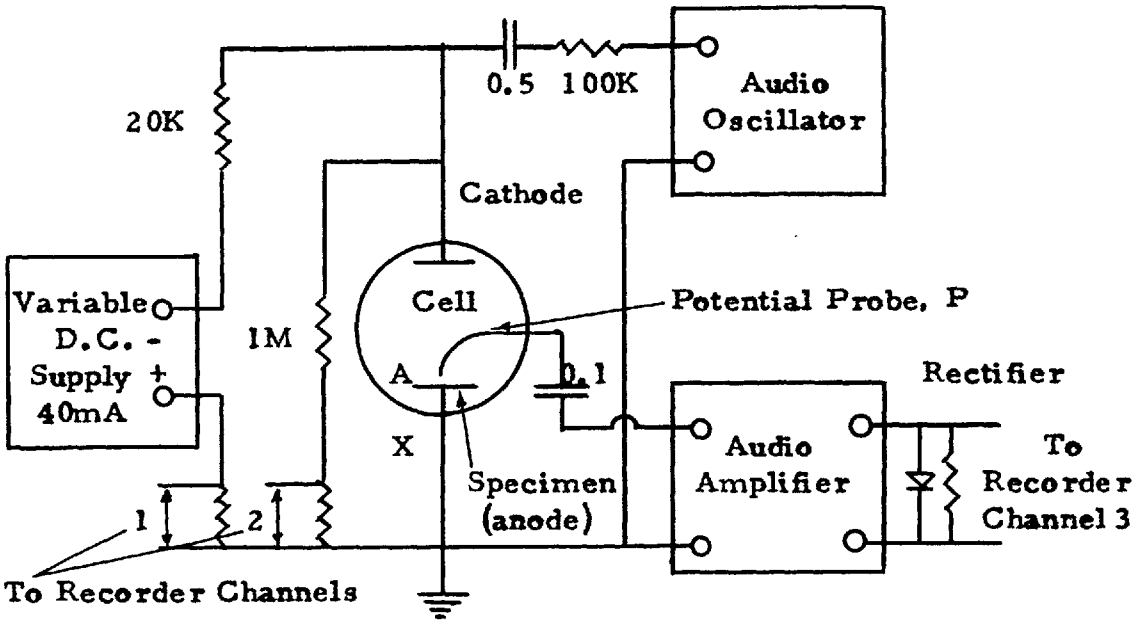

FIGURE 1. CIRCUIT DIAGRAM FOR ANODISING APPARATUS.

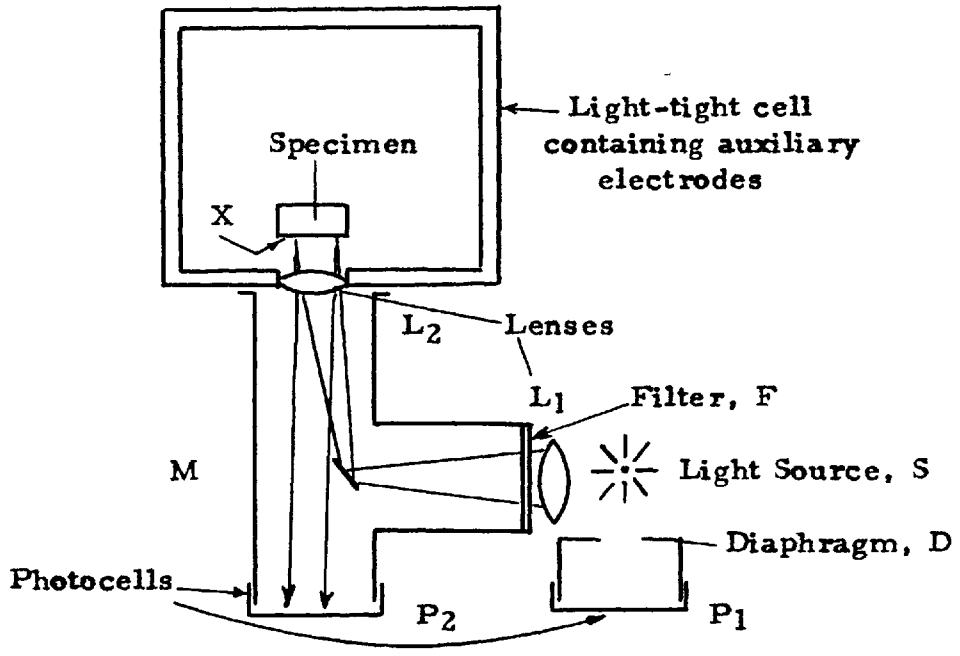

FIGURE 2. APPARATUS FOR THE MEASUREMENT OF THE OPTICAL THICKNESS OF OXIDE FILMS.

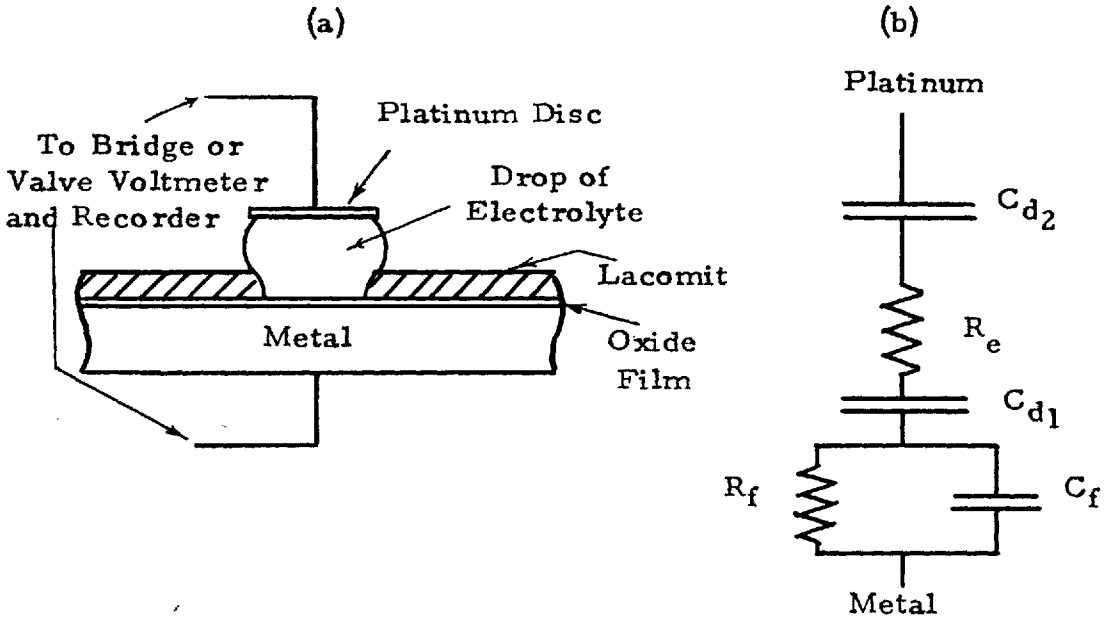

FIGURE 3 (a) CELL FOR MEASUREMENT OF RESISTANCE CAPACITANCE & POTENTIAL OF OXIDE FILMS.
(b) EQUIVALENT CIRCUIT OF CELL.

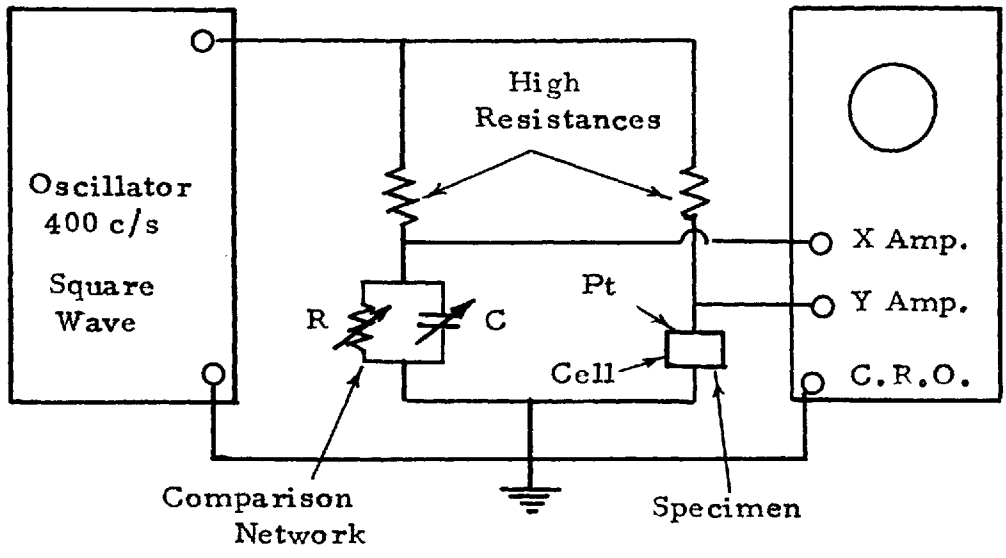

FIGURE 4. SCHEMATIC DIAGRAM OF BRIDGE CIRCUIT.

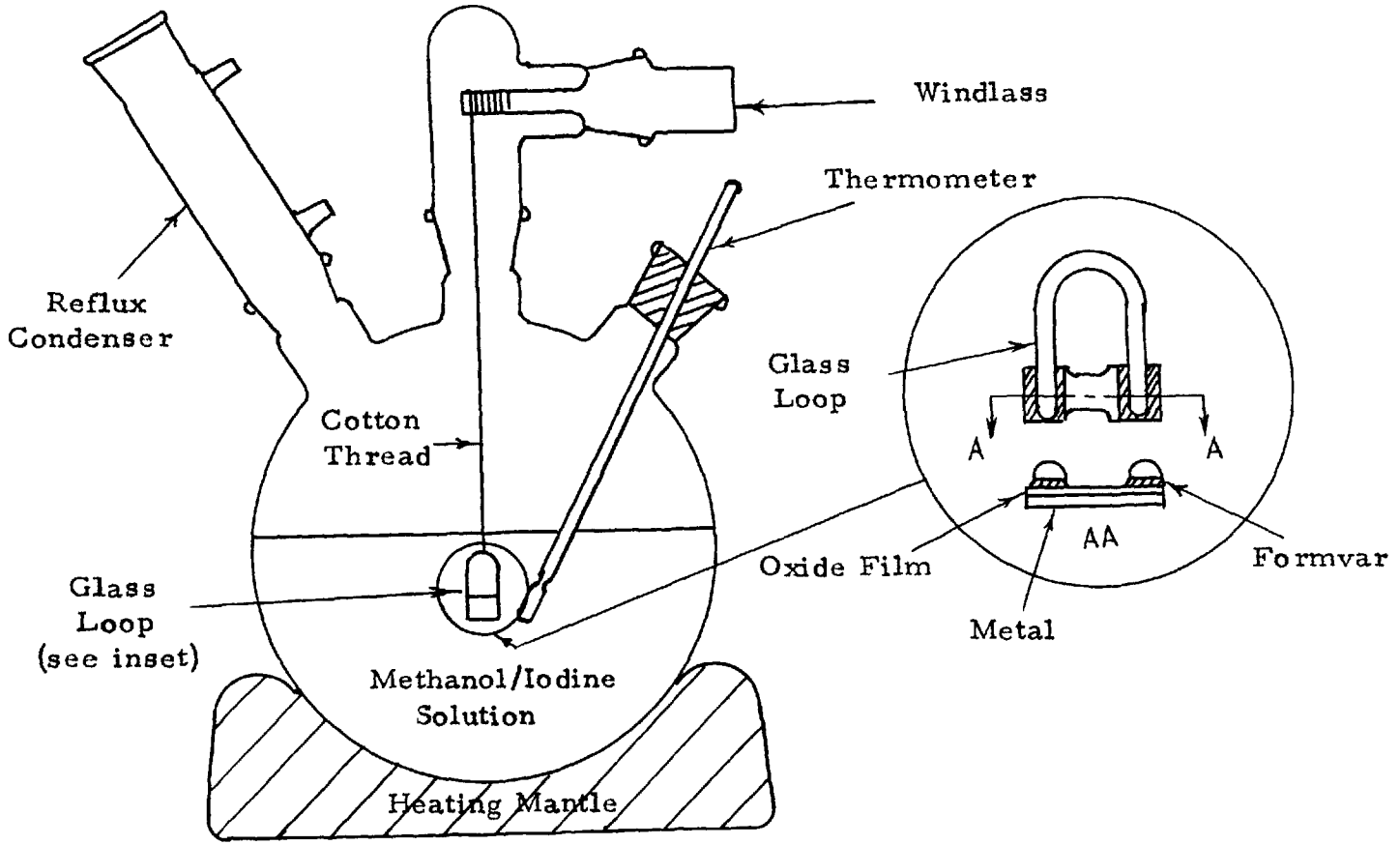

FIGURE 5. APPARATUS FOR CHEMICAL SEPARATION OF OXIDE FILMS FOR TENSILE TESTS.

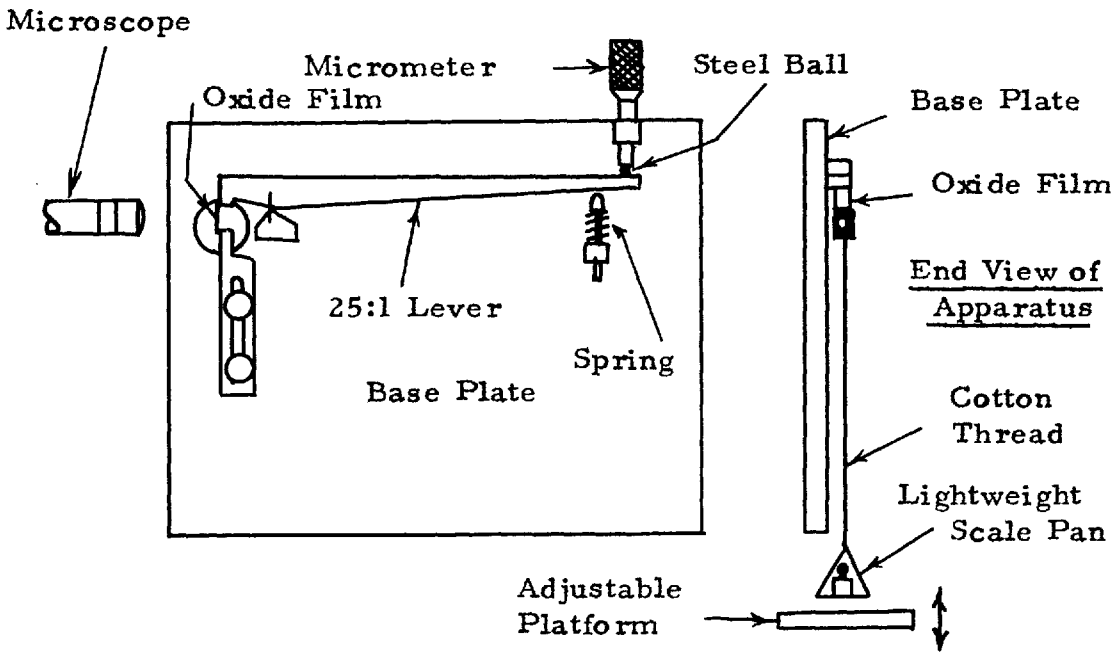

FIGURE 6. APPARATUS FOR MEASURING THE STRESS-STRAIN BEHAVIOUR OF SEPARATED OXIDE FILMS.

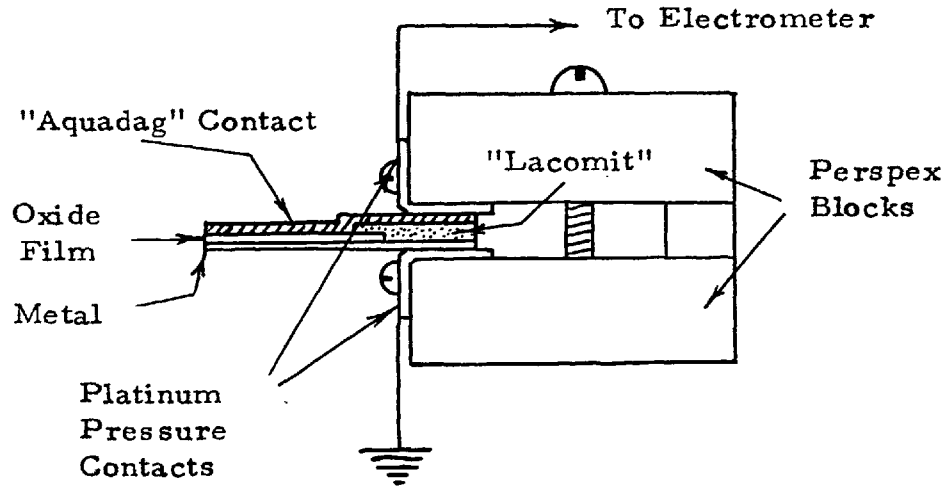

FIGURE 7. APPARATUS FOR MEASUREMENT OF THE ELECTRICAL RESISTANCE OF OXIDE FILMS USING THE DRY CONTACT METHOD.

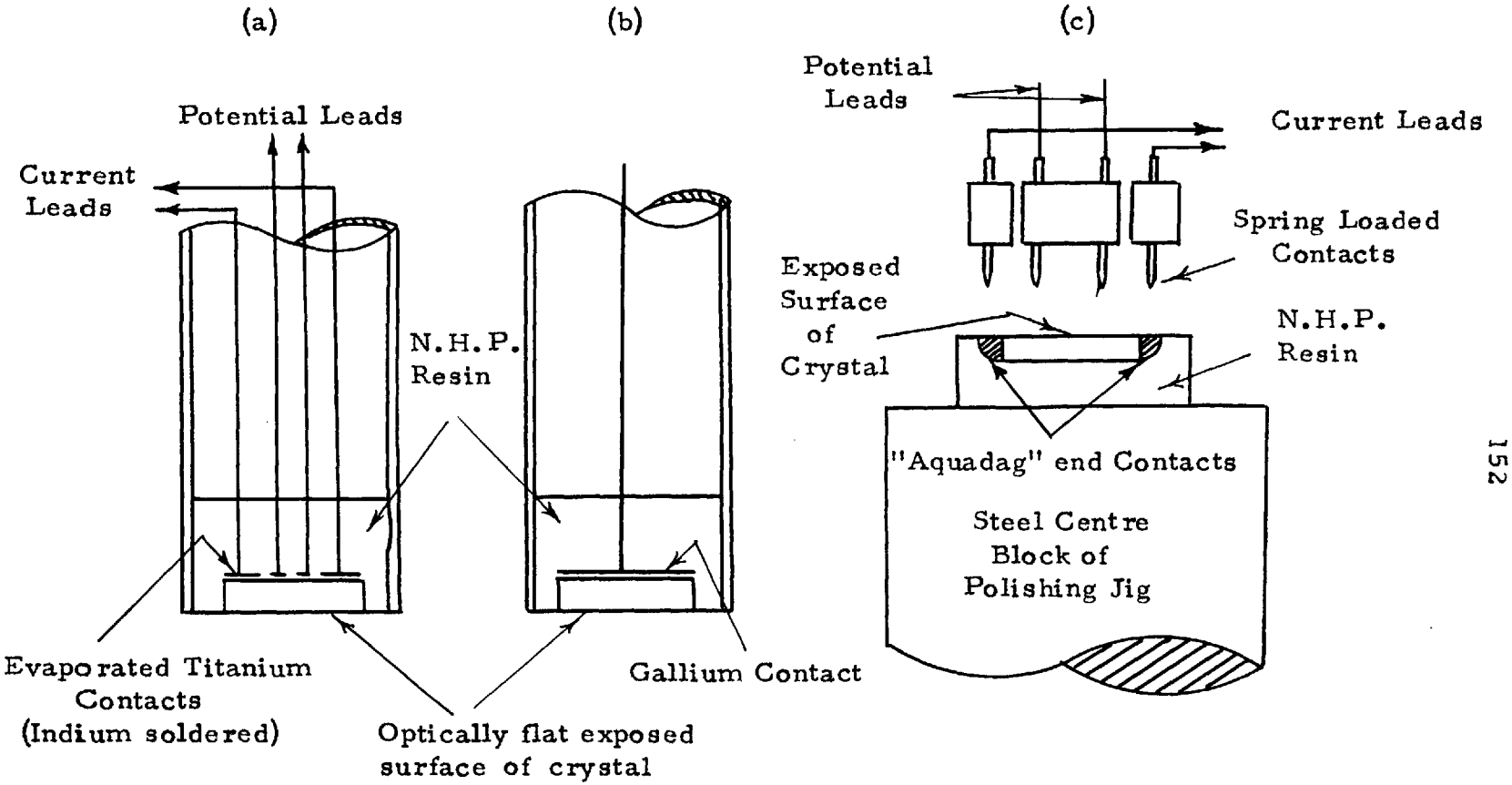

FIGURE 8. METHODS OF MOUNTING RUTILE SINGLE CRYSTAL SPECIMENS FOR ELECTROLYTIC TREATMENT AND CONDUCTIVITY MEASUREMENTS.

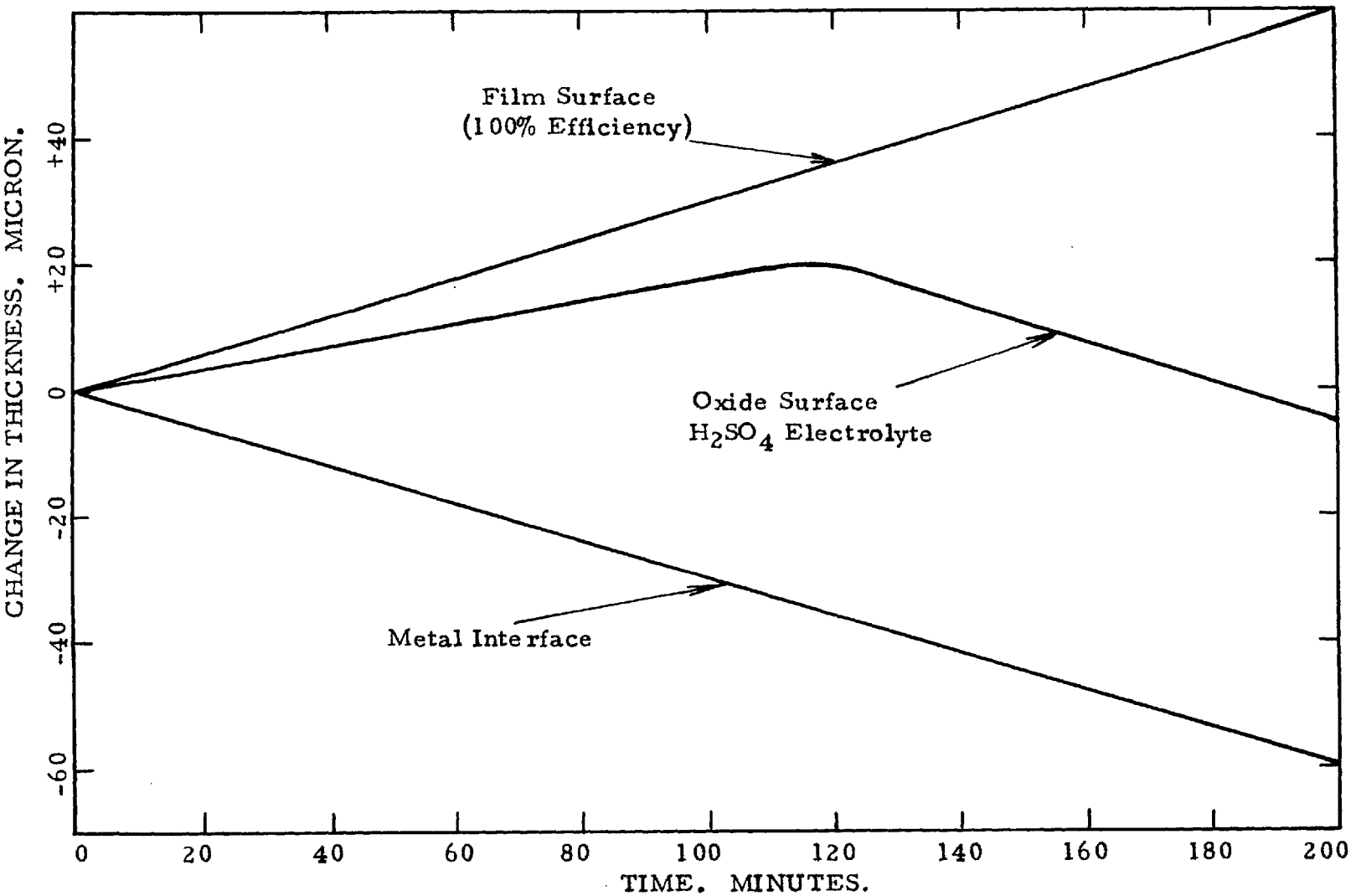

FIGURE 9. RATE OF GROWTH OF ANODIC FILMS IN SULPHURIC ACID SOLUTION (AFTER PHILLIPS [39]).

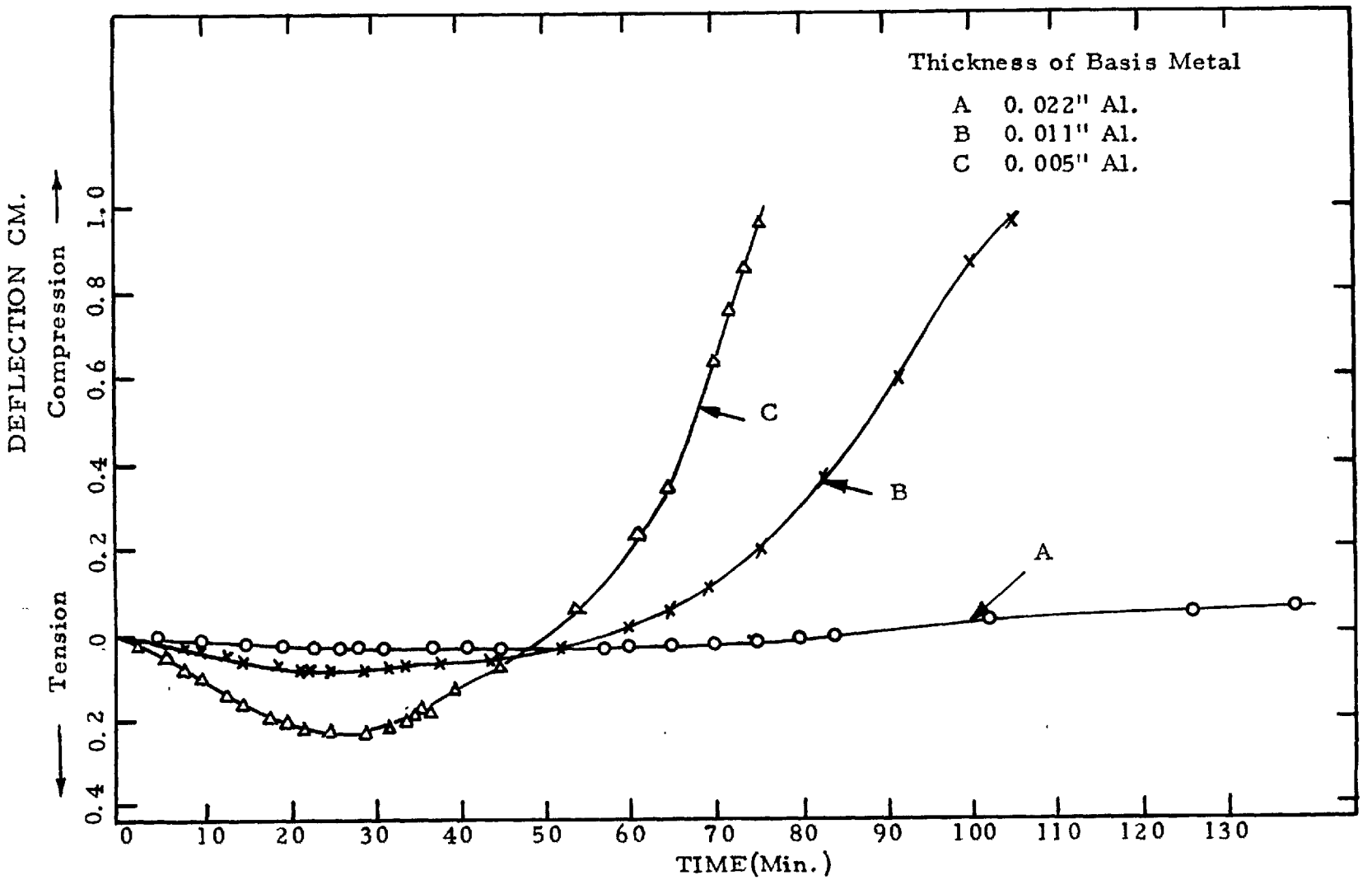

FIGURE 10. DEFLECTION OF ALUMINIUM FOIL DUE TO ANODISED FILMS GROWN ON ONE SIDE ONLY (IN H_2SO_4 SOLUTION).

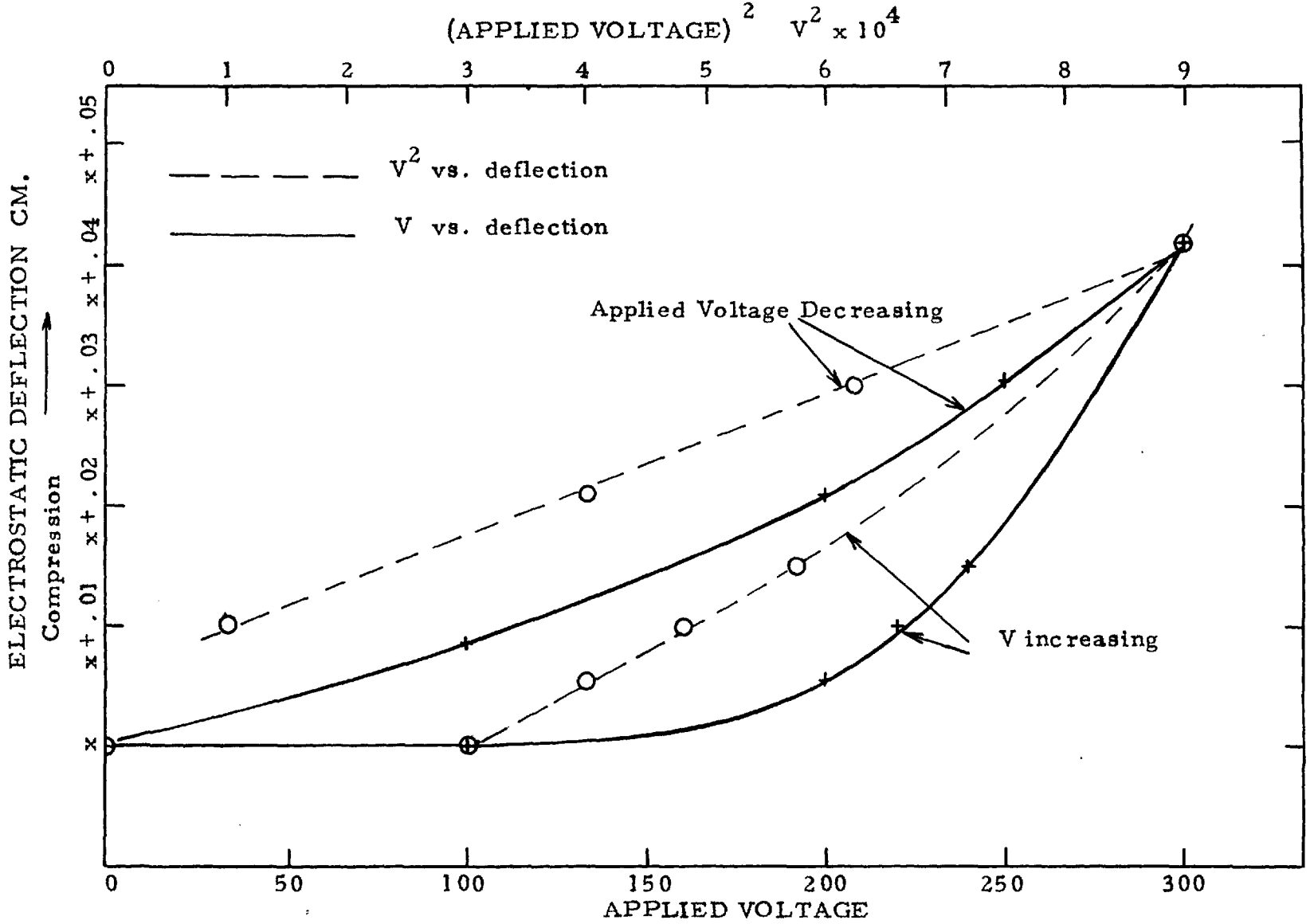

FIGURE 11. "ELECTROSTATIC" DEFLECTION OF AN ANODISED ALUMINIUM STRIP.

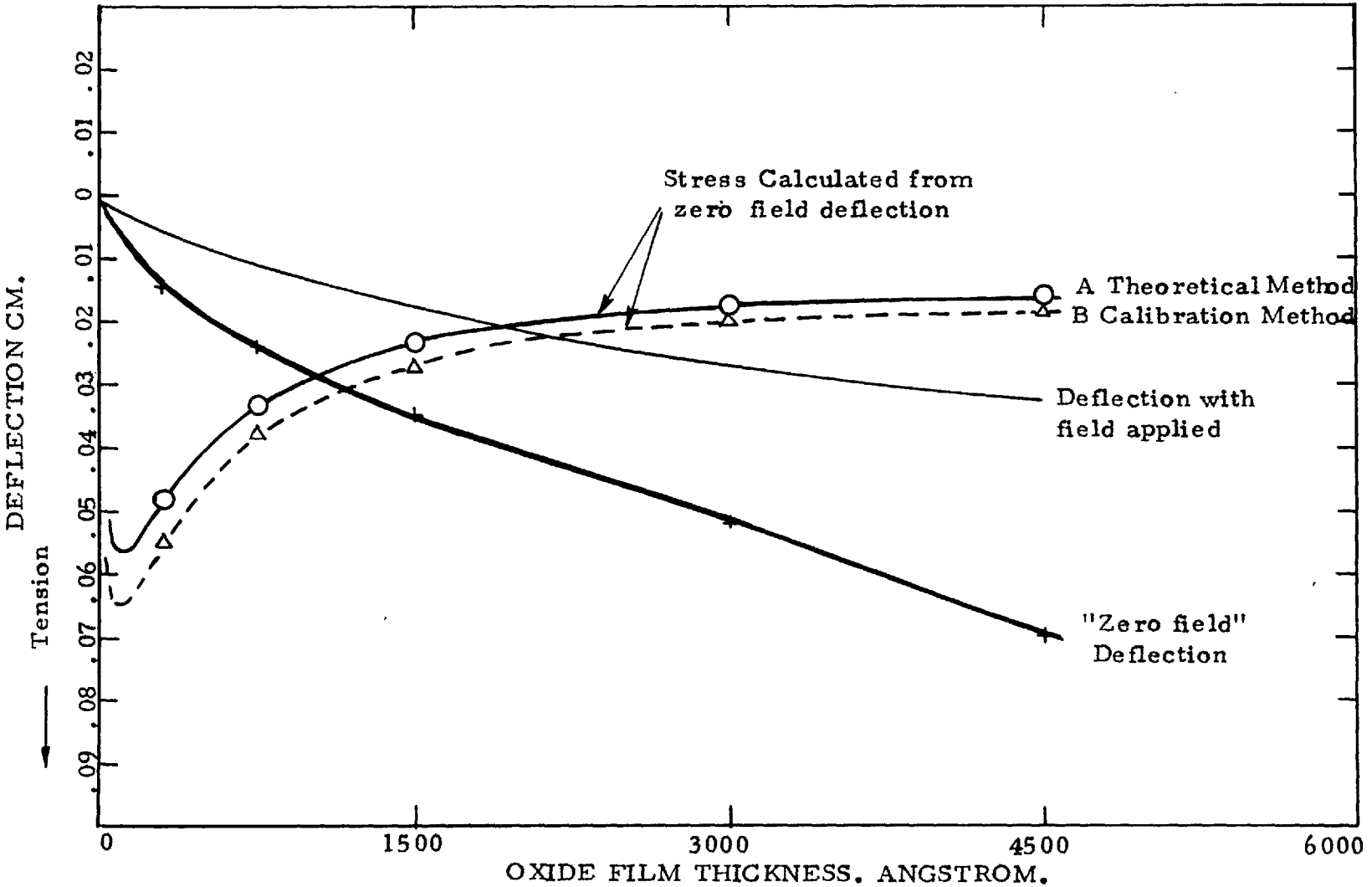

FIGURE 12. CALCULATED STRESS IN AN ANODIC FILM ON ALUMINIUM.

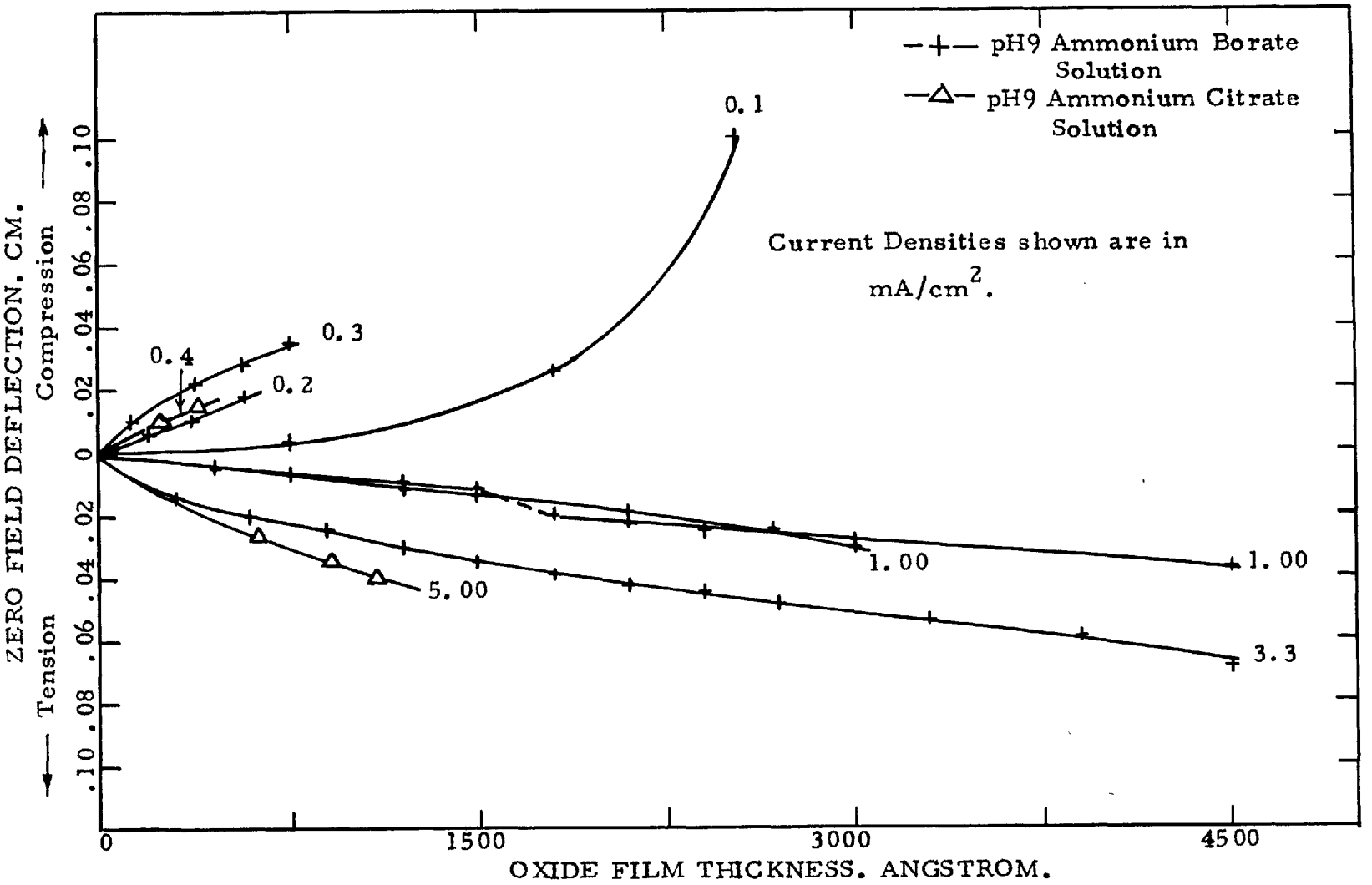

FIGURE 13. DEFLECTION OF ALUMINIUM FOIL ANODISED ON ONE SIDE AT DIFFERENT CURRENT DENSITIES.

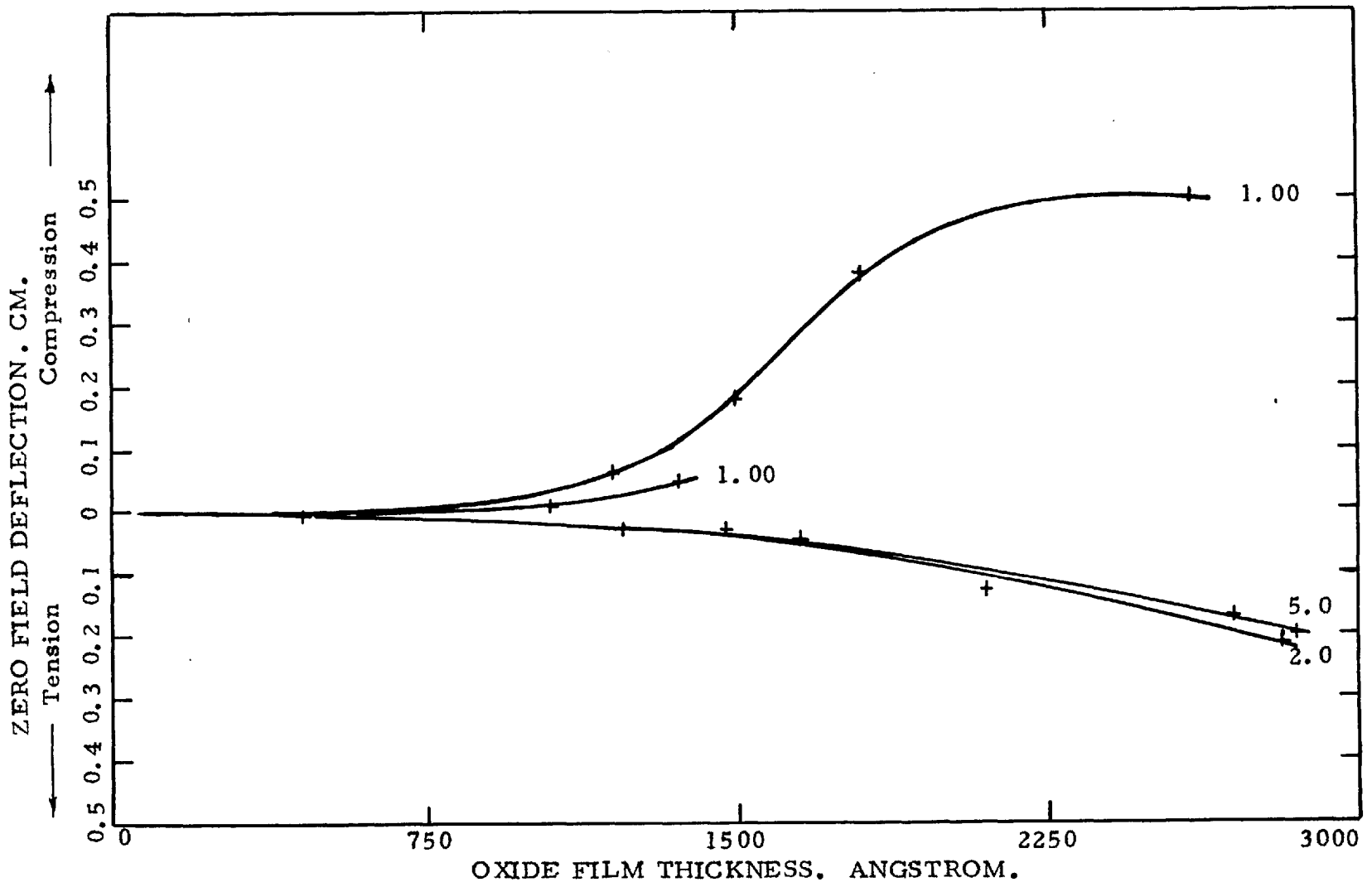

FIGURE 14. DEFLECTION OF ALUMINIUM FOIL ANODISED ON ONE SIDE (IN pH6 AMMONIUM CITRATE SOLUTION).

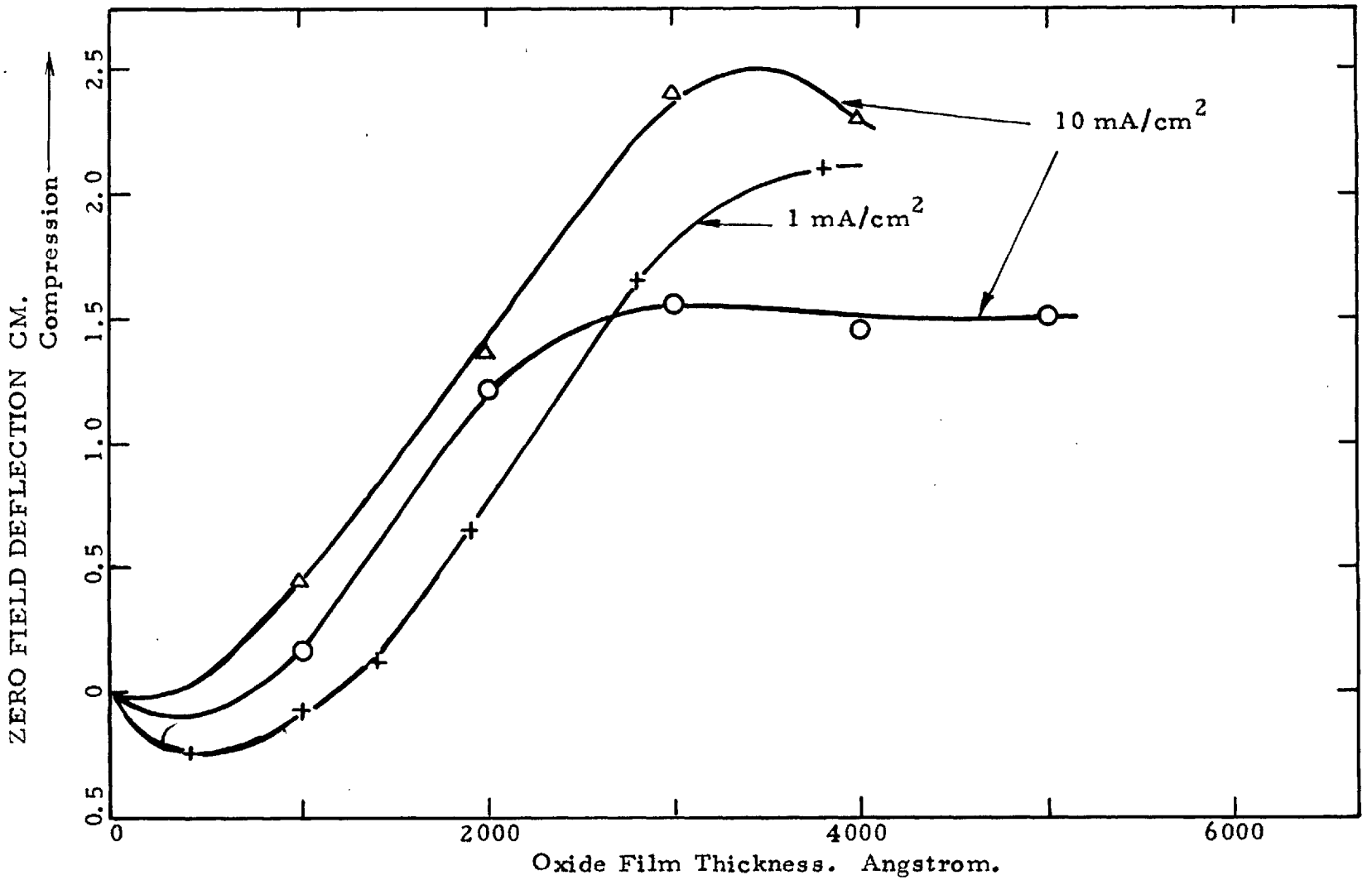

FIGURE 15. DEFLECTION OF ZIRCONIUM FOIL ANODISED ON ONE SIDE IN pH9 AMMONIUM BORATE SOLUTION.

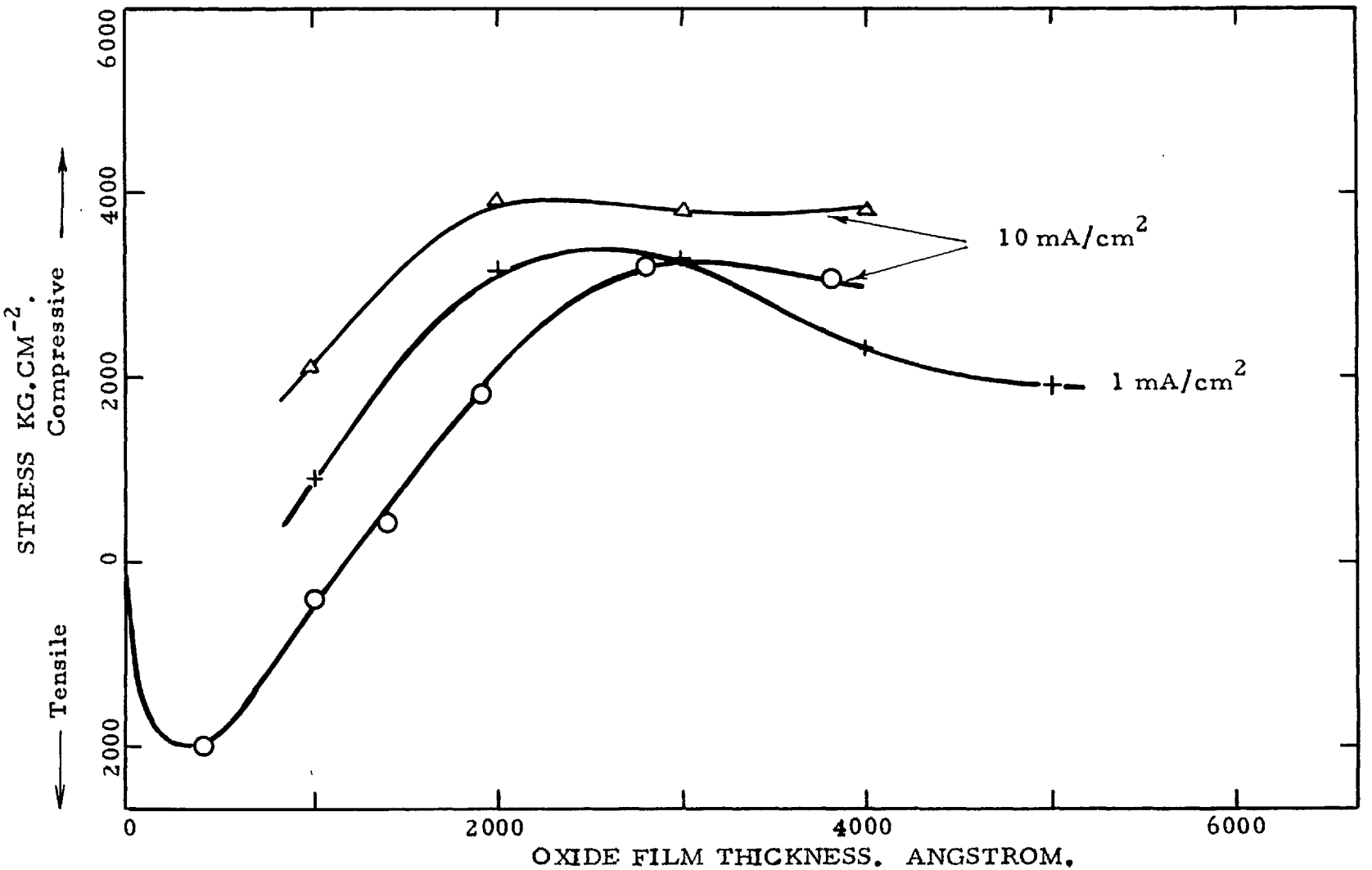

FIGURE 16. STRESSES IN ZIRCONIUM OXIDE FILMS.

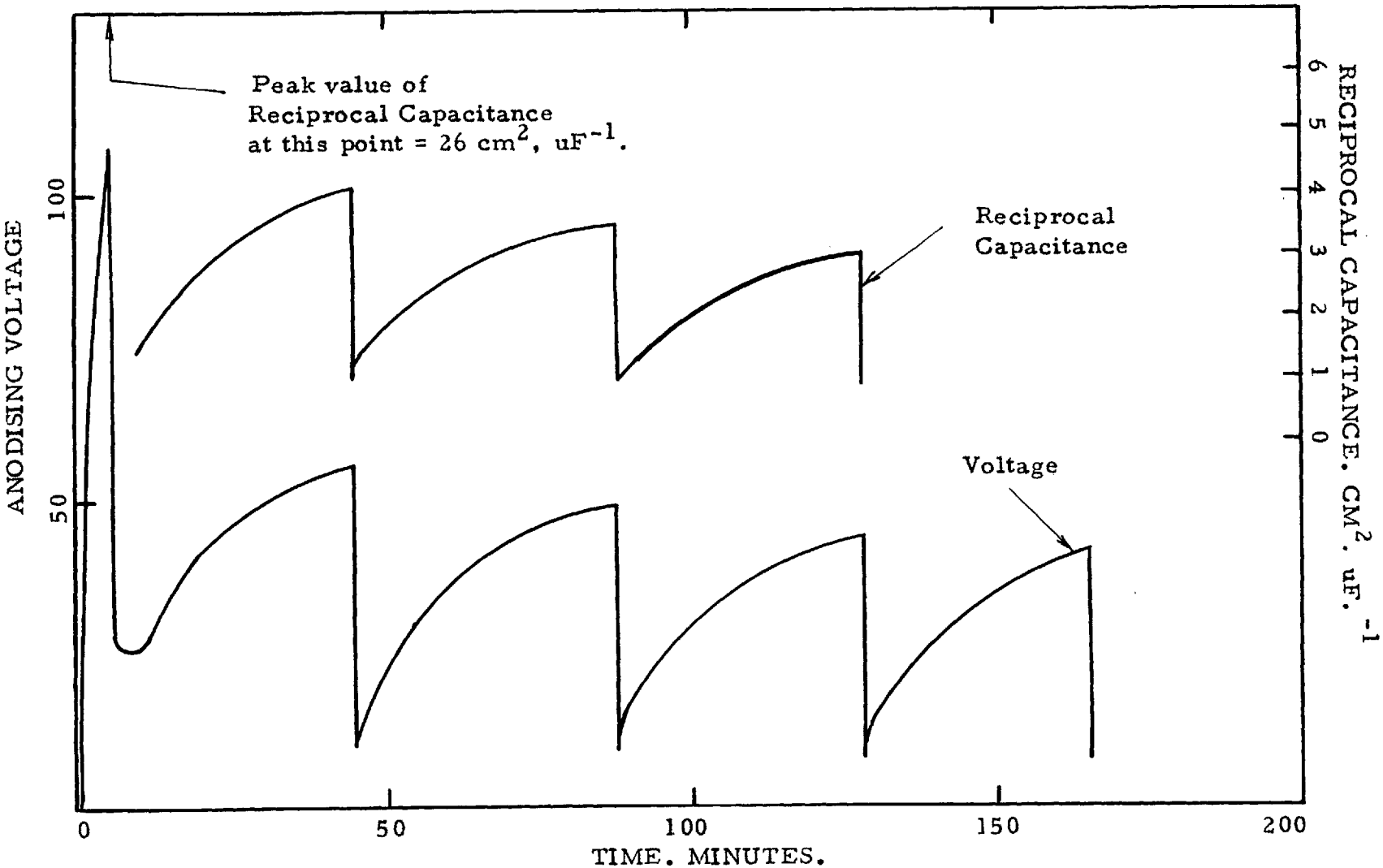

FIGURE 17. CYCLIC BEHAVIOUR OF VOLTAGE AND RECIPROCAL CAPACITANCE DURING THE ANODIC OXIDATION OF TITANIUM AT CONSTANT CURRENT DENSITY.

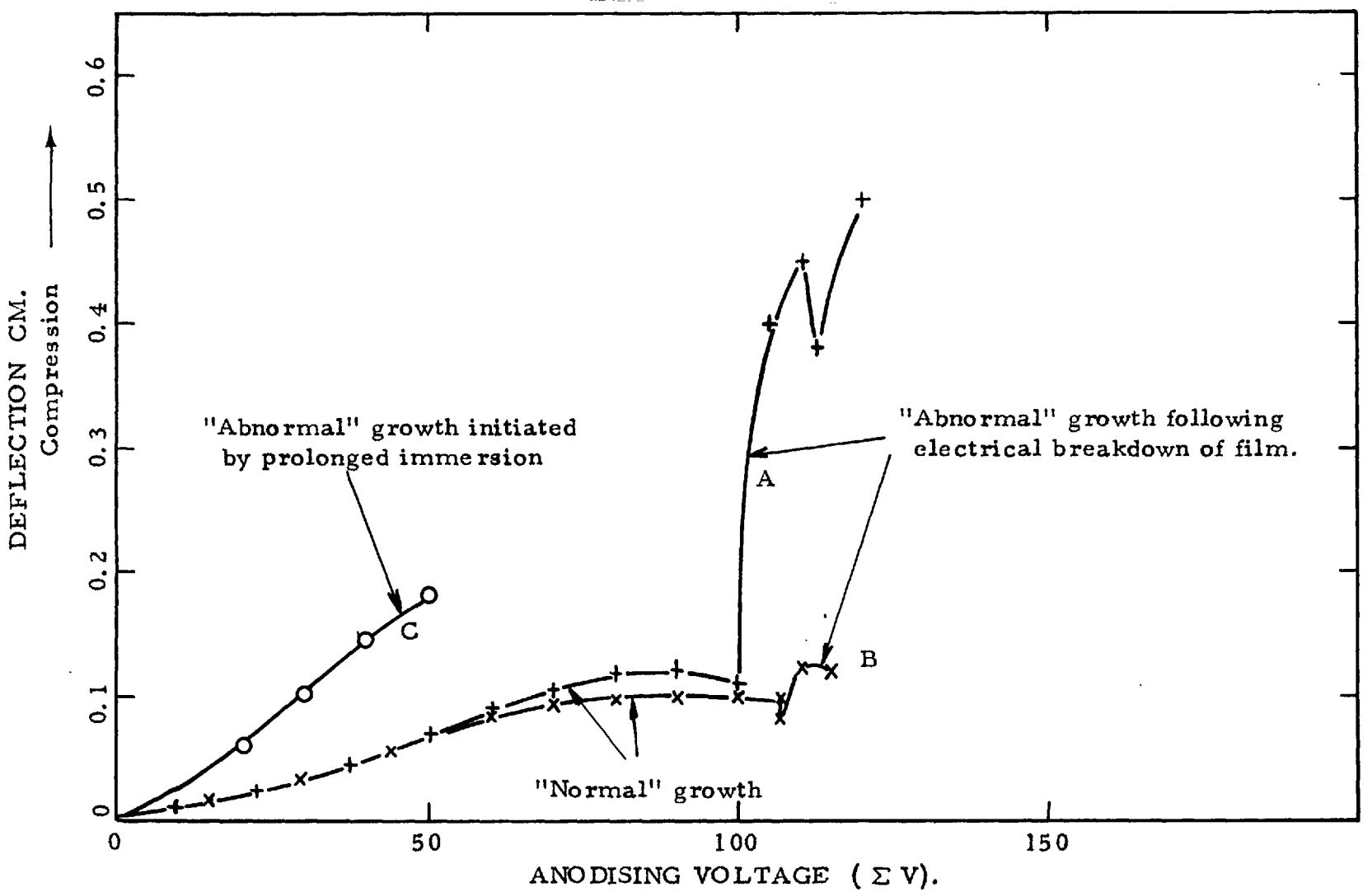

FIGURE 18. DEFLECTION OF TITANIUM FOIL ANODISED ON ONE SIDE IN pH9 AMMONIUM BORATE SOLUTION.

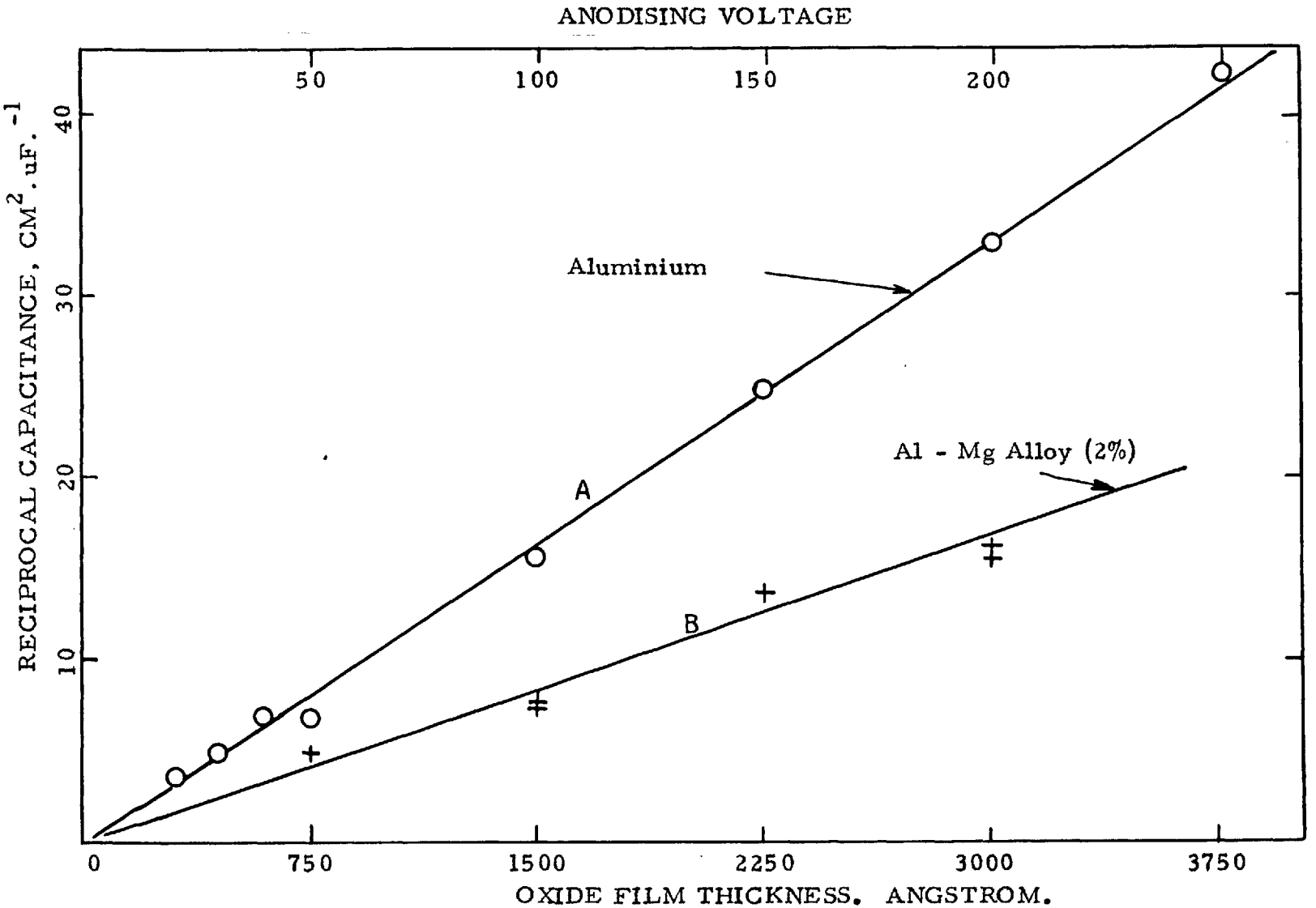

FIGURE 19. RECIPROCAL CAPACITANCE OF OXIDE FILMS ON 2S ALUMINIUM AND M57S ALLOY. (2% Mg).

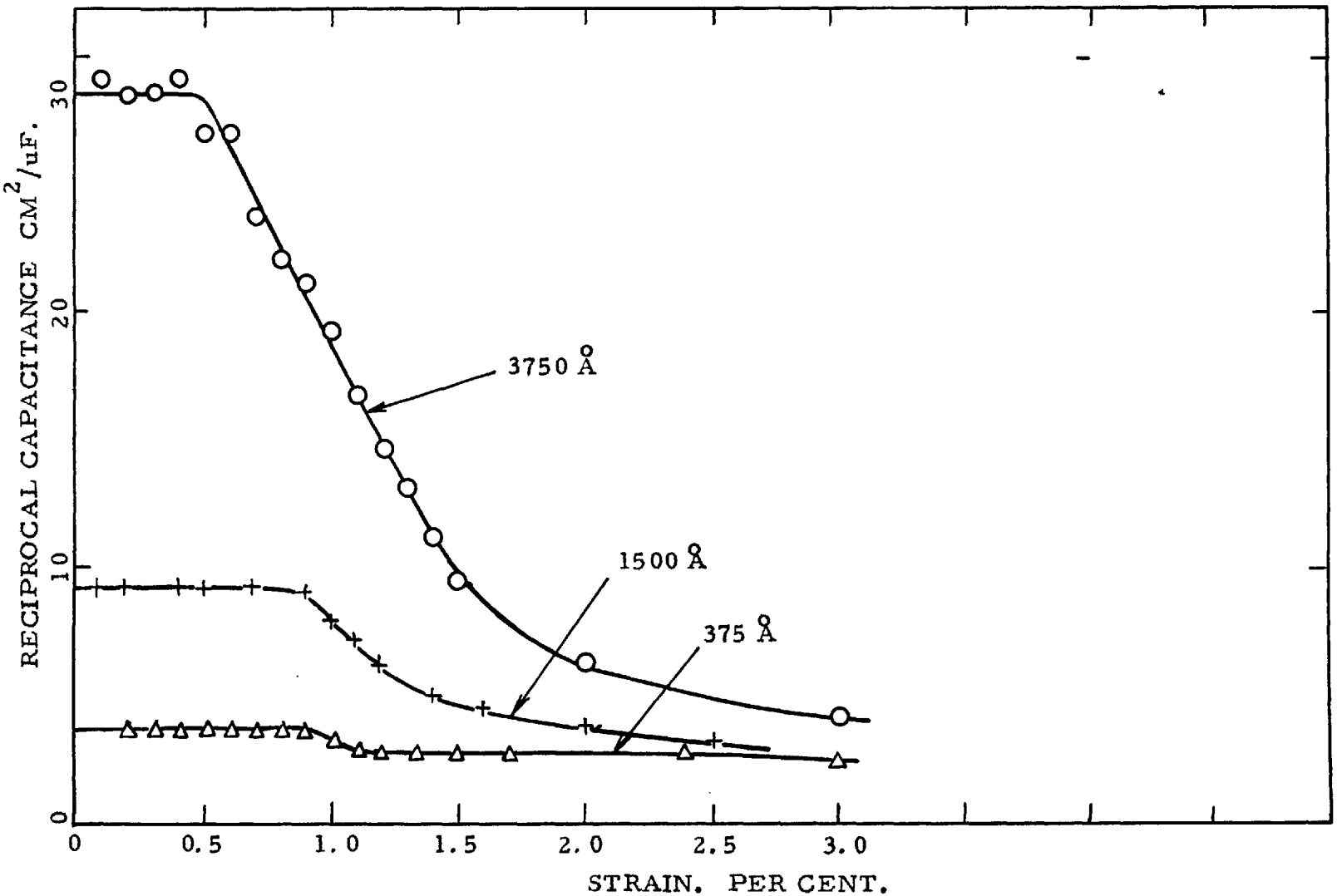

FIGURE 20. RECIPROCAL CAPACITANCE VS. STRAIN FOR ANODISED FILMS ON 2S ALUMINIUM.

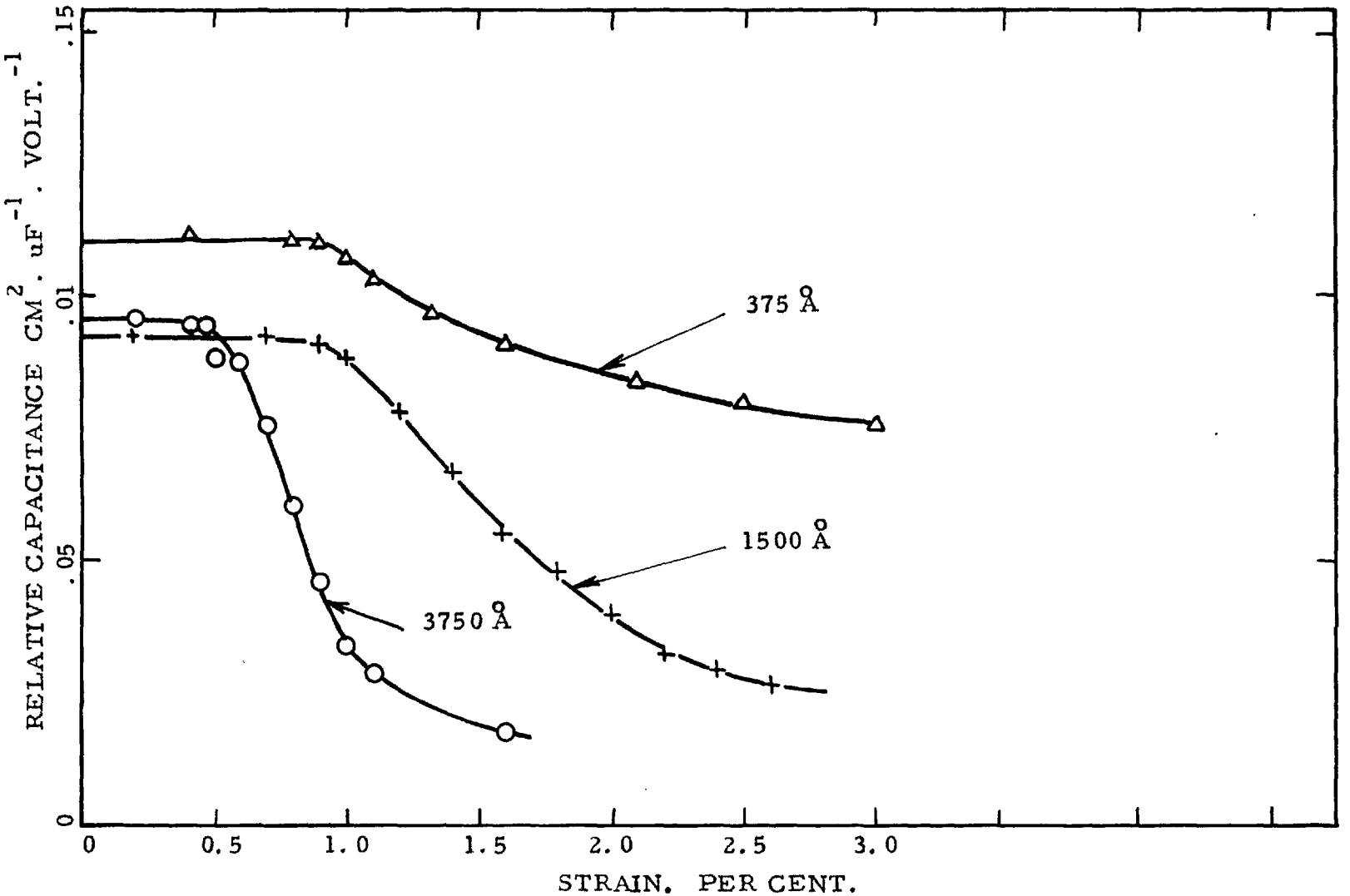

FIGURE 21. "RELATIVE CAPACITANCE" $^1/_{CV}$ VS. STRAIN FOR ANODISED FILMS ON 2S ALUMINIUM.

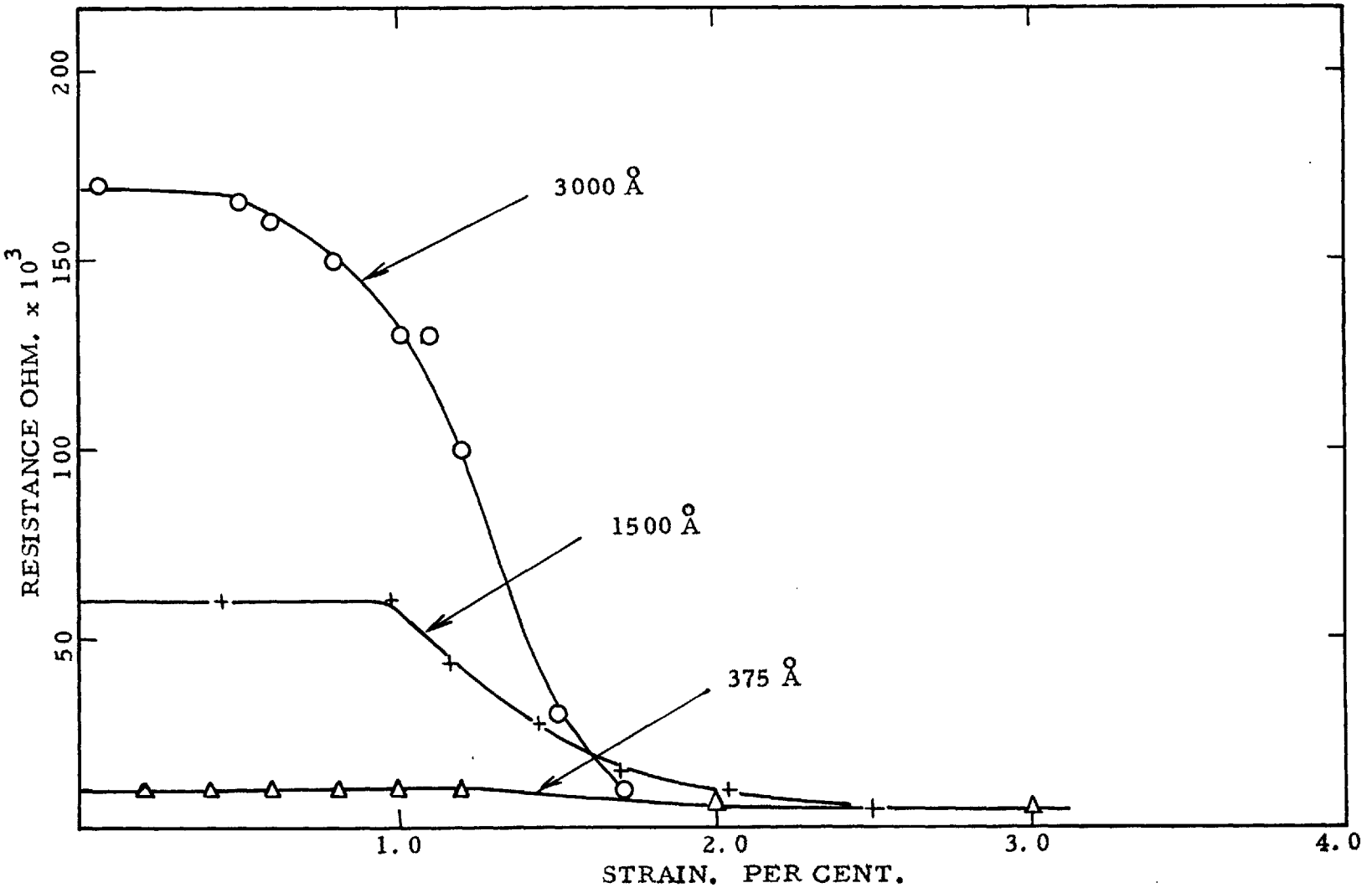

FIGURE 22. RESISTANCE VS. STRAIN CURVES FOR OXIDE FILMS ON 2S ALUMINIUM.

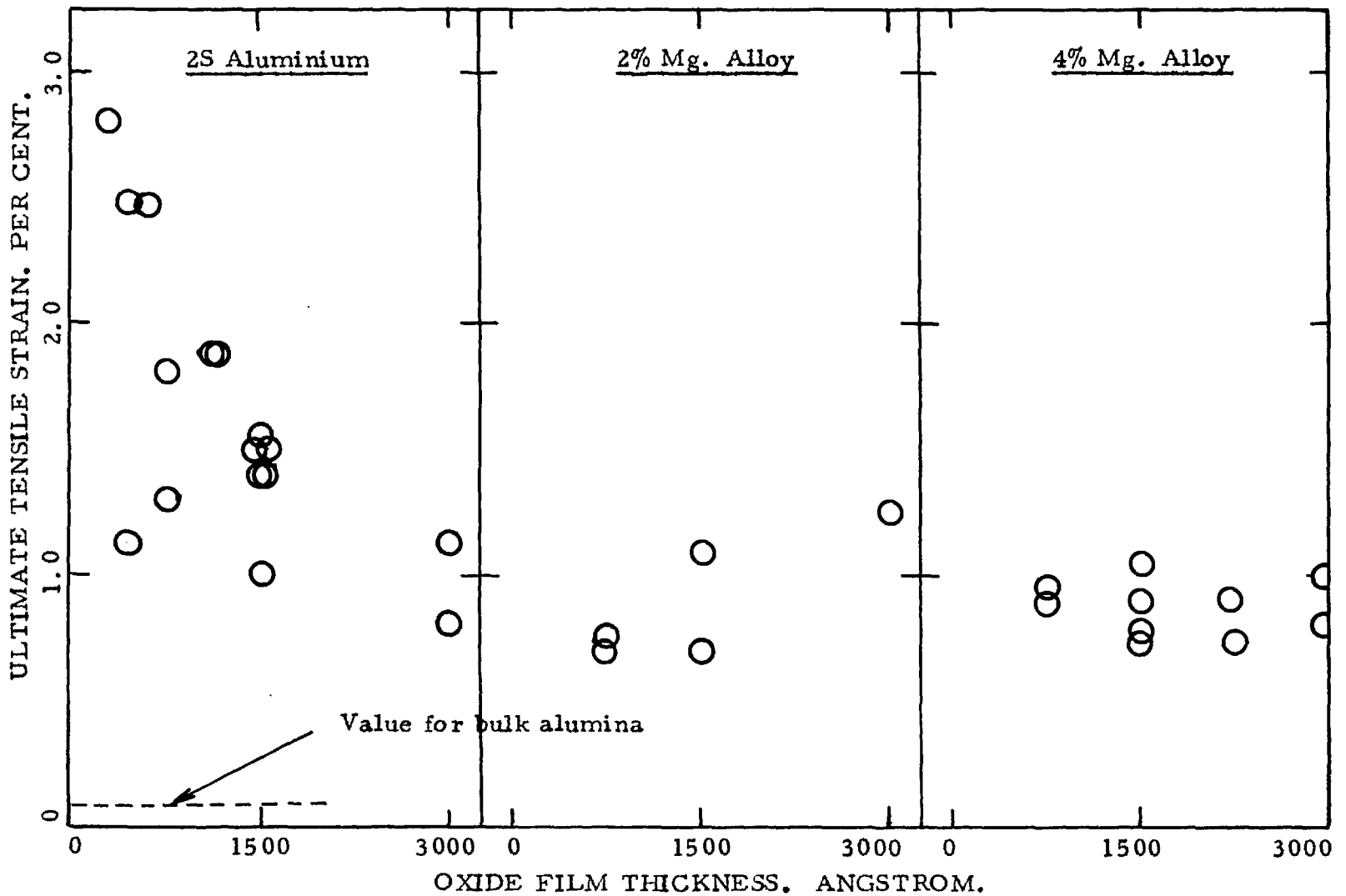

FIGURE 23. COMPARISON OF U.T.S. VALUES FOR ANODIC FILMS ON ALUMINIUM AND ALUMINIUM-MAGNESIUM ALLOYS BY CAPACITANCE-RESISTANCE METHOD.

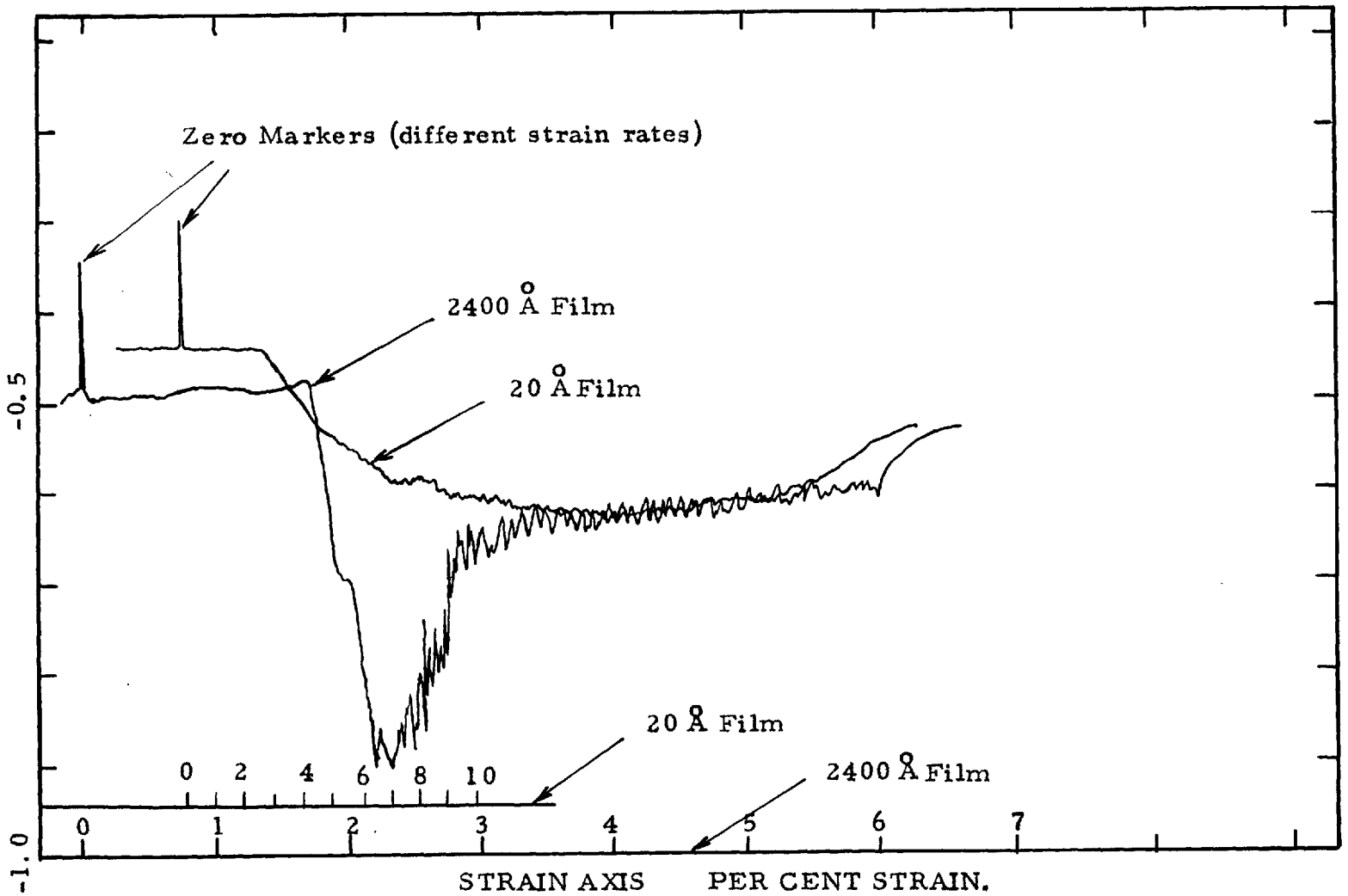

FIGURE 24. ELECTRODE POTENTIAL VS. STRAIN FOR ANODISED FILMS ON 2S ALUMINIUM.

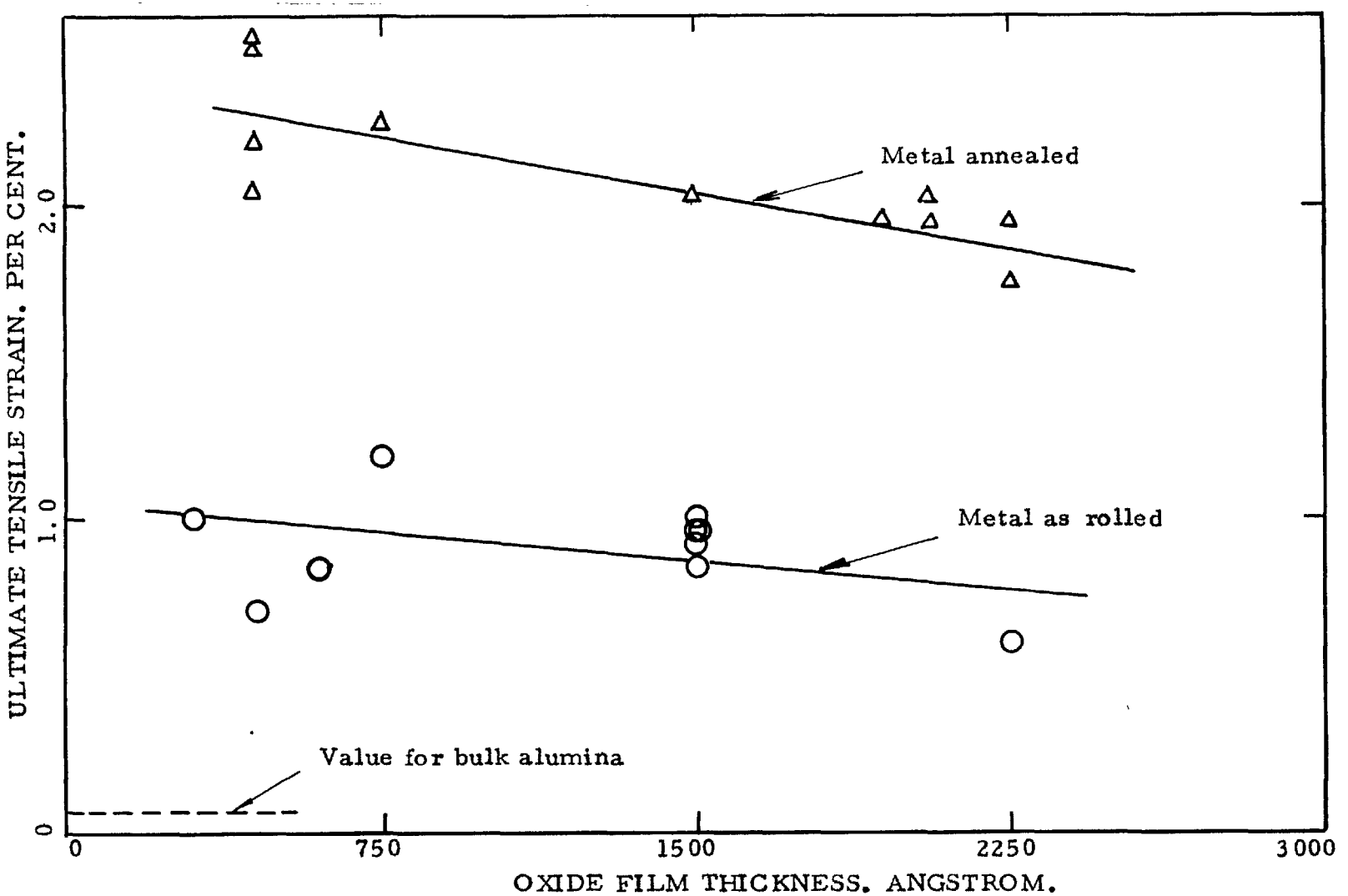

FIGURE 25. U.T.S. VALUES FOR ANODIC FILMS ON 2S ALUMINIUM (BY POTENTIAL METHOD).

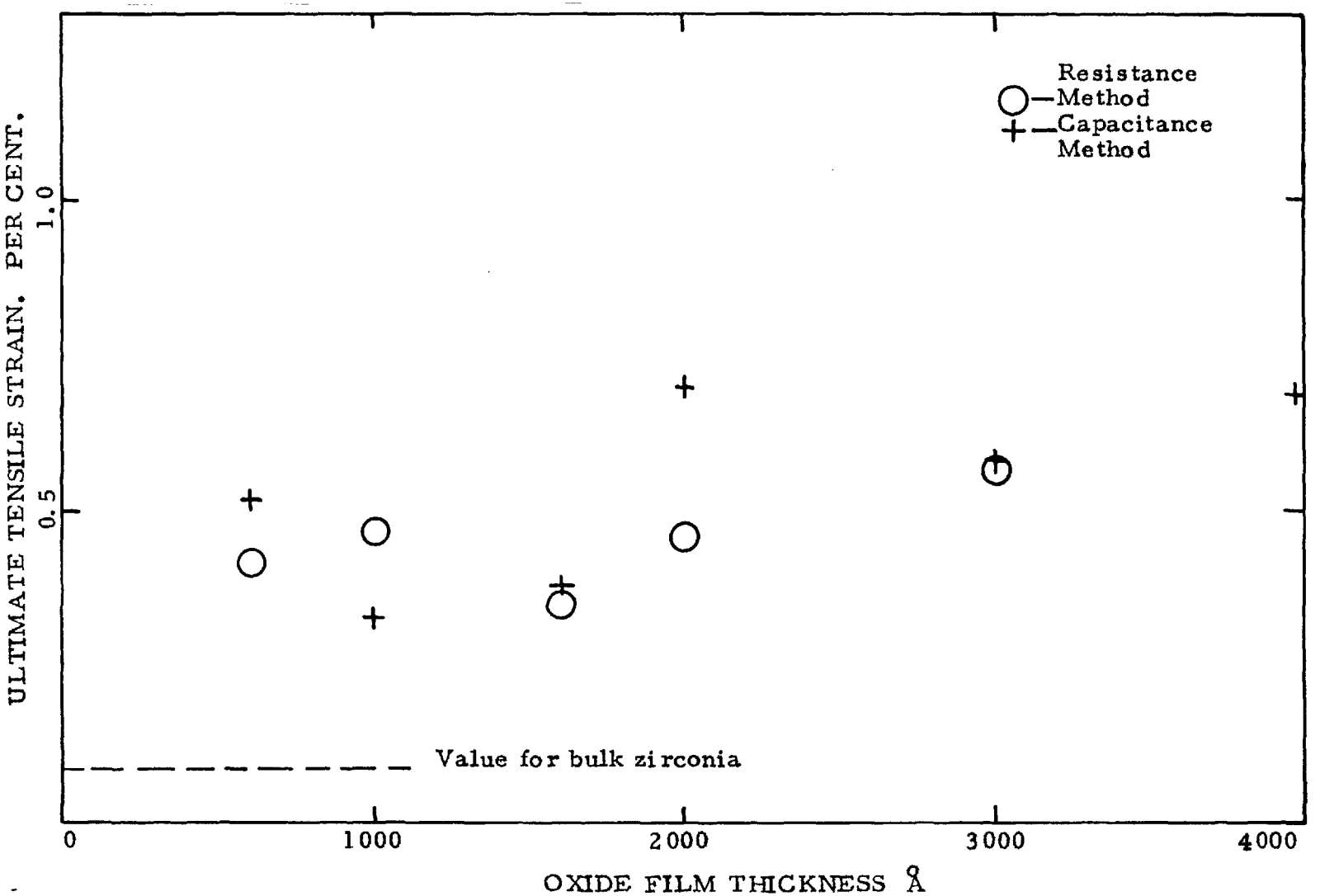

FIGURE 26. U.T.S. VALUES FOR ANODIC FILMS ON ZIRCONIUM.

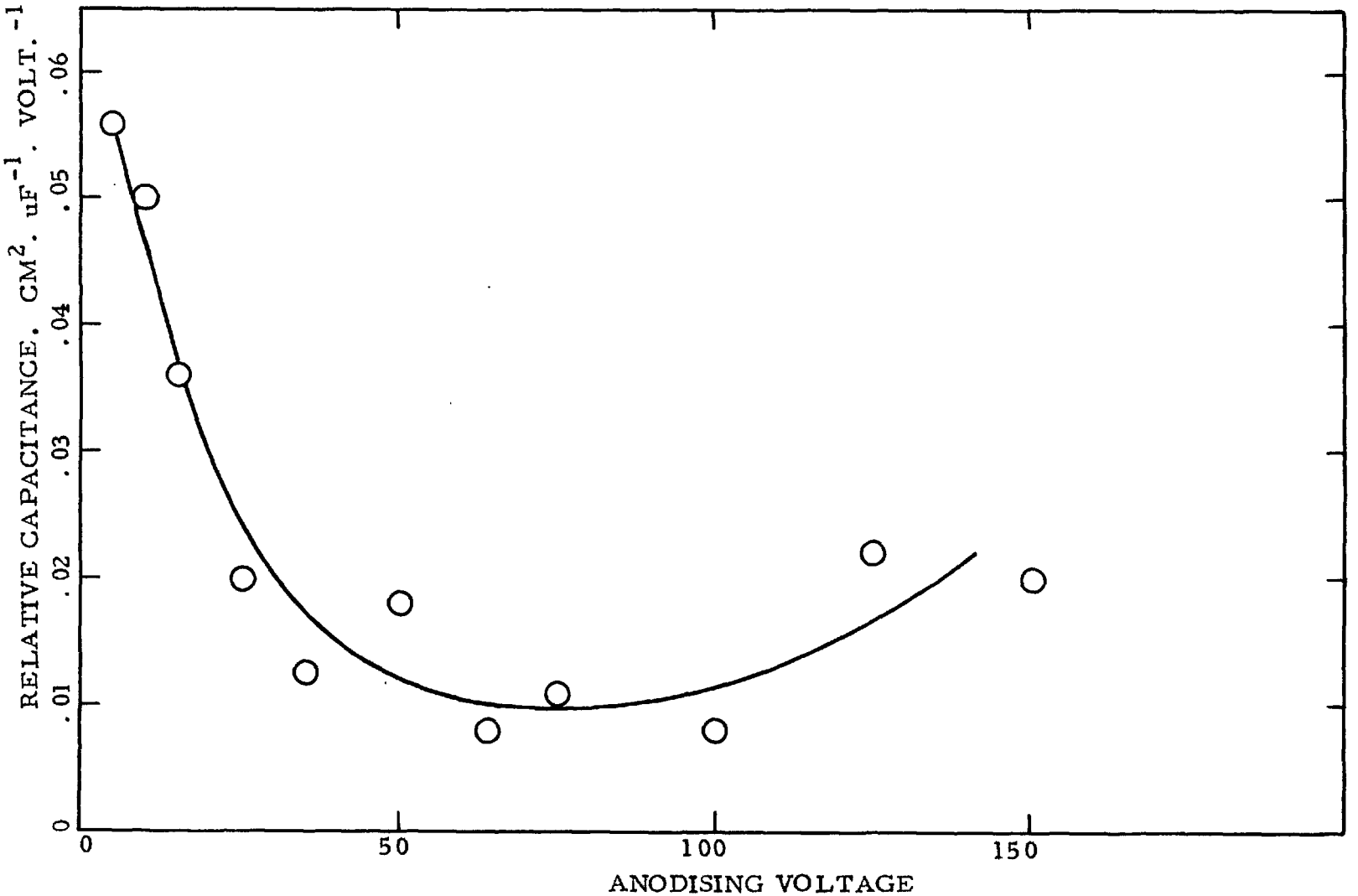

FIGURE 27. INITIAL VALUES OF RELATIVE CAPACITANCE FOR ANODIC FILMS ON TITANIUM.

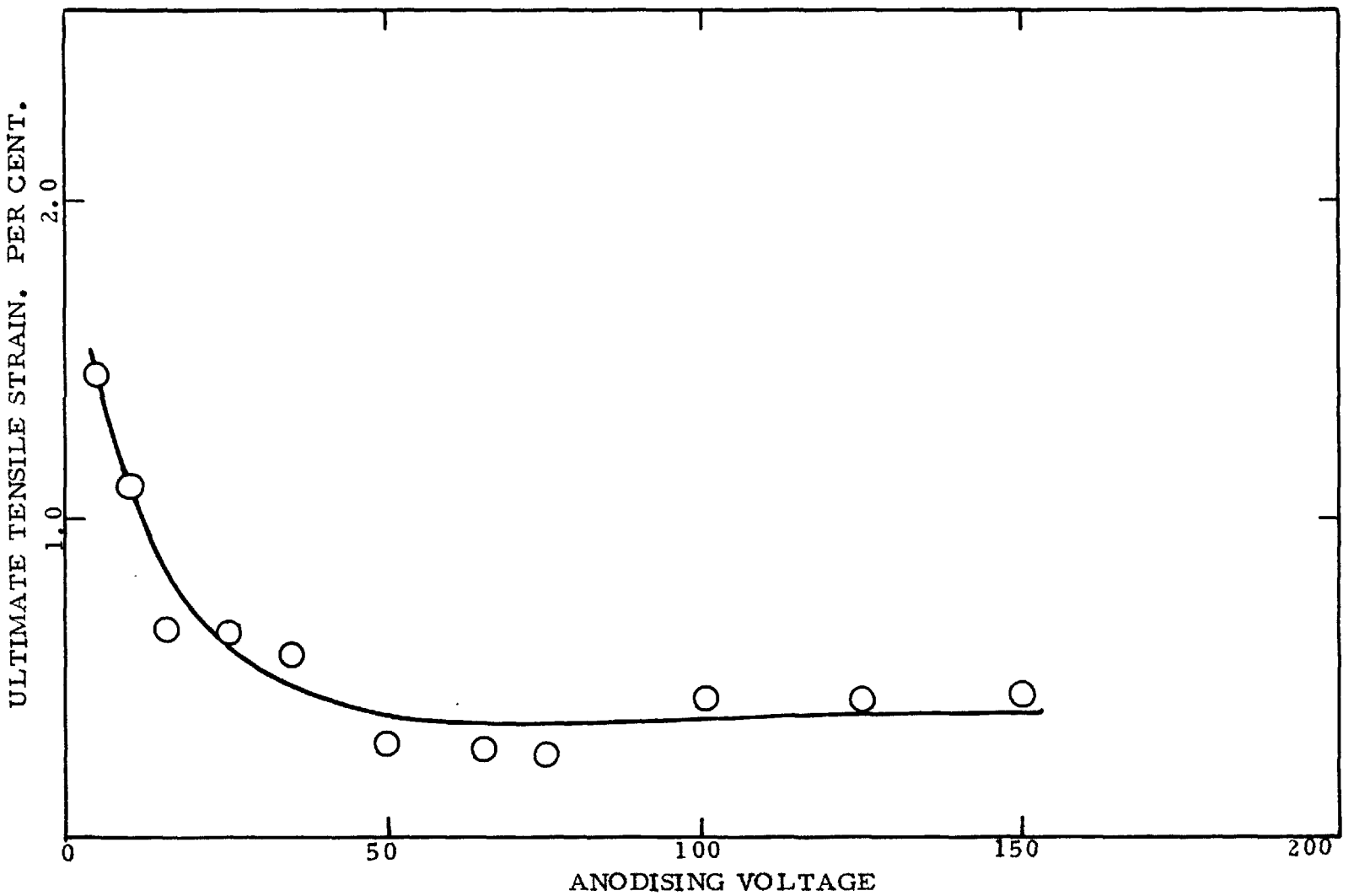

FIGURE 28. U.T.S. VALUES FOR ANODIC FILMS ON TITANIUM.

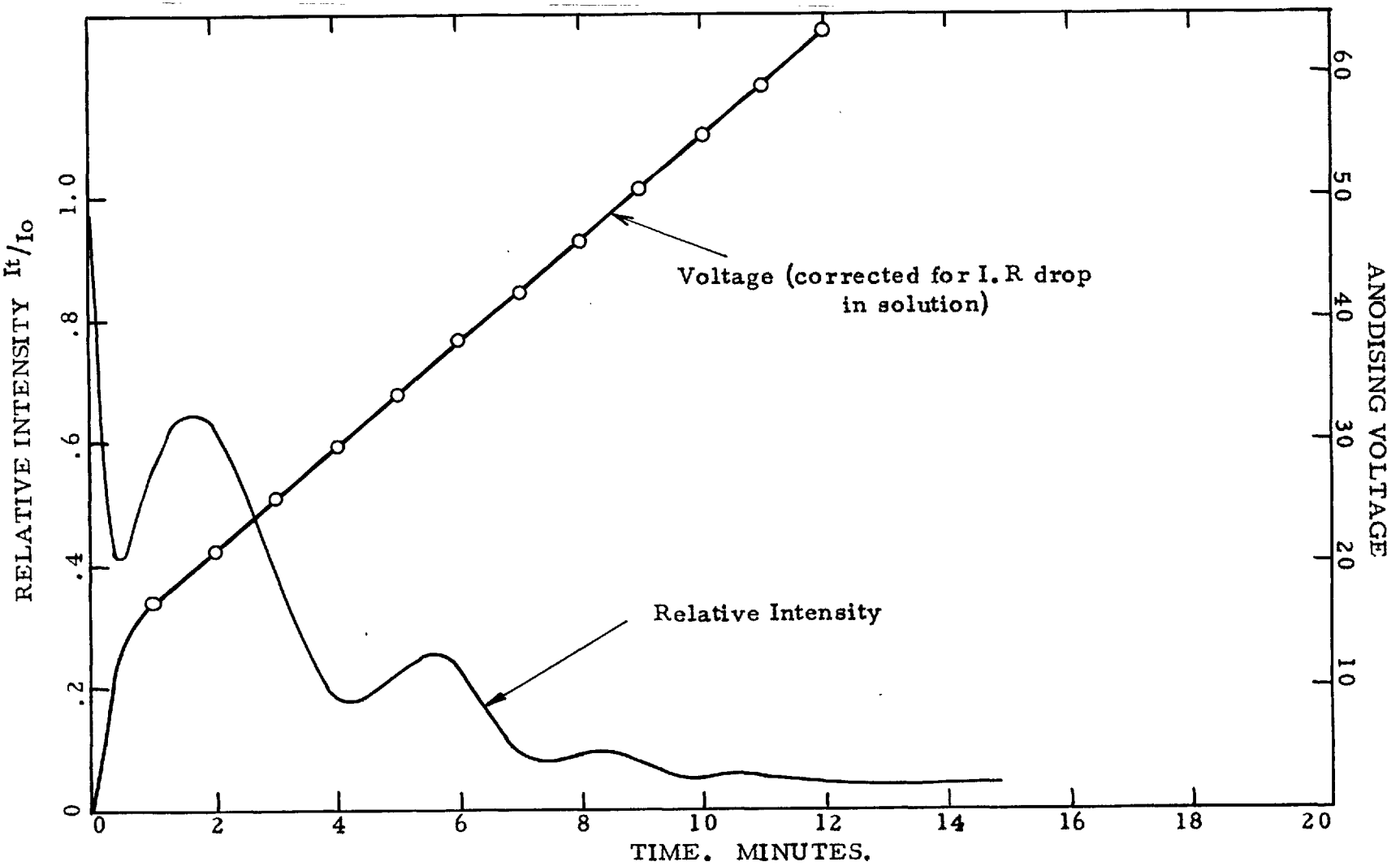

FIGURE 29. REFLECTED INTENSITY OF MONOCHROMATIC LIGHT DURING ANODIC OXIDATION OF URANIUM IN AMMONIA SOLUTION.

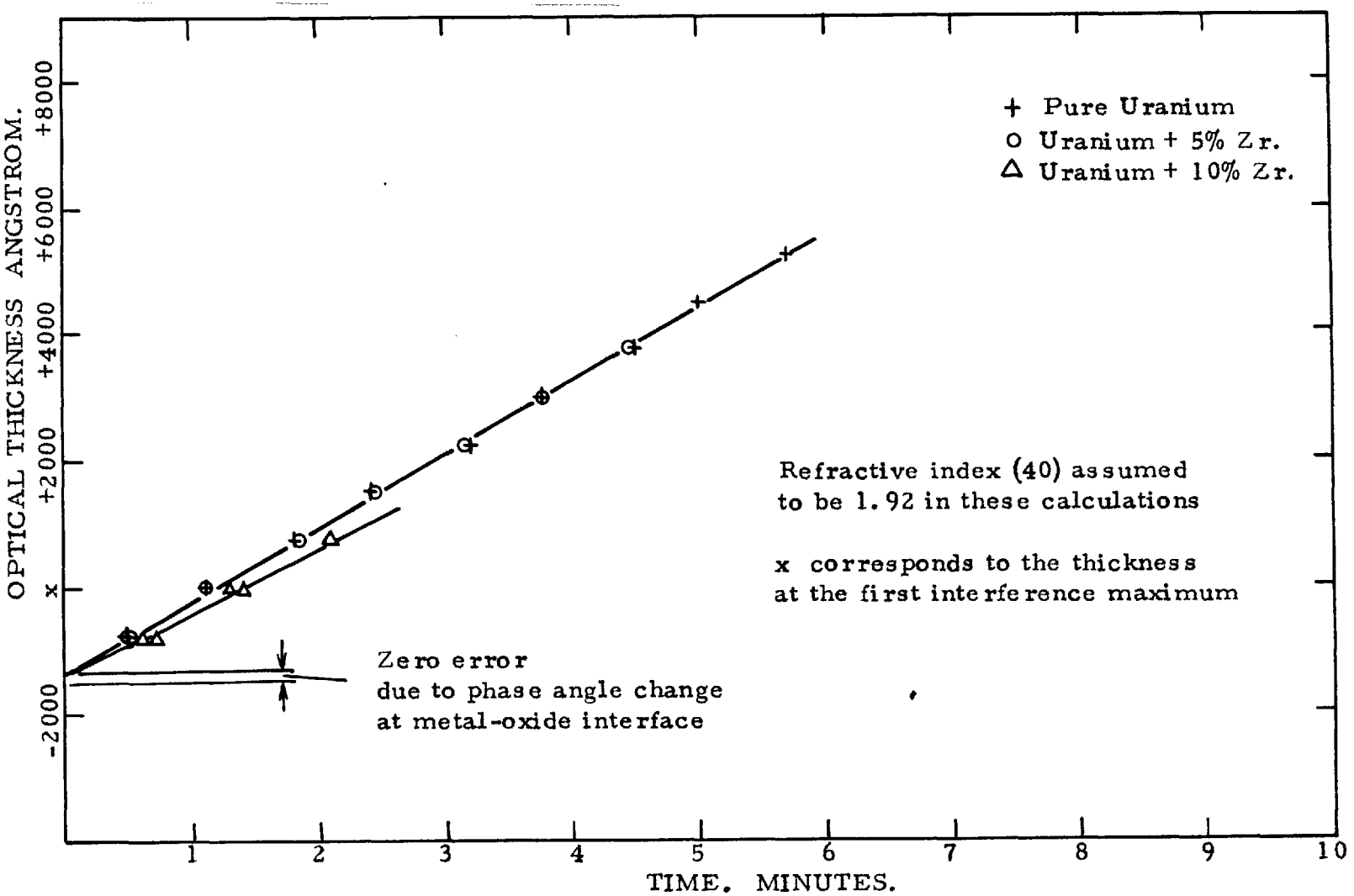

FIGURE 30. APPARENT RATE OF OXIDE GROWTH DURING ANODISATION OF URANIUM-ZIRCONIUM ALLOYS AT CONSTANT CURRENT DENSITY.

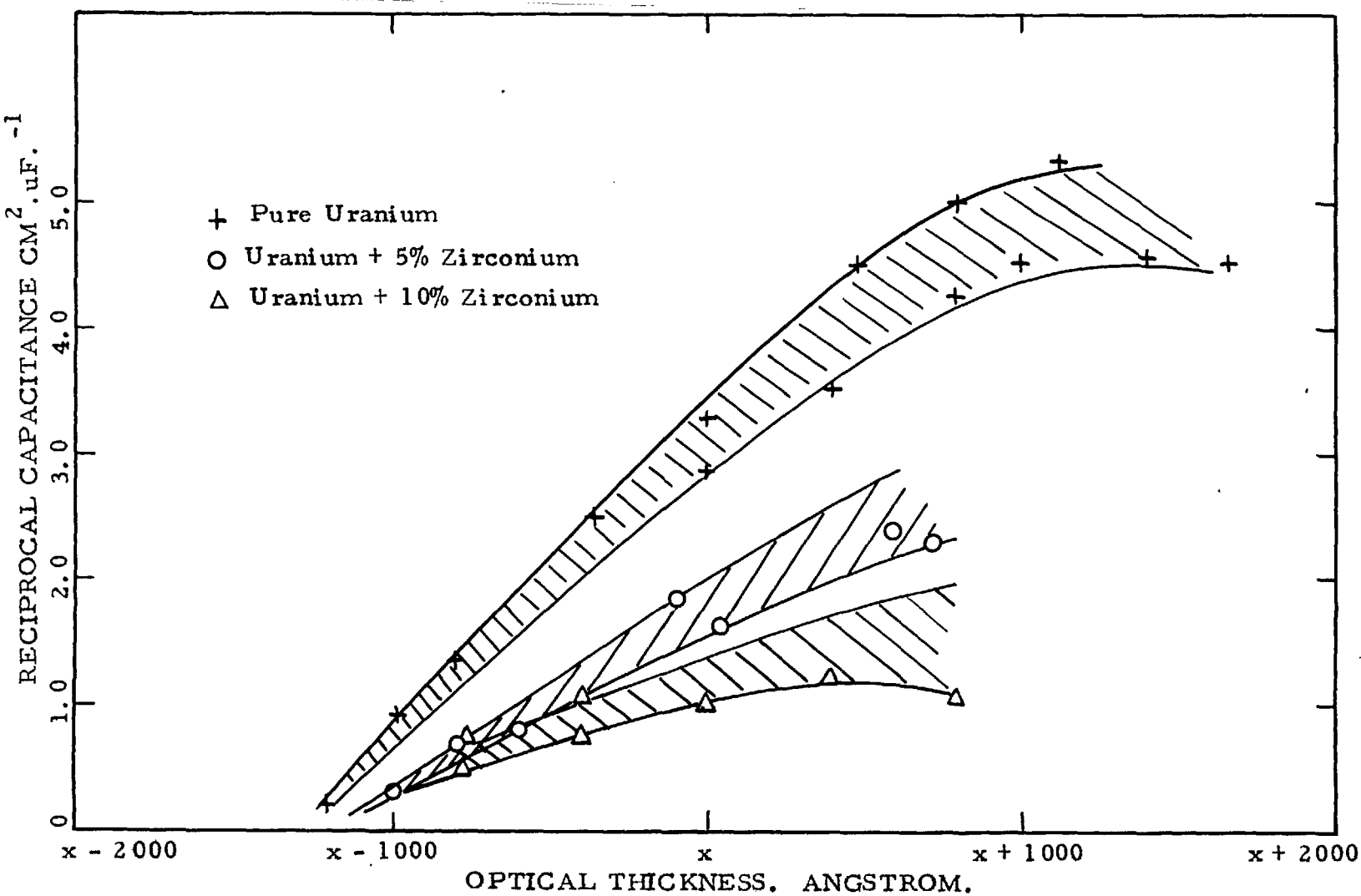

FIGURE 31. RECIPROCAL CAPACITANCE OF ANODIC FILMS ON URANIUM AND URANIUM-ZIRCONIUM ALLOYS.

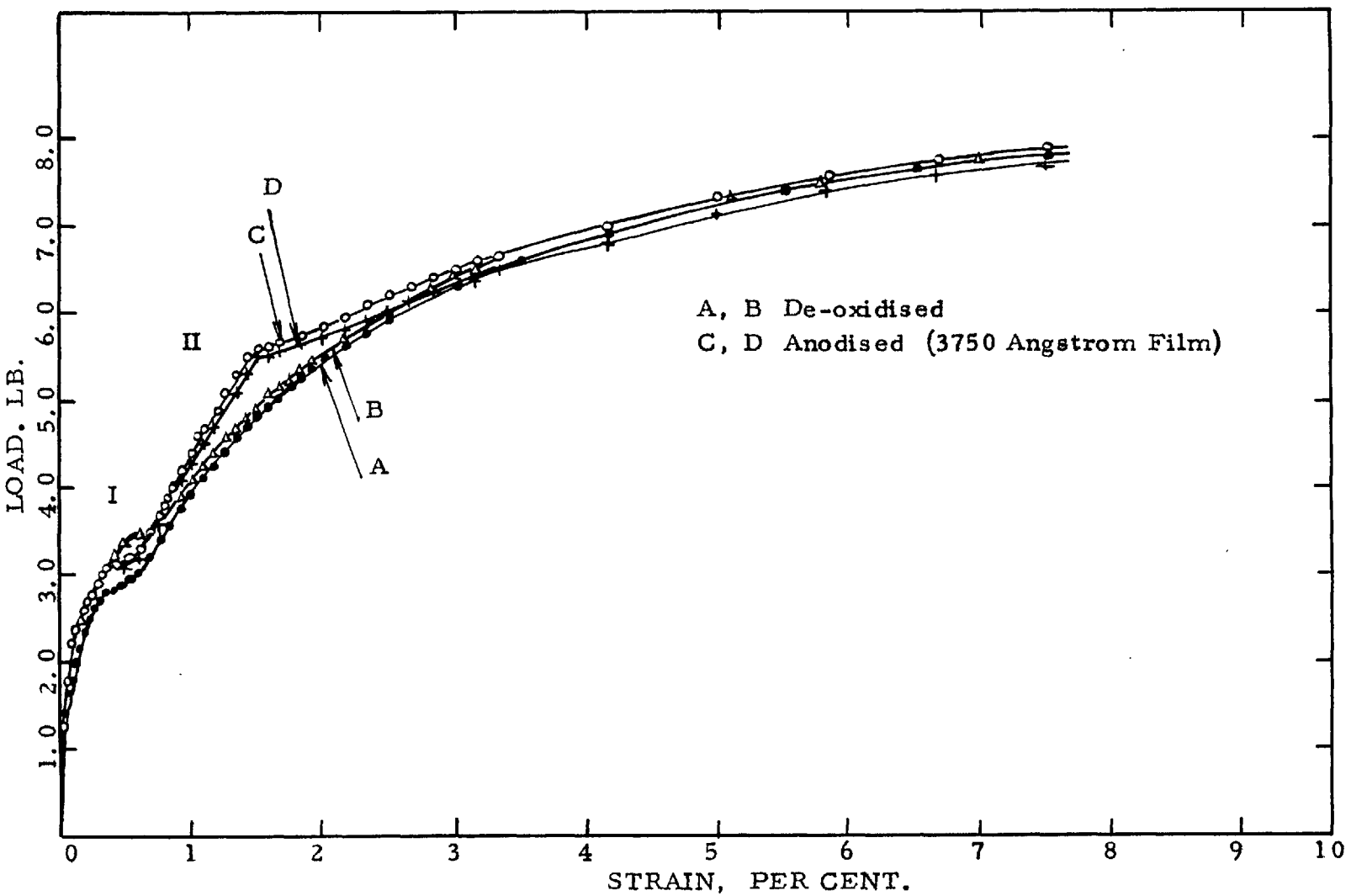

FIGURE 32. LOAD VS. STRAIN CURVES FOR THIN FOIL SPECIMENS OF 2S ALUMINIUM.

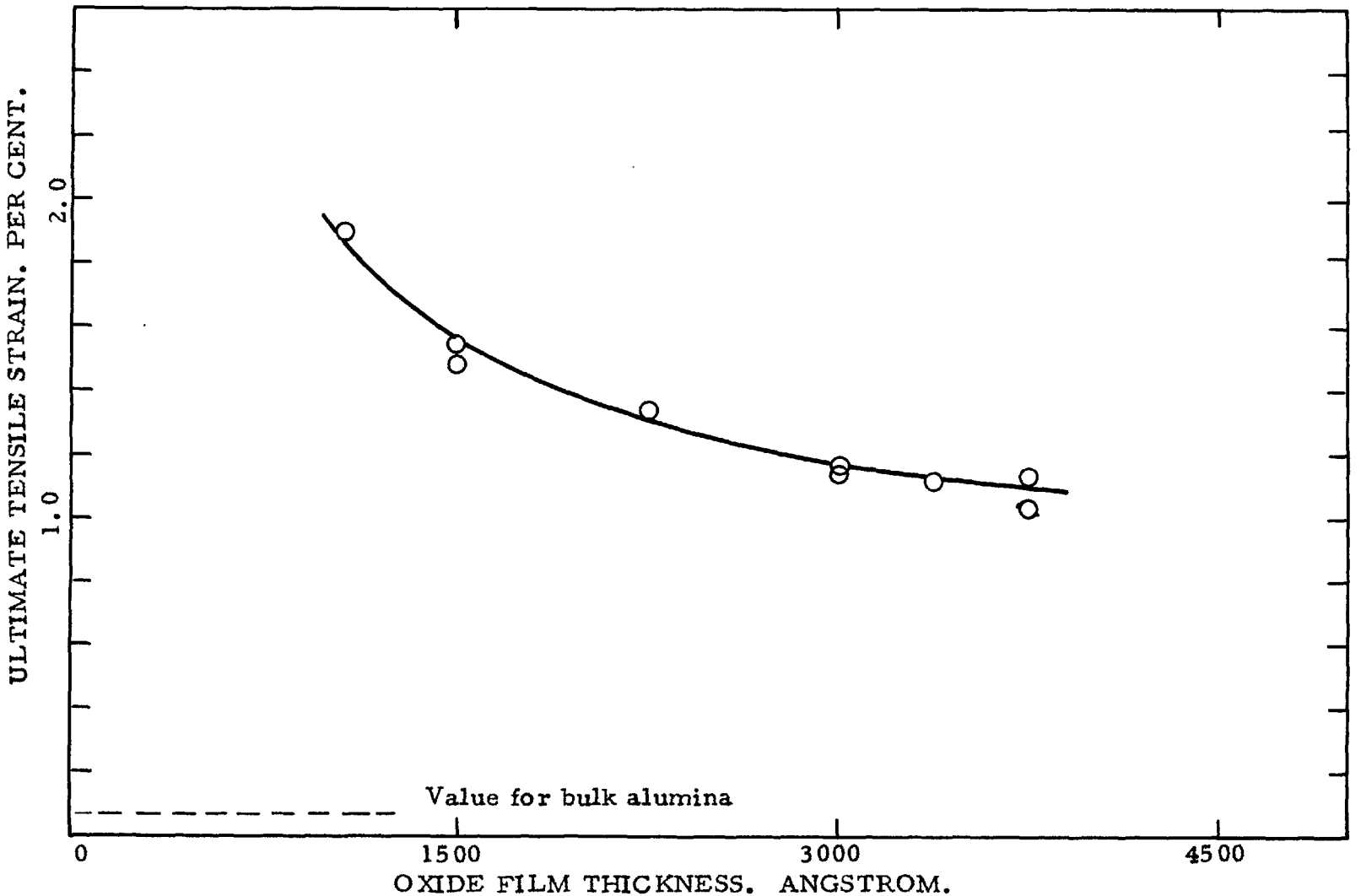

FIGURE 33. U.T.S. OF ANODIC FILMS ON ALUMINIUM FROM STRESS-STRAIN CURVES FOR FOILS.

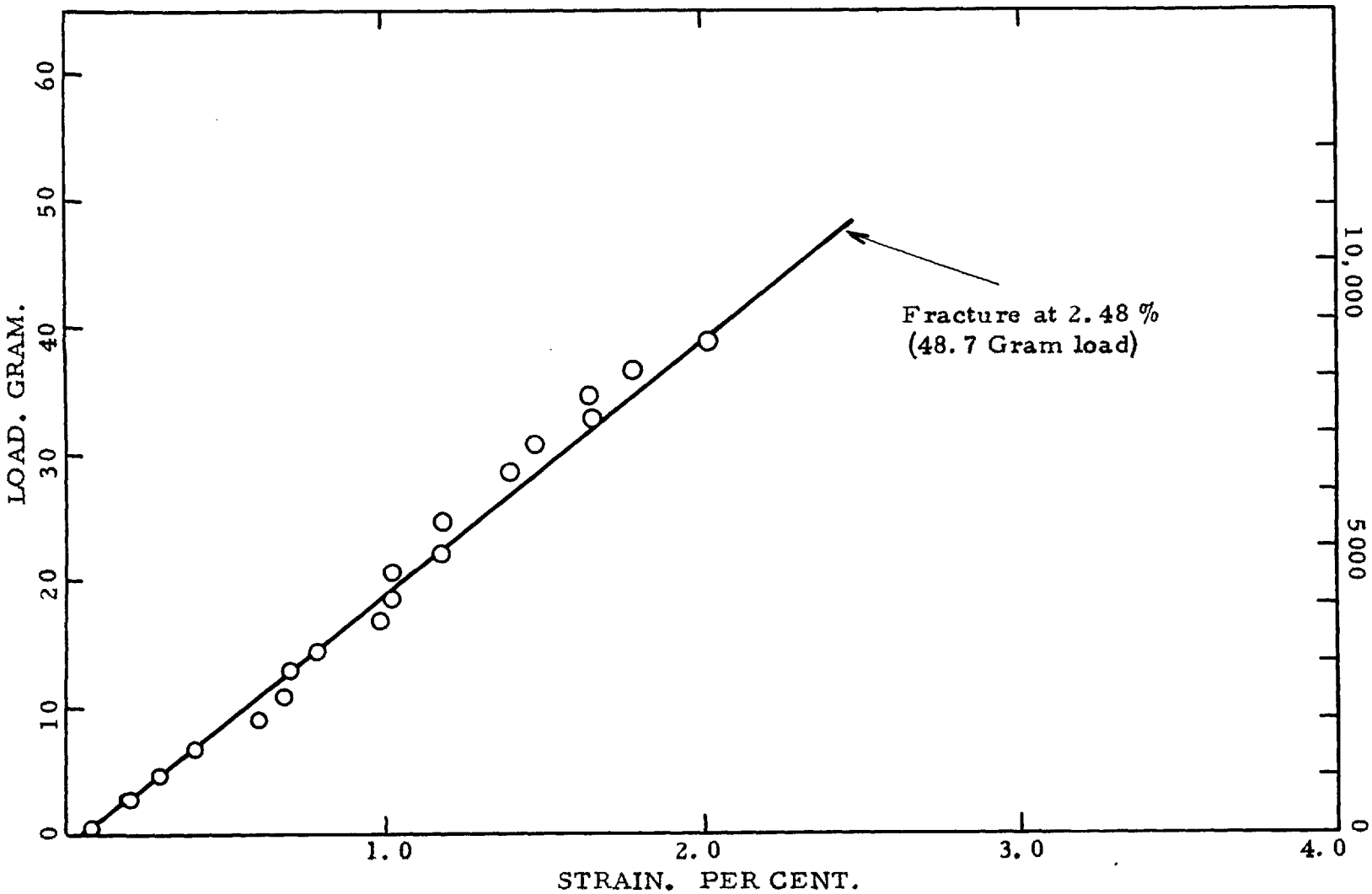

FIGURE 34. STRESS-STRAIN CURVE FOR A 1500 Å ANODIC OXIDE FILM SEPARATED FROM 2S ALUMINIUM.

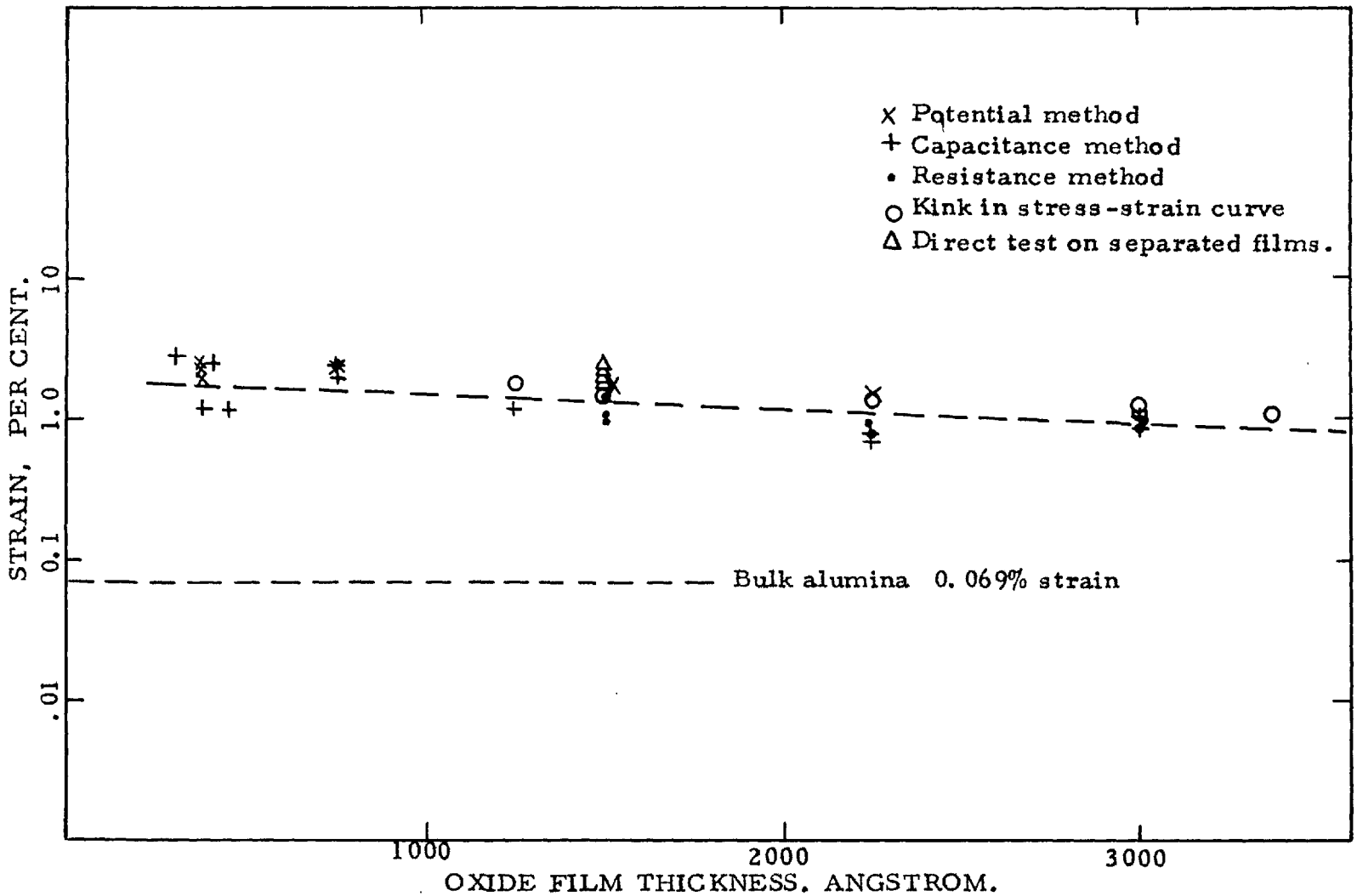

FIGURE 35. SUMMARY OF ULTIMATE TENSILE STRAIN DATA FOR ANODISED FILMS ON ANNEALED ALUMINIUM.

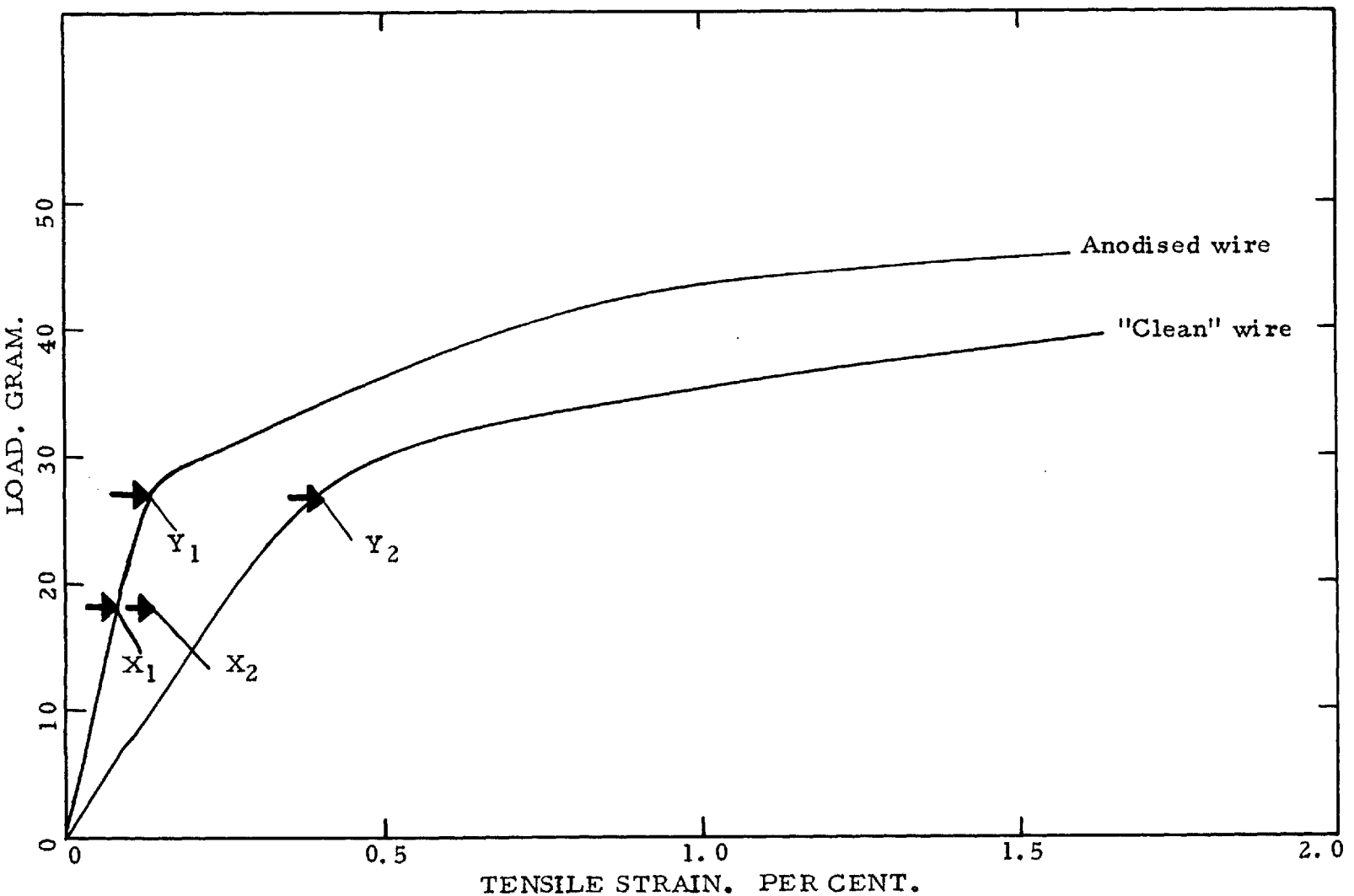

FIGURE 36. STRESS- STRAIN CURVES FOR "CLEAN" AND ANODISED ALUMINIUM WIRES.

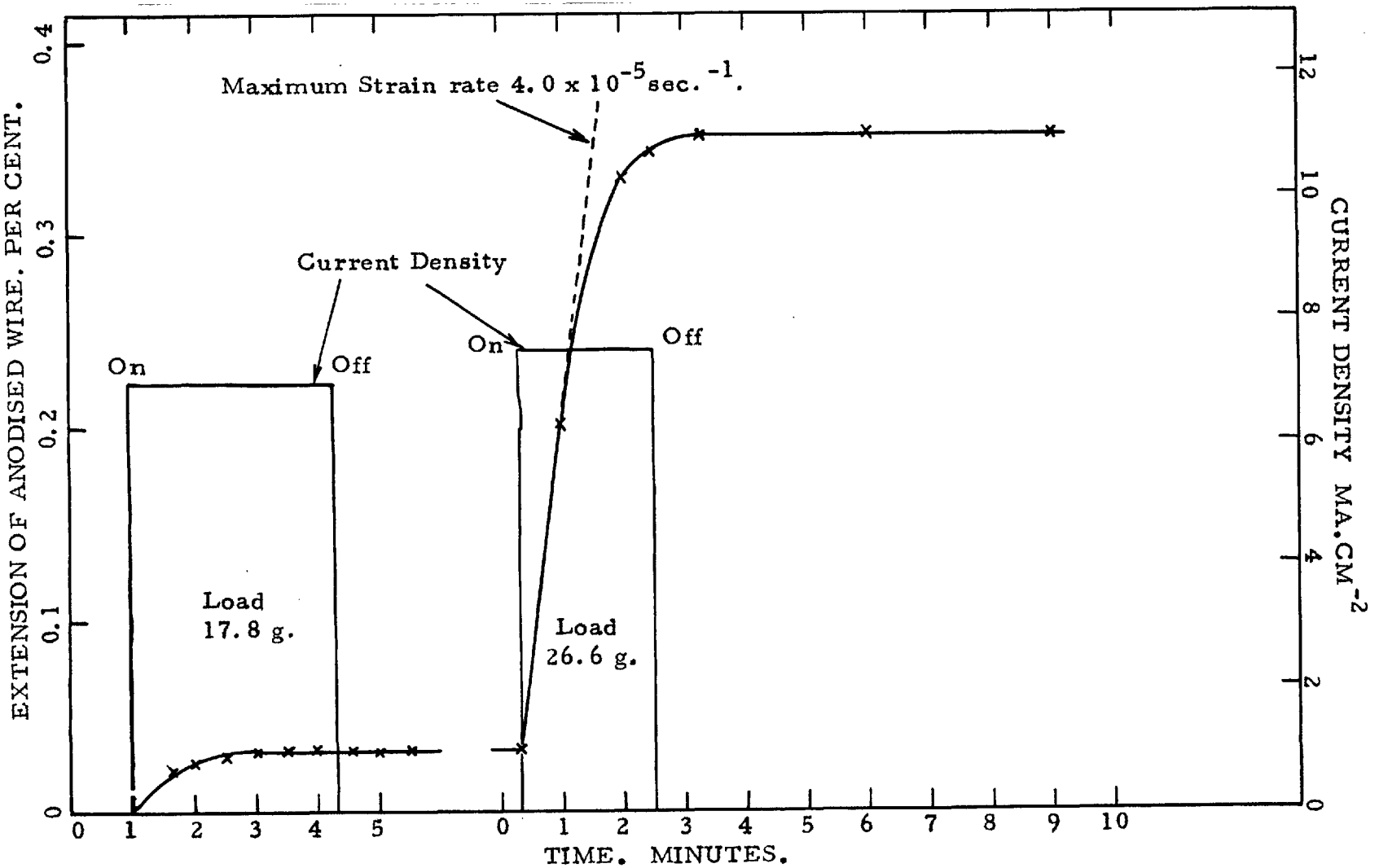

FIGURE 37. EXTENSION OF ANODISED WIRE SPECIMEN DUE TO AN APPLIED ANODIC CURRENT.

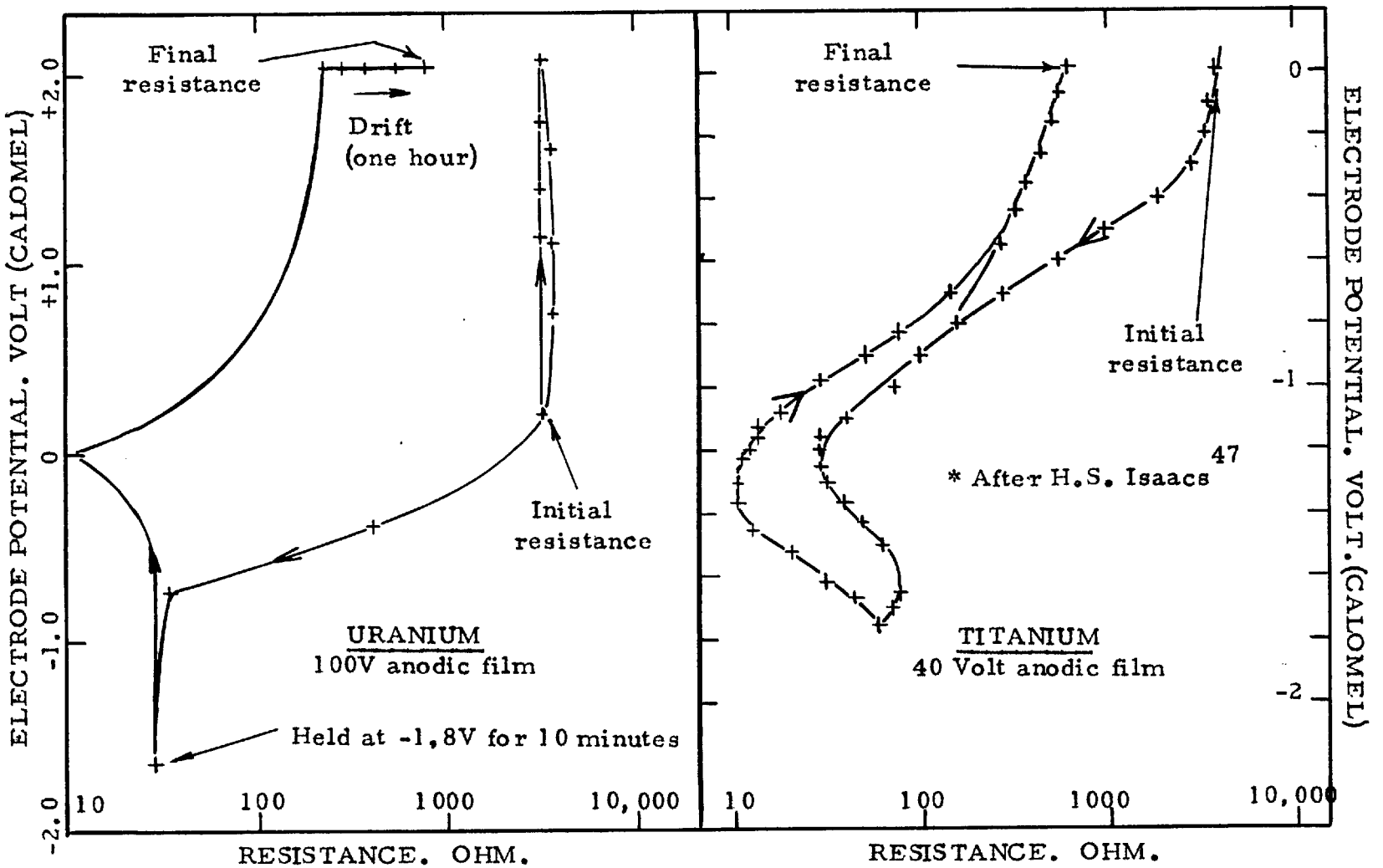

FIGURE 38. EFFECT OF CATHODIC POLARISATION ON THE APPARENT RESISTANCE OF ANODIC FILMS ON URANIUM, AND TITANIUM.*

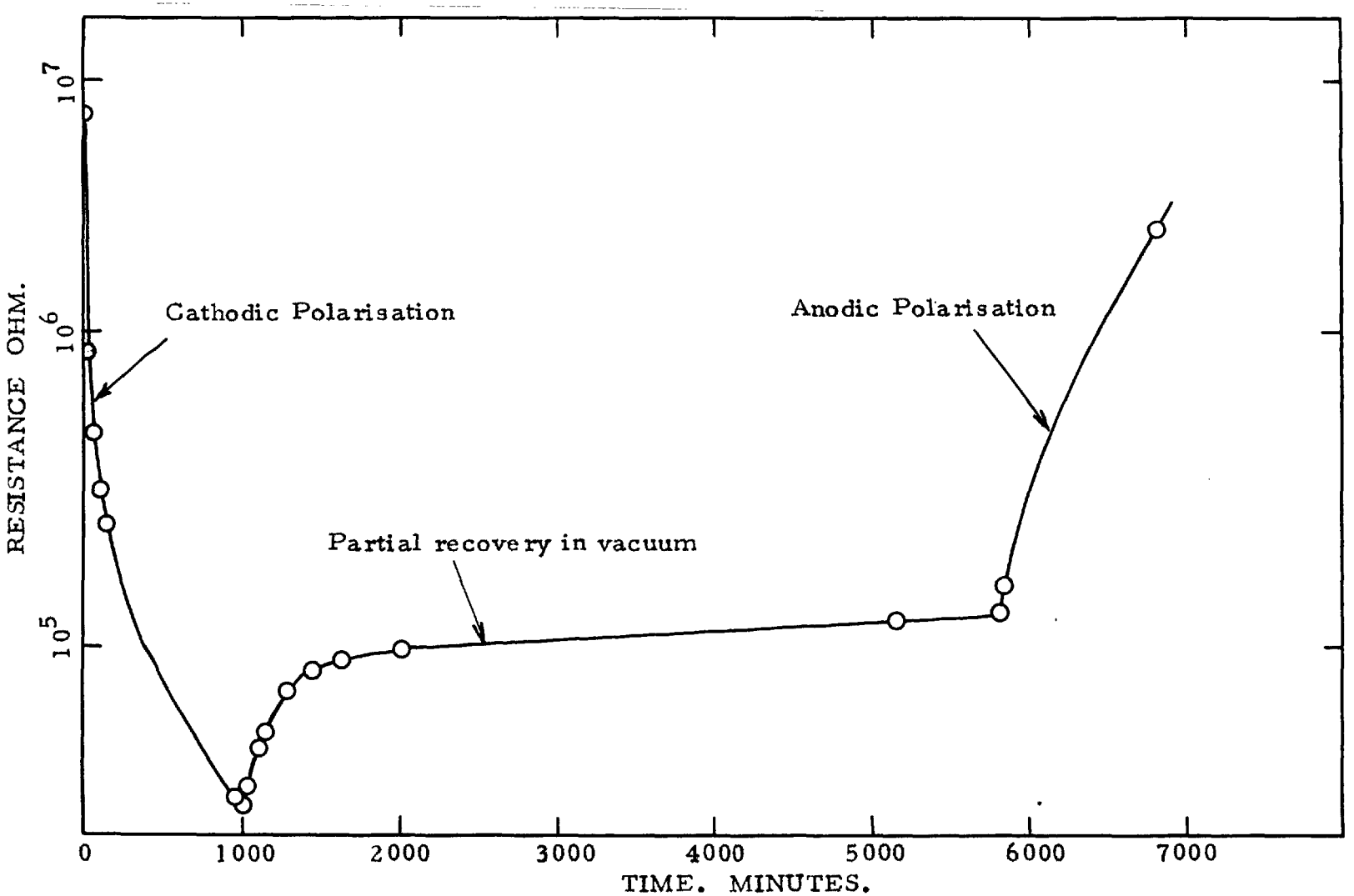

FIGURE 39. CHANGE IN RESISTANCE OF A SINGLE CRYSTAL OF RUTILE DURING ELECTROLYTIC TREATMENT.

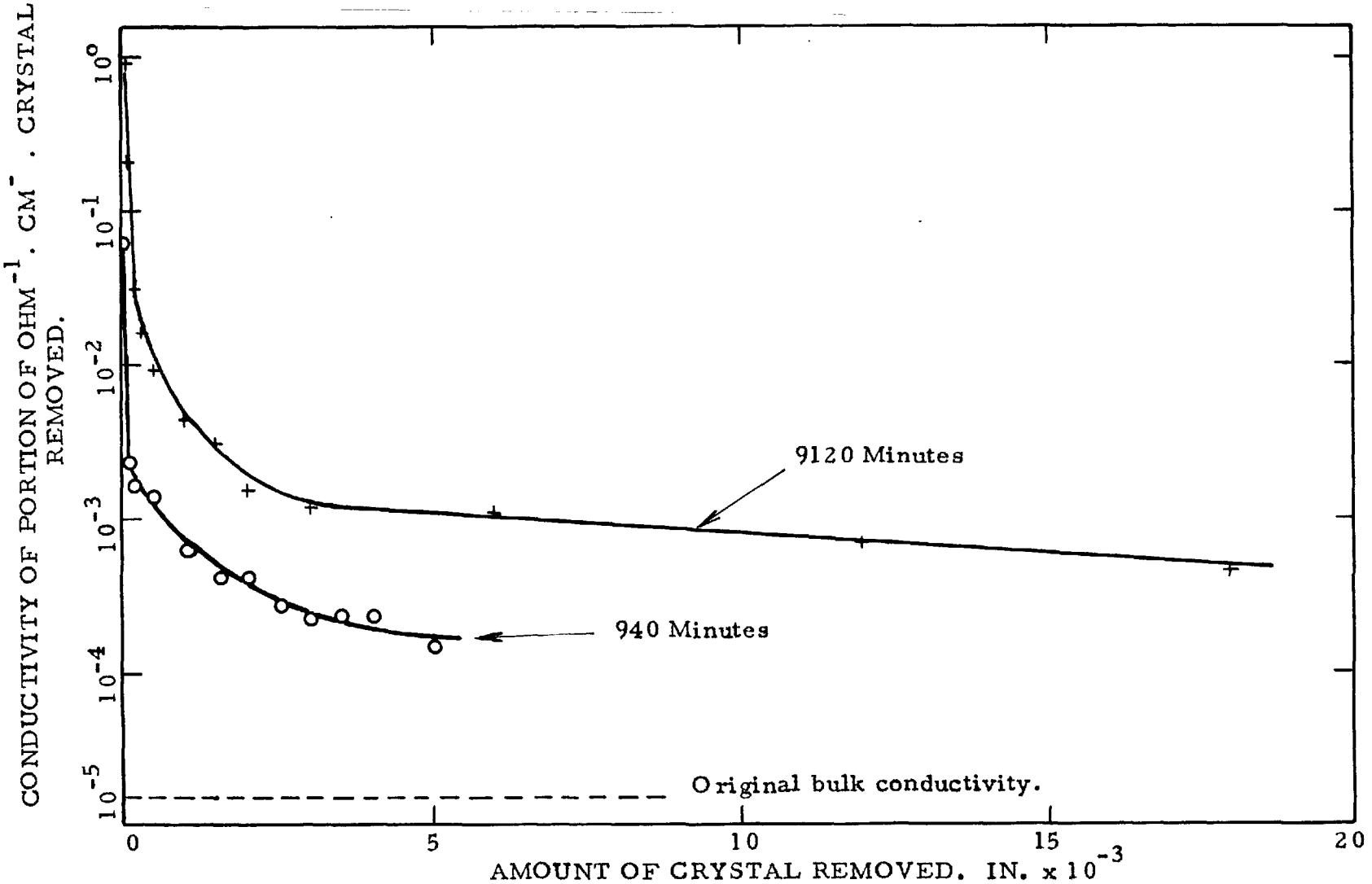

FIGURE 40. CONDUCTIVITY VS. THICKNESS PROFILES FOR CATHODICALLY TREATED RUTILE SINGLE CRYSTALS.

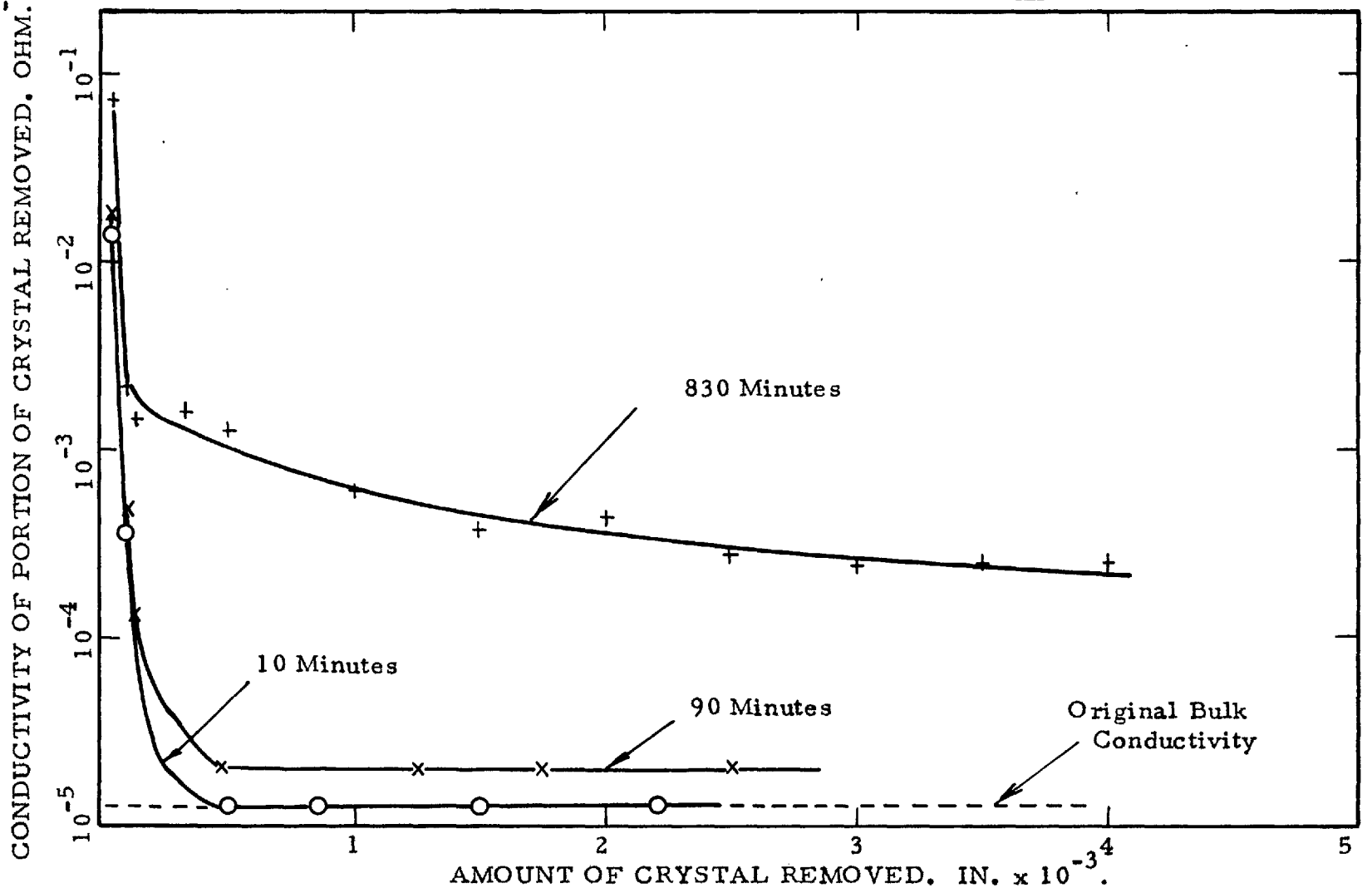

FIGURE 41. CONDUCTIVITY VS. THICKNESS PROFILES FOR RUTILE SPECIMEN "B" AFTER THREE PERIODS OF CATHODIC POLARISATION.

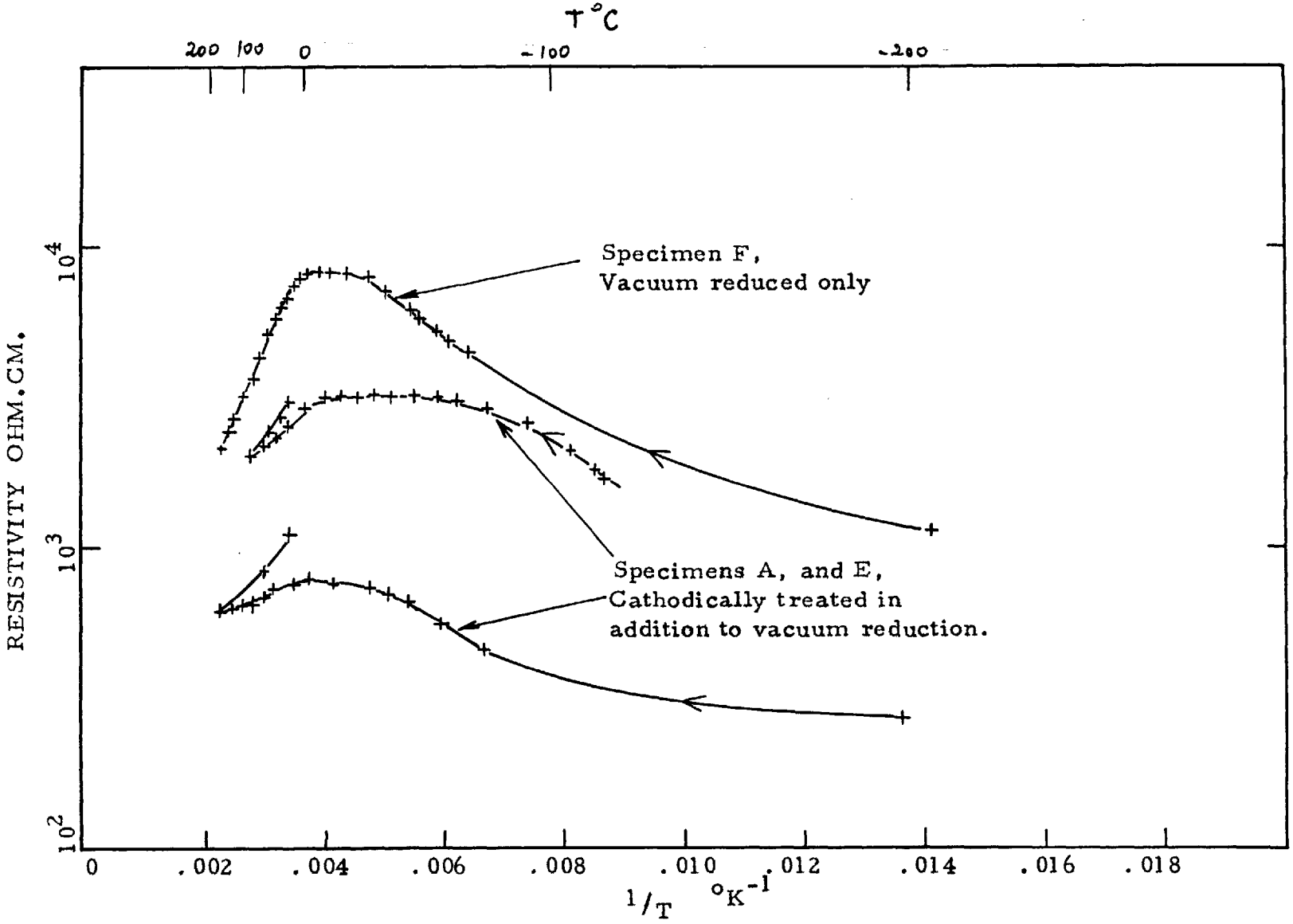

FIGURE 42. RESISTIVITY - TEMPERATURE PROFILES FOR RUTILE SINGLE CRYSTALS BEFORE AND AFTER CATHODIC TREATMENT.

[Reprinted from the Journal of Physical Chemistry, 63, 1486 (1959).]

THE SURFACE PROPERTIES OF LIQUID LEAD IN CONTACT WITH URANIUM DIOXIDE

By D. H. Bradhurst and A. S. Buchanan

Chemistry Department, University of Melbourne, Australia

Received March 10, 1959

The sessile drop technique has been used to measure surface tensions and contact angles of liquid lead on uranium dioxide surfaces. The influence on these properties of the metallic solute bismuth and the non-metallic solutes oxygen, sulfur, selenium and tellurium has been investigated. Oxygen is clearly the most effective in reducing the surface tension and contact angle of the molten lead.

Introduction

The present study forms part of an investigation on the stability of suspensions of uranium dioxide in liquid metals. As a preliminary approach to this problem it was decided to investigate the wetting of uranium dioxide by lead, and for this purpose the sessile drop technique of Humenik and Kingery[1,2] appeared admirably suited, since both contact angle of the liquid with the solid, and the surface tension of the former could be measured in the one experiment. Abrahams, Carlson and Flotow[3] have used this method for an investigation of the sodium–potassium alloy–uranium dioxide system. The sessile drop method has been adapted to the requirements of the lead–uranium dioxide system, and the influence of variables such as the constitution of the liquid, the stoichiometry of the uranium dioxide, and its density; nature and pressure of the surrounding atmosphere, and the temperature, have been investigated.

Experimental

The apparatus consisted of a 6″ by 1″ dia. molybdenum tube furnace, heated by induction and enclosed within a water-cooled Pyrex glass or silica tube. This tube was equipped with optical flats at each end, enabling the sessile drop and uranium dioxide plaque to be photographed under any desired conditions. The induction heater was of the radiofrequency type and enabled temperatures of greater than 1500° to be maintained indefinitely. The temperature was measured using a Cambridge optical pyrometer, and a Cu–advance alloy thermocouple, the latter checked in each run against the melting point of lead.

A vacuum line was connected to the furnace tube, and evacuated by a mercury diffusion pump and backing pump, giving a pressure of about 10^{-6} mm. Purified argon, carbon monoxide or hydrogen atmospheres could be introduced through a purification line consisting of a liquid oxygen trap, sodium–potassium alloy trap and two P_2O_5 drying columns.

A magnified image of the sessile drop and uranium dioxide plaque was focussed on to a photographic plate by an f4.5, 8″ focal length lens and microscopic eyepiece, mounted on an optical bench. Using an exposure of 60 seconds at f23, very sharp images were obtained. Measurements of drop dimensions and contact angle were made on traced enlargements (magnification 30 times) of these plates, and using Dorsey's[4] method of calculation, surface tensions could be reproducibly determined to within ±2%, and contact angles to within ±2°. Figure 1 shows that the measurements taken for calculation of surface tension are independent of the over-all height of the drop and its angle of contact with the plaque surface, and may be precisely determined. The equation used was

$$T = gdr^2(0.05200/f - 0.1227 + 0.0481f)$$

where

T = surface tension, dyne. cm.$^{-1}$
$f = y/r - 0.4142$
g = acceleration due to gravity, cm. sec.$^{-2}$
d = density of the lead, g. cm.$^{-3}$
r = radius of drop, cm.
y = distance from drop apex to the point of intersection of the two 45° tangents.

Lead samples (99.999%, supplied by the Metallurgy Department, University of Melbourne) were prepared in cylindrical pellet form (3.5 by 6.5 mm.) using a stainless steel punch. The lower surface of the pellet so obtained was hemispherical, ensuring a uniform advancing angle of contact on melting. The lead surface was scraped clean with a stainless steel blade before each pellet was made, after which ivory tipped forceps were used for handling. The extent of oxidation during handling was negligible. The pellet was weighed, then reweighed in the cases where surface active agents had been added. The additives were confined in a small hole drilled in the surface of the pellet and concentrations in the range 0.003 to 0.05 molal with respect to PbX (X = O, S, Se, Te) were used.

Uranium dioxide plaques were prepared by igniting "Baker's Analyzed" uranyl acetate at 1100° in air, then completely reducing the U_3O_8 formed to brown $UO_{2.00}$ in purified hydrogen at 900°. A weighed sample of this product was heated in air for 10 minutes at 200° during which time the composition was altered to $UO_{2.13}$. This non-stoichiometric oxide sinters more readily than $UO_{2.00}$,[5] and plaques of density 8.5 to 9.3 were obtained by cold pressing at 100,000 p.s.i. and sintering at 1400–1500° in dynamic vacuum of approximately 10^{-3} mm. For the study of the effect of plaque density on surface tension and contact angle, specially prepared samples of uranium dioxide of density 10.8 were obtained from the Industrial Group, U. K. Atomic Energy Authority.

The plaque surfaces were ground flat and lightly polished on a silicon carbide stone, then reduced to stoichiometric UO_2 prior to each run as described above. The plaque and preweighed pellet were inserted into the molybdenum susceptor of the induction furnace and levelled horizontally and

(1) M. Humenik and W. D. Kingery, This Journal, **57**, 359 (1953).

(2) W. D. Kingery, USAEC report, NYO-3144.

(3) B. M. Abrahams, R. D. Carlson and H. E. Flotow, USAEC report, NESC-104, 1957.

(4) N. E. Dorsey, *J. Wash. Acad. Sci.*, **18**, 505 (1928).

(5) P. Murray, E. P. Rodgers and A. E. Williams, AERE report, M/R-893, 1952.

longitudinally with the aid of a cathetometer. The furnace was evacuated and then heated to a temperature of 750°, to assist degassing. Photographs were taken at 700, 750, 600 and 500° and were spaced at intervals of 30, 45, 50 and 60 minutes, respectively.

Photomicrographs of the plaque surface and features of the lead surface, were taken when necessary at the completion of a run and the solidified drop was checked for uniform diameter.

Results

The initial work was concerned with the measurement of surface tension of lead–bismuth alloys as a function of composition, and Fig. 2. shows the isotherm obtained for 700°. The relationship appears to be linear as was also found for the Fe–Ni system at higher temperatures.[2] An interesting result which emerged from this work was evidence for the sensitivity of both surface tension and contact angle of lead towards oxygen present as dissolved oxide. Figure 3 shows two contact angle *vs.* composition curves obtained in atmospheres of hydrogen and cylinder argon, respectively. The cylinder argon used at the time contained some oxygen, as shown by the blackening of the UO_2 surface surrounding the solidified drop, and the appearance of microcrystalline tetragonal lead oxide on the lead surface after solidification.[6] In hydrogen at 700°, uranium dioxide would be present as $UO_{2.00}$ and any PbO would be reduced to lead. The lower contact angle with the argon atmosphere was almost certainly due to oxygen dissolved in the liquid phase, the effect obviously being much less for bismuth than for lead. Subsequent work on the addition of lead oxide to the liquid lead has confirmed this explanation. Furthermore, an order of surface activity has been established for lead oxide, lead sulfide, lead selenide and lead telluride dissolved in liquid lead. Figure 4 shows the surface tension isotherms for these solutes, while Table I gives the order of surface activity and indicates clearly the unique position of oxygen as a solute.

TABLE I

System	Maximum reduction in surface tension % at 750°, dyne cm.$^{-1}$	Work of adhesion in contact with $UO_{2.00}$, dyne cm.$^{-1}$
Pure Pb		61.4
PbO + Pb	22.2	198.0
PbS + Pb	7.0	137.0
PbSe + Pb	5.0	132.0
PbTe + Pb	2.5	133.0

Oxygen present in non-stoichiometric forms of uranium dioxide in the range $UO_{2.00}$ to $UO_{2.67}$ was converted to lead oxide by the molten lead, and produced similar depressions in surface tension and contact angle to those obtained by direct additions of lead oxide.

Surface tension and contact angle were found to be independent of the density of the uranium dioxide plaque, identical values being obtained for plaques of density 6.5, 9.3 and 10.8.

Discussion

The surface activity of the solute elements has been shown to be in the order O>>S>Se≃Te (Table I and Fig. 4). The considerable effect of the first member of this series in lowering the surface free energy of liquid lead indicates an appreciable excess concentration of solute species in the surface of the liquid, and moreover, the entities in the surface must have a significantly lower field of force than that operating between the atoms of the liquid lead. This suggests that the PbO dissolved in the lead has an appreciable covalent character in its bonding. In additional support of this view is the fact that the solubility of oxygen in lead is relatively low (Table II), and furthermore it has been observed in the present experiments that PbO comes out of solution in the liquid lead when the temperature is reduced; its solubility must therefore be quite inappreciable at low temperatures.

(6) D. H. Bradhurst and A. S. Buchanan, to be published.

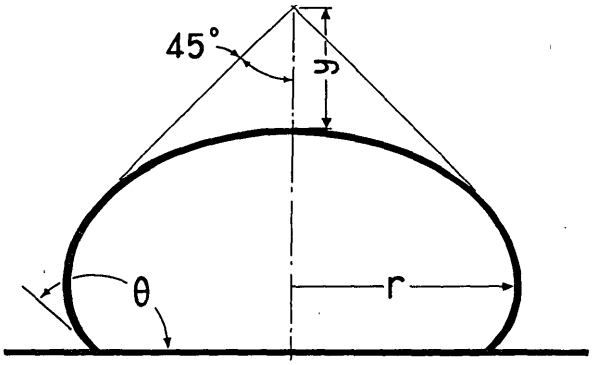

Fig. 1.—Profile of a typical sessile drop showing the measurements made for calculation of surface tension.

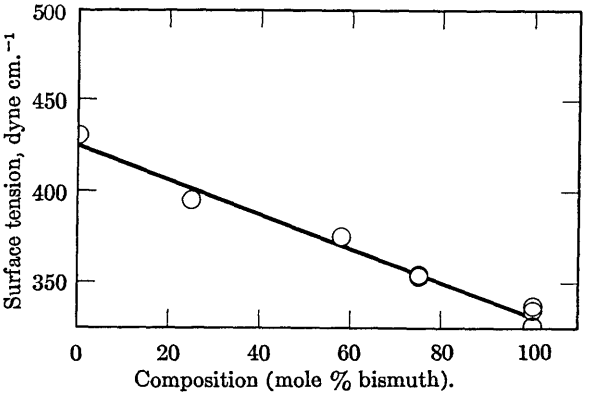

Fig. 2.—Surface tension *vs.* composition isotherm for lead-bismuth alloys at 700°.

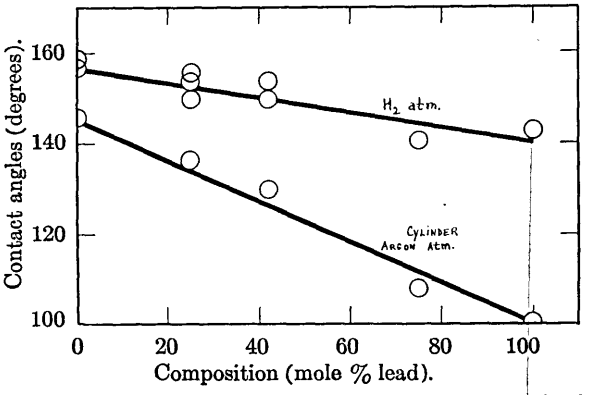

Fig. 3.—Two contact angle *vs.* composition curves of different slopes for lead-bismuth alloys in hydrogen and cylinder argon atmospheres.

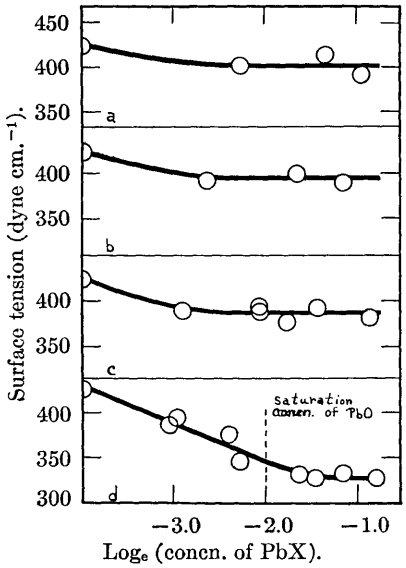

Fig. 4.—Surface tension *vs.* concentration isotherms for lead containing solutes (a) PbTe, (b) PbSe, (c) PbS, (d) PbO, at 750°. Note that the maximum depression in surface tension in (d) corresponds approximately to the saturation concentration of PbO at this temperature.

TABLE II

Solute	Solubility in liquid lead at 750°, wt. %[7,8]
O	0.20
S	0.46
Se	2.5
Te	10.8

The order of surface activity described above does not appear to be the same in all metals, *e.g.*, in liquid iron, the order is O<S<Se>>Te.[9]

It may be noted from Fig. 4 that the maximum lowering of surface tension of lead with oxygen as a solute coincides approximately with the saturation concentration[7] of the solution at the experimental temperature. If indeed the surface activity of oxygen dissolved in liquid lead is associated with appreciable covalent character of the bonding in PbO, then it is surprising that the other members of the solute series S, Se, Te, display so little surface activity since the larger ions $S^{=}$, $Se^{=}$, $Te^{=}$, should be more readily polarized by Pb^{++}, giving enhanced covalent character to the bonding. Even if the solute species consisted largely of independent ions S″, Se″, Te″, the considerable size of these entities should mean that they are difficult to accomodate within the bulk of the liquid lead and should therefore exhibit surface activity (Table III).

TABLE III

Species	Radius, Å. Covalent	Radius, Å. Ionic (X″)	Ionization potential[10] for loss of 1 electron (e.v.)
Oxygen	0.74	1.4	13.61
Sulfur	1.04	1.8	10.36
Selenium	1.17	1.98	9.75
Tellurium	1.37	2.2	8.96
Lead (Pb^{++})		1.2	

The relative lack of surface activity of the solutes S, Se, Te, appears to be associated with increasing metallic character, particularly in the case of the latter two. This leads to enhanced solubility (Table II) with less tendency to form a surface layer in the liquid. We have observed in the present experiments that PbS, PbSe and PbTe dissolve very rapidly in the liquid lead, and moreover, do not come out of solution appreciably when the lead is cooled, in comparison to PbO as a solute (although Greenwood[11] has observed the formation of very small PbS crystals on a solidified lead surface, using a magnification of 900 times).

The metallic character of selenium and tellurium particularly in the molten state[12] is undoubted, the elements both existing in a metallic form which exhibits slight electronic conductivity and appreciable photoconductivity, indicating ready excitation of electrons to the conduction bands (*cf.* ionization energies in Table III). Furthermore, the compounds PbS, PbSe and PbTe all exhibit electronic conductivity, the electronic mobilities being PbS 640, PbSe 1400 and PbTe 2100 cm.^{2}/volt sec. and associated with this is the metallic appearance of these compounds. It is likely therefore that the solutes S, Se and Te are readily accommodated in the bulk of the liquid lead, existing either as a solution of neutral atoms, or more probably, with some transfer of electrons to the conduction bands of the liquid metal. It may be noted in this respect that the covalent radii of Se and Te in particular are close to the radius of Pb^{++}.

As the works of adhesion indicate (Table I), the solute oxygen is the most effective in enhancing the wetting of UO_2 by liquid lead, but this effect is not considerable until quite high temperatures are attained. There is therefore some advantage in having traces of oxygen in liquid lead where wetting of oxide surfaces is desired.

This work was supported by a grant from the Australian Atomic Energy Commission, and forms part of a program of work on the surface chemistry of liquid metal systems.

(7) F. D. Richardson and L. E. Webb, *Trasn. Inst. Min. and Met.*, **64**, 529 (1955).

(8) M. Hansen, "Constitution of Binary Alloys," McGraw-Hill Book Co., Inc., New York, N. Y., 2nd ed., 1958, pp. 1099–1112.

(9) W. D. Kingery, THIS JOURNAL, **62**, 878 (1958).

(10) Landolt and Börnstein, "Zahlwerte und Funktionen aus Chemie," Vol. 1, Part 1, pp. 211–212.

(11) J. N. Greenwood and H. W. Worner, *J. Inst. Metals*, **65**, 435 (1939).

(12) W. Klemm, *Proc. Chem. Soc.*, 329 (1958).

Reprinted from the
AUSTRALIAN JOURNAL OF CHEMISTRY
VOLUME 14, NUMBER 3, PAGES 409–416, 1961

SURFACE PROPERTIES OF MOLTEN BISMUTH–BISMUTH CHLORIDE IN CONTACT WITH URANIUM DIOXIDE

By D. H. Bradhurst and A. S. Buchanan

SURFACE PROPERTIES OF MOLTEN BISMUTH–BISMUTH CHLORIDE IN CONTACT WITH URANIUM DIOXIDE

By D. H. BRADHURST and A. S. BUCHANAN*

[*Manuscript received February* 15, 1961]

Summary

The wetting of uranium dioxide by liquid bismuth has been investigated by means of measurements of surface tension of the liquid and contact angle of the liquid on the solid. Bismuth chloride in low concentration was found to be a very effective surface active agent in improving the wetting of the solid by the metal.

I. INTRODUCTION

In general pure liquid metals and alloys do not wet oxide surfaces. On the other hand, appreciably improved wetting can be achieved by the solution of certain non-metallic elements in the metal phase. Oxygen has proved to be one of the more effective surface active solutes in this respect and contact angles of less than 90° can be attained in certain cases. Whilst this phenomenon is of some assistance in securing a stable dispersion of an oxide in a liquid metal, the effects are frequently of insufficient magnitude and other more effective non-metallic solutes were therefore sought. Recent work on the miscibility of metal–molten salts (Cubicciotti 1953 ; Bredig 1955, 1956 ; Grjotheim, Grønvold, and Krogh-Moe 1955 ; Corbett 1957 ; Ohlberg 1958) indicated that certain of these systems might be suitable. The bismuth–bismuth chloride system was investigated from the point of view of its surface tension and contact angle on oxide surfaces and hence of its ability to wet these surfaces. Bismuth trichloride shows appreciable solubility (a fraction of 1 mole %) in metallic bismuth at temperatures above the melting point of the latter (271 °C). As the temperature is increased the range of solubility increases and is of the order of several mole % at 500 °C. At higher concentrations of bismuth trichloride there is an extensive range of composition in which two mutually saturated liquid phases exist and complete solution is only attained at a temperature of the order of 800 °C (Yosini *et al.* 1959).

II. EXPERIMENTAL

(*a*) *Preparation of Bismuth–Bismuth Trichloride Sample*

Dehydration of bismuth chloride was achieved by repeatedly melting bismuth chloride (B.D.H.) under vacuum in a round-bottomed distillation flask equipped with a side arm and sample tube constricted at the inlet. Part of the material was then distilled into the sample tube under approximately 40 cm pressure of dried argon. The tube was sealed and samples obtained were subsequently handled in a dry box. The bismuth chloride prepared in this way had a melting point of approximately 235 °C and was of satisfactory purity for the

* Chemistry Department, University of Melbourne.

surface tension measurements which were made using the maximum bubble pressure method.

The bismuth–bismuth chloride samples used in the contact angle measurements were prepared by introducing a sample of bismuth chloride into a preweighed silica sample tube containing a weighed amount of pure bismuth and the weighed solid specimen of uranium dioxide and then sealing under argon using an oxy-gas torch. Check analyses for chloride showed that the amount of hydrolysis which occurred during the sealing process was negligible.

(b) Measurements of Surface Tension and Contact Angle

Surface tensions at the bismuth chloride end of the system were measured by the maximum bubble pressure technique. The apparatus consisted of a Pyrex vessel containing the Bi–$BiCl_3$ mixture immersed in a bath of molten sodium nitrate–potassium nitrate. A Pyrex capillary tube passed through the stopper and the tube could be raised or lowered precisely by means of a brass stop and micrometer screw gauge firmly clamped to a steel vacuum frame. The vessel was connected to the vacuum and gas purification line. Bismuth trichloride was first distilled into this vessel as described above, and argon was admitted to atmospheric pressure. The stopper containing the capillary assembly was then inserted, the lower half of the tube placed in the molten-salt bath, and the vessel evacuated, and refilled with argon. When the temperature was steady at the value required for measurement, the capillary tip was lowered into the surface and argon or nitrogen was passed through at a rate corresponding to the formation of one bubble per 6–7 sec. The maximum pressure p_m just before the " breakaway " point was measured with a *m*-xylene (density 0·859 g cm^{-3}) manometer having a mirror-backed scale. The optimum depth of immersion of the capillary tip proved to be about 0·02 cm.

The surface tension was calculated from the formula

$$\gamma=\tfrac{1}{2}r(h_2\rho_{2g}-h_1\rho_{1g}),$$

where r=average radius (cm) of the capillary (measured by a travelling microscope),
h_1=depth of tip below liquid surface (cm),
ρ_1=density of liquid (g cm^{-3}),
h_2=difference in manometer liquid heights (cm),
ρ_2=density of manometer liquid (g cm^{-3}).

The capillaries were prepared by drawing out Pyrex tubing in an oxy-gas flame, scratching the surface with a file, and snapping the capillary. After several attempts, a tip could be prepared which was perpendicular to the bore of the tube. Tips prepared in this way, as others have found (Boardman, Palmer, and Heymann 1948), have a sharper circumference than ground tips, and give a cleaner, more definite " breakaway " point.

Measurements of contact angle were carried out by taking photographs of a plate of uranium dioxide dipping into the liquid phase of a bismuth–bismuth trichloride melt, enclosed in either a Pyrex glass or silica tube. The tubes were sealed under approximately 1 atm of argon, as described above.

These tubes were heated in a cruciform tube furnace, permitting observation at elevated temperatures. Photographs were taken using an f4·5 anastigmatic lens, and quarter-plate camera mounted on an optical bench. Photographs of the profile of the UO_2 plaque in the liquid were taken at 300 and 800 °C for a series of bismuth–bismuth trichloride mixtures ranging in composition from 0–100% bismuth.

III. Results

The values obtained for the maximum bubble pressure in molten bismuth trichloride showed a gradual increase for any one set of readings (Table 1). However, replacement of the cleaned and dried capillary tip gave the original values, suggesting that the rise was probably due to constriction of the capillary by deposited material. The Pyrex glass was wetted by the molten bismuth trichloride, and appreciable capillary rise was observed when the capillary tip first touched the liquid surface. The minimum pressure was therefore taken to be the most reliable and the results shown in Table 1 compared favourably with previous values (Jaeger and Kahn 1916).

Table 1

CALIBRATION OF CAPILLARY FOR MAXIMUM BUBBLE PRESSURE MEASUREMENTS OF SURFACE TENSION

Substance	Maximum Bubble Pressure (cm *m*-xylene)	Temperature (°C)	γ (dyne cm^{-1})	Time (min)
$BiCl_3$	4·21	286	66·9±0·3	3
	4·21	288	66·9	5
	4·75	286	74·9	10
	4·19	285	66·1±0·3	3
	4·19	289	66·1	5
	4·47	290	70·4	9
H_2O	4·68	15	73·3±0·3	—
	4·70	15	73·5±0·3	—

This method was used for bismuth–bismuth trichloride mixtures at 300 °C and, as shown in Table 2, there was little change in surface tensions up to 24 mole % bismuth.

At the bismuth-rich end of the phase diagram, maximum bubble pressure measurements were carried out at temperatures up to 320 °C but a slightly more elaborate purification procedure was required in order to prevent oxidation of the molten bismuth. The cylinder nitrogen used in these experiments was dried by passing it through a liquid air trap and phosphorus pentoxide column.

Oxygen was then removed by a second column containing magnesium turnings, electrically heated to 400 °C. This procedure ensured the maintenance of a bright metal surface during measurements and individual readings remained

constant indefinitely. The surface tension *v.* concentration isotherm obtained at 300 °C is shown in Figure 1. Due to the large miscibility gap which exists at this temperature no measurements could be performed in the range 40–98 mole % bismuth.

TABLE 2

SURFACE TENSION OF BISMUTH–BISMUTH TRICHLORIDE MIXTURES

Bismuth (mole %)	Surface Tension (dyne cm^{-1})	Temperature (°C)
0	66·1±0·3	272
10·0	66·3±0·3	283
24·4	66·9±0·3	272

The 300 °C isotherm was used to estimate the surface excess concentration of solute, and the area per molecule by the application of the Gibbs adsorption isotherm (see Fig. 2).

Bismuth trichloride proved a very effective solute in reducing the contact angle of molten bismuth on UO_2. The contact angle was reduced to zero on addition of about 5 mole % of bismuth trichloride, and the wetting was irreversible

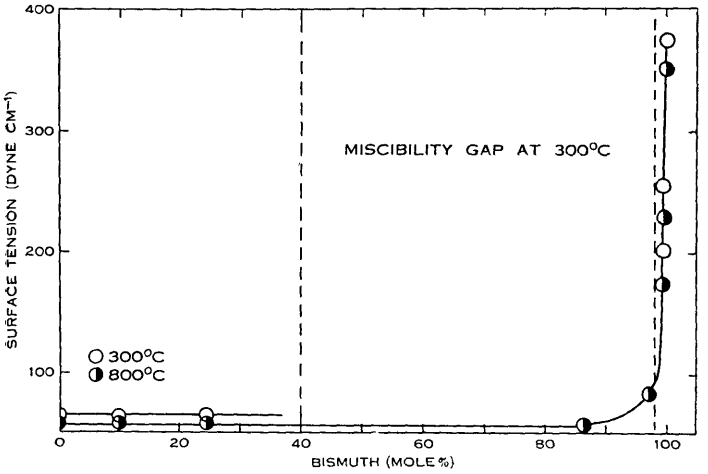

Fig. 1.—Surface tension isotherms for bismuth–bismuth trichloride at 300 and 800 °C.

as has been observed in other systems studied (Bradhurst 1960). Figure 3 shows three photographs of the contact angle between UO_2 and different Bi–$BiCl_3$ melts, illustrating wetting and non-wetting values, and Figure 4 shows the isotherms obtained for contact angle *v.*. composition, at 300 and 800 °C respectively.

Above 300 °C the mixtures consisted of a two-phase liquid with bright metallic bismuth at the bottom and a dark salt-rich phase at the top. For

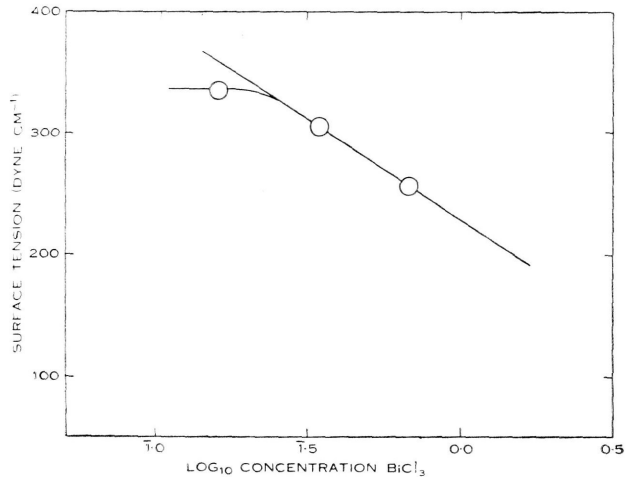

Fig. 2.—Gibbs adsorption isotherm for bismuth–bismuth trichloride at 300 °C. Slope = —164 ; $\Gamma = 9 \cdot 1 \times 10^{14}$ molecules cm^{-2}.

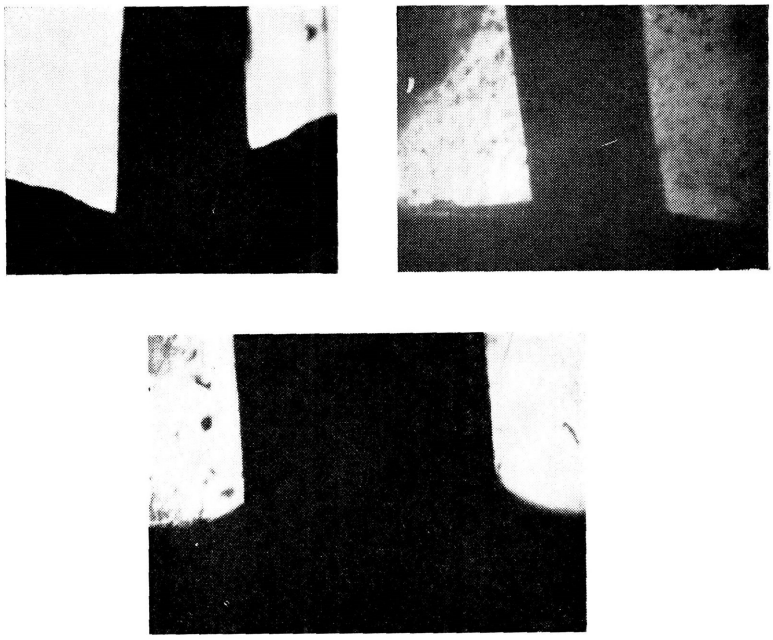

Fig. 3.—Photographs of the contact angle of bismuth–bismuth trichloride on uranium (in the form of compressed plates inserted in the melt). Reduction in contact angle is shown with increasing bismuth trichloride concentration from top to bottom on photographs.

metal-rich mixtures the whole liquid became bright and metallic as the miscibility gap was passed on heating. The dark salt-rich phase reappeared on cooling and the observation of this transitional point was used by Yosini to construct the phase diagram for the system.

During each determination, the silica tube walls remained very clean, showing that there must have been very little of the mixture existing in the vapour phase, as the partial pressure due to argon alone was approximately 4 atm at 800 °C. Some difficulty was experienced with optical distortion due to the slightly striated silica tube walls, but the contact angle could still be determined in the better photographs to within $\pm 2°$.

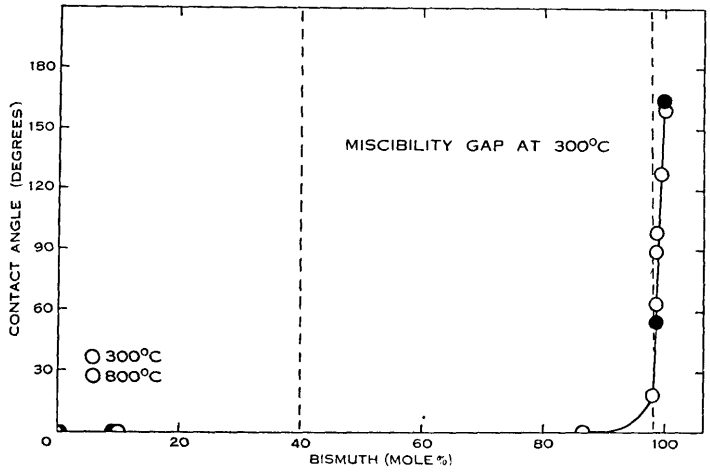

Fig. 4.—Isotherms for the contact angle of bismuth–bismuth trichloride melts on uranium dioxide at 300 and 800 °C.

IV. Discussion

A considerable amount of work has been done in recent years on bismuth–bismuth halide systems (Corbett 1958*a*, 1958*b*; Cubicciotti 1958; Cubicciotti and Keneshea 1958; Yosini *et al.* 1959), but very little has been done on metal-rich mixtures, or at temperatures above 400 °C, apart from phase studies alone. In other systems which we have studied, such as metal–metal oxides, surface activity was definitely present (Addison 1954; Livey and Murray 1955; Bradhurst and Buchanan 1959) but the oxide was usually so insoluble that the metal was saturated before appreciable reduction in surface tension or contact angle had occurred. On the other hand in the bismuth–bismuth trichloride–uranium dioxide system complete wetting by pure bismuth trichloride was replaced by almost complete non-wetting for pure bismuth, as the composition changed from 0–100% bismuth, and from the isotherms of Figures 1 and 4 it is apparent that bismuth trichloride must be strongly surface active when dissolved in molten bismuth.

Wetting of UO_2 by liquid bismuth trichloride is not surprising in view of its relatively low surface tension (66 dyne cm^{-1}) and its surface activity in

molten bismuth will be due to the great difference in surface tensions of the two substances (surface tension of bismuth is 380 dyne cm^{-1} at 300 °C). In the mixed liquid the surface is probably almost entirely composed of bismuth trichloride and, in effect, a non-metallic chloride surface is presented to the UO_2 which itself probably has a surface composed largely of oxide ions (Livey and Murray 1955).

Vapour pressure and partial molal volume measurements (Cubicciotti 1958 ; Cubicciotti and Keneshea 1958) on bismuth trichloride–bismuth systems have shown that marked positive deviations from Raoult's law occur at 400 °C as bismuth is added to molten bismuth trichloride and that the volume of the system decreases initially when Bi is added to $BiCl_3$. Early work on conductivities by Aten (1909) showed that the conductivity of bismuth trichloride increased initially with the addition of metallic bismuth. It is also known (Corbett 1958*a*, 1958*b*) that salt-rich solutions are diamagnetic. The two main schools of thought on the nature of the species existing in these solutions have been due to Corbett (1958*a*, 1958*b*), whose work supports polymers of the type $(BiCl)_n$, and Cubicciotti (1958), who has postulated the existence of Bi_n^{+m} polymers. This second postulate is supported by the conductivity, magnetic, and volume measurements. The species Bi_2 has been identified in the gaseous phase (Bracket and Brewer 1954, USAEC report), and dissolved in lead (Kelley 1936). On the other hand, stoichiometric BiCl has been identified as a component of bismuth trichloride–bismuth melts below 327 °C, and the polymeric form Bi_2Cl_4 has been used (Corbett 1958*a*, 1958*b*) to explain the positive deviations from Raoult's law observed by Cubicciotti.

Recent measurements (Cubicciotti 1958) of partial molal volumes of bismuth and bismuth trichloride have led to postulates of a chloride " quasi-lattice " (again at temperatures less than 400 °C) which can incorporate added bismuth in " octahedral holes ". Using calculated values of ionic radii it has been shown that this model may be adapted to explain the changes in partial molal volume of bismuth in bismuth trichloride for limited ranges of temperature and concentration. In the metal-rich miscible range at 300 °C added chloride ion would likewise be fitted into octahedral holes with only a small expansion in the liquid bismuth " quasi-lattice ".

The pronounced surface activity of chloride found in the present work indicates that this ion is not easily accommodated within the liquid metal " lattice ", and expansion at elevated temperatures is required for this purpose. However, in the work on liquid lead (Bradhurst and Buchanan 1959) and the solutes O, S, Se, and Te it was observed that the least readily accommodated species, oxygen (having the greatest non-metallic character) was the solute exhibiting the most pronounced surface activity. The lack of metallic character would appear to be of considerable importance in the present case also since both chloride ions and chlorine atoms could be readily accommodated in the bismuth lattice with very little expansion, and hence size of the species concerned cannot be the only criterion of miscibility (Table 3).

Application of the Gibbs adsorption isotherm to the measurements on the reduction in surface tension with increase of bismuth chloride concentration at

300 °C (Fig. 2) in the 98–100% bismuth region gives an area per surface molecule of about 11 Å^2. The area for the chloride ion is about 10·3 Å^2. This procedure is very approximate but provides some support for the view that the surface species may be chloride ions or oriented BiCl ion pairs in view of the other evidence for entities of this kind.

TABLE 3
RADII OF POSSIBLE SPECIES IN BISMUTH–BISMUTH TRICHLORIDE

Species	Bi	Cl^-	Cl
Radius (Å) (Bragg 1937)..	1·78	1·81	0·99

The high electronegativity of chlorine (3·0 on Pauling's scale) gives something of a measure of its non-metallic character and inability to yield electrons to the conduction bands of the molten bismuth and hence become easily assimilated in the metallic medium. Oxygen on the same scale has an even higher electronegativity (3·5) and displays surface activity in liquid metals although limited by its quite low solubility in this respect.

V. REFERENCES

ADDISON, C. C. (1954).—*J. Chem. Soc.* **1954**: 2861.
ADDISON, C. C. (1955).—*J. Chem. Soc.* **1955**: 2262.
ATEN, A. (1909).—*Z. Phys. Chem.* **66**: 641.
BOARDMAN, N. K., PALMER, A. R., and HEYMANN, E. (1948).—*Trans. Faraday Soc.* **51**: 259.
BRACKET, E., and BREWER, L. (1954).—USAEC Rep. UCRL 3712.
BRADHURST, D. H. (1960).—M.Sc. Thesis, Melbourne.
BRADHURST, D. H., and BUCHANAN, A. S. (1959).—*J. Phys. Chem.* **63**: 1486.
BRAGG, W. L. (1937).—"Atomic Structure of Minerals." (Oxford Univ. Press.)
BREDIG, M. A. (1955).—*J. Amer. Chem. Soc.* **77**: 1454.
BREDIG, M. A. (1956).—Proc. 3rd Symp. High Temperature, Berkeley.
CORBETT, J. D. (1957).—*J. Amer. Chem. Soc.* **79**: 3020.
CORBETT, J. D. (1958*a*).—*J. Amer. Chem. Soc.* **80**: 4757.
CORBETT, J. D. (1958*b*).—*J. Phys. Chem.* **62**: 1149.
CUBICCIOTTI, D. (1953).—USAEC Rep. AECD 3623.
CUBICCIOTTI, D. (1958).—*J. Phys. Chem.* **62**: 843.
CUBICCIOTTI, D., and KENESHEA, F. J. (1958).—*J. Phys. Chem.* **62**: 463.
GRJOTHEIM, K., GRØNVOLD, F., and KROGH-MOE, F. (1955).—*J. Amer. Chem. Soc.* **77**: 5824.
JAEGER, F. M., and KAHN, J. (1916).—*Proc. Acad. Sci. Amst.* **19**: 381–97.
KELLEY, K. K. (1936).—Bull. U.S. Bur. Min. No. 393.
LIVEY, D. J., and MURRAY, P. (1955).—*Plansee Proc.* **1955**: 375–404.
OHLBERG, S. M. (1958).—USAEC Rep. NAA-SR-2939.
YOSINI, T. J. ET AL. (1959).—*J. Phys. Chem.* **63**: 230.

Reprinted from the
AUSTRALIAN JOURNAL OF CHEMISTRY
VOLUME 14, NUMBER 3, PAGES 397–408, 1961

SURFACE PROPERTIES OF LIQUID SODIUM AND SODIUM–POTASSIUM ALLOYS IN CONTACT WITH METAL OXIDE SURFACES

By D. H. Bradhurst and A. S. Buchanan

SURFACE PROPERTIES OF LIQUID SODIUM AND SODIUM–POTASSIUM ALLOYS IN CONTACT WITH METAL OXIDE SURFACES

By D. H. BRADHURST* and A. S. BUCHANAN*

[*Manuscript received February* 15, 1961]

Summary

Dissolved oxygen was shown to be surface active in liquid sodium from measurements of surface tension and of contact angle of the liquid on various oxide surfaces. When sufficient oxygen was present wetting of UO_2 by liquid sodium could be brought about at temperatures above approximately 300 °C. Observations on the wetting of several solid oxides by sodium gave some support to the hypothesis that wetting was more effective on those oxides with larger cations. Sodium–potassium alloys showed non-wetting contact angles when relatively free of oxygen but wetting occurred when the oxygen content of the liquid was increased.

I. INTRODUCTION

The ability of a liquid metal to wet an oxide surface has recently become of interest in nuclear reactor technology, where the production of a stable suspension of nuclear fuel uranium dioxide in a medium of high thermal conductivity such as a liquid metal could form the basis of a homogeneous reactor.

As a preliminary approach to the problem the wetting of uranium dioxide by lead was studied (Bradhurst and Buchanan 1959*a*) by a sessile-drop technique similar to that used by Humenik and Kingery (1953).

It was found that oxygen had a significant surface active effect in molten lead, and the present study is an extension of this work to include molten sodium and sodium–potassium alloy. The dependence of the surface tension and contact angle of these liquid metals on such variables as the liquid constitution, nature of the solid oxide, type of atmosphere, and temperature has been investigated.

II. EXPERIMENTAL

Measurements of surface tension by the sessile-drop technique were carried out by focusing a magnified image of the liquid metal drop (on a prepared oxide plaque) on to a photographic plate. An f4·5 8-in. focal length lens was used in conjunction with a microscopic eyepiece and bellows mounted on an optical bench. Using an exposure of 60 sec at f23 very sharp images were obtained. Measurements of drop dimensions and contact angle were made on traced enlargements (magnification 30 times) of these plates, and using Dorsey's (1928) method of calculation surface tensions could be reproducibly determined to within ± 4–5%. Contact angles were determined to within $\pm 2°$.

*Chemistry Department, University of Melbourne.

The measurements required for calculating surface tension are independent of the overall drop height and its angle of contact with the oxide surface. The equation used was

$$T=gdr^2(0\cdot05200/f-0\cdot1227+0\cdot0481f), \quad (1)$$

where T=surface tension (dyne cm^{-1}),
$f=y/r-0\cdot4142$,
g=acceleration due to gravity (cm sec^{-2}),
d=density of the liquid metal (g cm^{-3}),
r=drop radius (cm),
y=distance from the drop apex to the point of intersection of the two 45° tangents.

The alkali metals studied (sodium and sodium–potassium alloy) were handled by two different techniques.

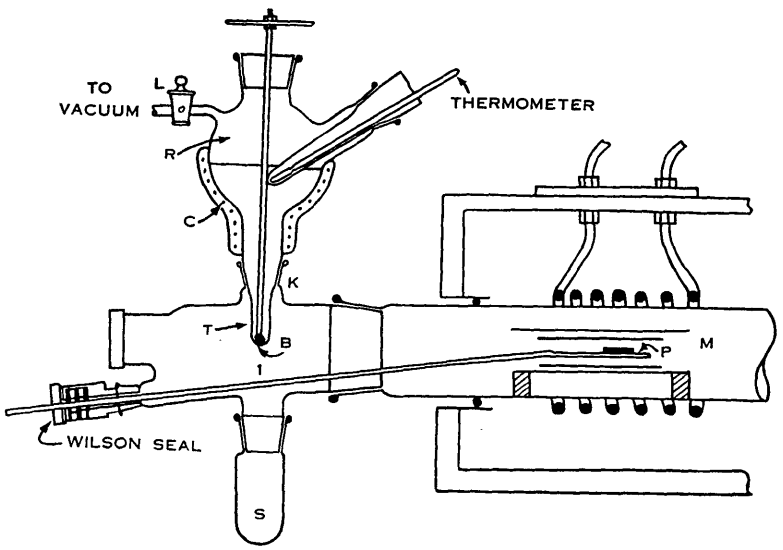

Fig. 1.—The sessile-drop apparatus for measuring surface tension and contact angle with liquid alkali metals.

(a) *Dynamic Vacuum Technique*

The apparatus consisted of a 6 by 1 in. diameter molybdenum tube furnace, heated by induction and enclosed within a water-cooled Pyrex glass tube. This tube is shown in Figure 1, together with the apparatus for introduction of the liquid alkali metals.

A vacuum line was connected to the furnace tube, and evacuated by a mercury diffusion pump, cold trap, and backing pump, giving a pressure of about 5×10^{-6} mmHg. Purified argon, hydrogen, or carbon monoxide atmospheres could be introduced through a purification line consisting of a liquid air trap, a column of heated magnesium turnings, and two P_2O_5 drying columns.

The reservoir, R, and the furnace tube containing the sliding platform, P, were evacuated to the limit of the pumping system and the susceptor and oxide

plaque were thoroughly degassed by heating in vacuum to 700 °C. The platform containing the plaque was then moved to a position just below T, and by means of the heating coils, C, on the alkali metal reservoir the temperature was raised sufficiently to ensure that the metal was molten down to the introduction tip, T (120–130 °C for sodium). A Teflon sleeve was used at K, lightly lubricated with Silicone vacuum grease, and proved satisfactory at the temperatures used.

By means of the ball valve, B, liquid metal was allowed to pass into the sampling tube, S, until a steady and controllable dropping rate was obtained. A single drop was then allowed to fall on the prepared oxide surface.

The platform was then moved carefully into the centre of the furnace, and levelled with the aid of a cathetometer focused on the image of the drop on the glass screen of the camera. A series of photographs of plaque and drop was then taken at different temperatures.

The liquid metal contained dissolved oxide approximately equal to the saturation concentration at the temperature of introduction. Excess oxide remained in the reservoir as a skin on the surface of the metal and the drops drawn off from the dropping tip beneath were always bright and free of bulk oxide.

The brightness of the metal surface was found to be a sensitive indicator of the presence of oxygen, and at pressures greater than 10^{-3} mmHg (McLeod gauge) perceptible dulling of the surface of liquid sodium occurred. This was undoubtedly due to small quantities of desorbed oxygen from the cold walls of the furnace tube and the susceptor itself, which although not affecting the total pressure of the system appreciably were sufficient to form a significant amount of oxide on the surface of the comparatively small sample. Providing a vacuum of 10^{-5} mmHg or better could be maintained in the furnace tube, the metal surface remained bright indefinitely (a period of greater than 28 hr was recorded for Na–K alloy) and no difficulty was experienced in making measurements.

Figure 5 (*b*) shows a series of photographs of molten sodium, on stoichiometric uranium dioxide, achieved by this method.

(*b*) *Sealed-Tube Technique*

It was found necessary to use sealed-tube techniques in order to study contact angles at temperatures greater than approximately 250 °C, as volatilization of the molten sodium was too rapid *in vacuo* above this temperature and clear photographs could not be taken. Furthermore, even in a purified argon atmosphere (argon passed through heated Mg turnings) there was sufficient residual oxygen in the system, either from the argon itself, or from outgassing of the cooled Pyrex walls of the furnace tube, to form appreciable amounts of oxide on the surface of the molten metal, which itself acted as an extremely efficient oxygen getter above 250 °C.

This problem was overcome by using the apparatus shown in Figure 2. It consisted of a simple Pyrex tube with a bulb blown at one end, and a side arm into which was sealed a metal oxide plaque. A sample of B.D.H. commercial sodium was cut from the centre of a block, introduced into the bulb, and the

tube quickly evacuated to 10^{-5} mmHg. The tube was flame heated to degas the walls, and, if necessary (as in the case of UO_2) the oxide surface was heated in hydrogen to approximately 500 °C to remove the oxygen in excess. The sodium was then melted and distilled carefully under vacuum by flame heating until a sample of clean bright sodium rested on the glass wall at position *C*. During the distillation, a vacuum of 10^{-5} mmHg or better was maintained, and heating was controlled very carefully to ensure that the temperature did not reach values at which discoloration of the walls occurs due to reaction of sodium and the Pyrex glass.

After admitting argon, sealing, and drawing off the tube at *A* and *D*, a drop of sodium was rolled into *E*, and by means of flame heating and tilting the tube the drop could be manoeuvred onto the prepared plaque. The residual amount of sodium at *C* was then strongly heated to act as an oxygen getter. The tube was resealed and drawn off at *F*, to allow the sample to be placed in an electrically heated cruciform furnace. The sample was observed and photographed using the same optical system as used for the induction heated furnace.

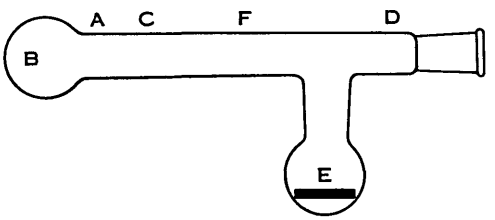

Fig. 2.—The sealed tube apparatus for observation on sessile drops of alkali metals at elevated temperatures.

The quality of the image produced through the curved wall of the sealed tube was, of course, inferior to that obtainable with the optical flats of the larger furnace tube, but the contact angle could still be determined to within $\pm 2°$ in many cases. Surface tension values were less accurate and were probably not more reliable than $\pm 10\%$. However, a series of photographs on the one system gave reliable comparisons. An error in calculation of up to $\pm 5\%$ was caused in some cases by reduction of the factor f in equation (1) due to the combined effects of small drop radius and the low density of sodium which reduces the " flatness " of the drop.

Analysis for oxygen was carried out on samples collected in method (*a*) by the butyl bromide method (White 1954 ; Smythe and de Bruin 1958). At the conclusion of each run butyl bromide was distilled into the sample tube, *S* (Fig. 1), from a prefrozen sample tube attached to the main vacuum line. After reaction had occurred with the sodium sample, the mixture was leached with water and the alkali produced was titrated potentiometrically with standard HNO_3 to pH 7. The sample size was then determined by a Mohr estimation of the total bromide.

Oxide plaques were prepared by cold pressing the powdered oxide at 100,000 p.s.i. and sintering either in air or in a controlled atmosphere. In the case of UO_2, a weighed sample of $UO_{2\cdot00}$ was heated in air for 10 min at 200 °C, during which time the composition was altered to $UO_{2\cdot13}$. This non-stoichiometric oxide sinters more readily than $UO_{2\cdot00}$ (Murray, Rodgers, and Williams 1952), and plaques of density 8·5 to 9·3 were obtained by cold pressing and sintering at 1500 °C in dynamic vacuum of approximately 10^{-3} mm. The plaque surfaces were ground flat and polished on a silicon carbide stone, then reduced to stoichiometric UO_2 prior to each run as described above.

III. Results and Discussion

Considerable evidence was found for surface activity of dissolved oxygen in molten sodium. Figure 3 shows the lowering of surface tension, as measured by the sessile-drop technique (*a*).

The sodium which contained oxygen possessed sufficient (0·034 wt. %) to give approximate saturation in the temperature range 100 to 250 °C, but not enough to form a coherent solid oxide film on the liquid sodium surface since the surface remained bright during all measurements.

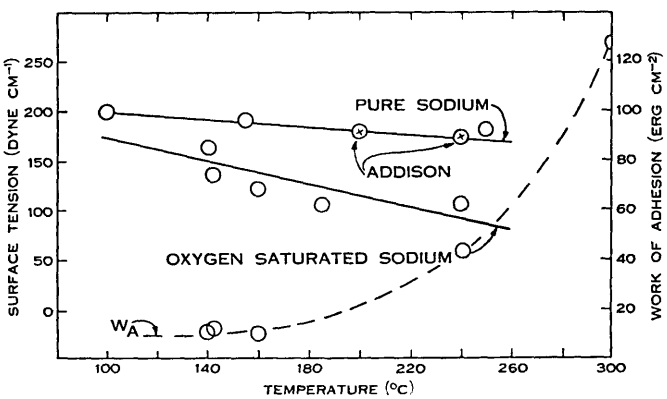

Fig. 3.—Variation with temperature of surface tension of liquid sodium and work of adhesion of liquid sodium on uranium dioxide.

It may be seen from Figure 3 that the lowering in surface tension obtained was proportional to the temperature. An increase in the effect is to be expected since increase in temperature will increase the solubility of oxygen as oxide. The curve for oxygen-free sodium is also shown, and was considerably above that for sodium in the presence of oxygen. In the latter case the extrapolated value of surface tension at the melting point is not far below that of pure sodium, which is again to be expected since the solubility of oxygen in sodium at 100 °C is very small (USAEC 1955) and very little lowering of surface tension should occur at this temperature.

The values obtained for the work of adhesion shown in Figure 3 were calculated from the " oxygen saturated " values for the contact angle, shown as curve *A* in Figure 4. It is interesting to note that the contact angle did not fall

below 90° until the temperature was increased to greater than 300 °C, even though sufficient oxide was present to allow saturation at all temperatures up to 300 °C.

It may be seen from Figure 3 that the decrease in surface tension obtained was accompanied by an increase in the wetting of uranium dioxide by molten sodium, as indicated by the increased work of adhesion. Furthermore, this wetting was found to be irreversible, as in all other cases studied, low values of contact angle being maintained on cooling to the melting point.

The curves *A* and *C* in Figure 4 represent the extremes in the contact angle values obtained in the presence of saturation and minimum oxygen concentrations respectively. It is possible that curve *C* would have been even higher if a more thorough oxygen " gettering " technique could have been employed, but it is

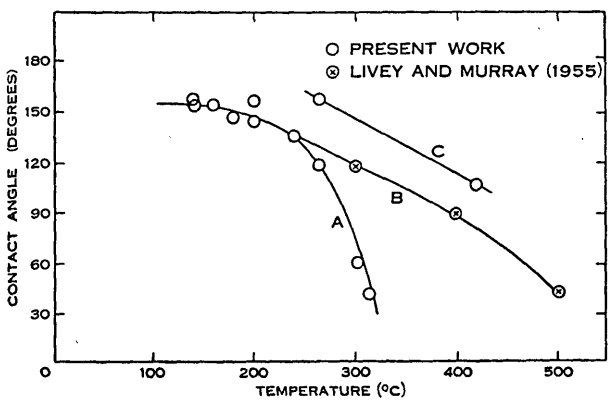

Fig. 4.—Variation with temperature of the contact angle on uranium dioxide of liquid sodium (containing various amounts of oxygen as solute).

A, O_2-saturated Na ; *B*, Na+some O_2 ; *C*, oxygen-free Na.

significant that the values obtained were higher than those of Livey and Murray (1955), and Taylor and Ford (1955), indicating that insufficient attention has been paid in the past to the effect of traces of oxygen on the surface tension of metals.

Further evidence in support of the surface activity of oxygen in sodium was provided by the occurrence of " spreading wetting " (Osterhoff and Bartell 1927) of sodium on oxide surfaces. A drop of sodium on a calcium oxide surface was allowed to evaporate progressively *in vacuo*, thus increasing the concentration of residual oxygen and causing a decrease in contact angle. Eventually the surface tension decreased sufficiently to cause spreading of the molten sodium, which is shown in Figure 5. The spreading is indicated by an approach of the drop towards the wall of the Pyrex glass tube through which the photographs were taken.

A second series of photographs (Fig. 6) shows the reduction of contact angle with increase in oxygen concentration, but spreading wetting did not occur at this low temperature, due to the relatively small saturation concentration of oxygen.

As in the work with lead and lead oxide, the process of solution of sodium oxide in molten sodium was accompanied by random motion of the solid oxide particles (Bradhurst and Buchanan 1959*b*) on the liquid surface, after which reduction of contact angle invariably occurred. Furthermore the high contact angle values obtained in curve *C* (Fig. 4) for sodium on uranium dioxide were only possible when the uranium dioxide was in its stoichiometric form, $UO_{2\cdot00}$, any higher oxides yielding the excess oxygen to the molten sodium, with conse-

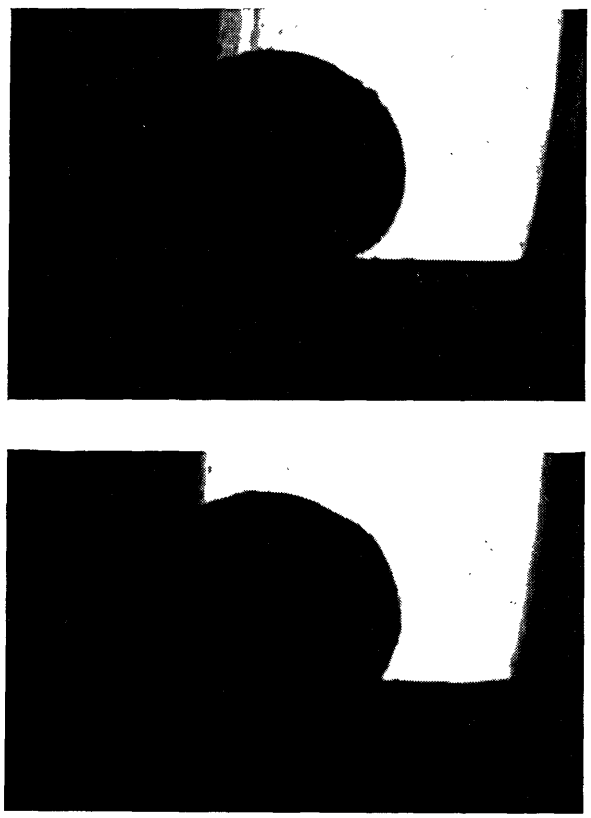

Fig. 5.—Spreading of liquid sodium on calcium oxide due to increased solution of oxygen in the sodium.

quent reduction of surface tension and contact angle. This behaviour is similar to that of lead. When a plaque of U_3O_8 ($UO_{2\cdot67}$) was used in conjunction with sodium already containing a small amount of oxygen, reaction occurred with sufficient rapidity at 250 °C to disintegrate the plaque, possibly with the formation of a sodium uranate.

The relative lowering of surface tension of sodium by dissolved oxygen was greater than that obtained for lead (Table 1). This may be due to the greater difficulty of accommodating the large oxygen anion in the liquid consisting of small sodium ions, and hence a greater surface excess of oxide is established.

The more pronounced ionic character of the solid oxides of sodium would tend to favour the existence of independent ions in molten sodium rather than any molecular species which may exist in molten lead (Bradhurst and Buchanan 1959*a*).

(*a*) *Dependence of the Contact Angle on the Radius Ratio of the Solid Oxide* [$M^{++}:O^{=}$]

Livey and Murray (1955), in a recent study of wetting of oxides by liquid metals, suggested that the non-wetting behaviour of most metals was due to mutual repulsion between oxygen anions on the oxide surface (which occupy the greater proportion of the surface) and the electron " cloud " of the liquid metal.

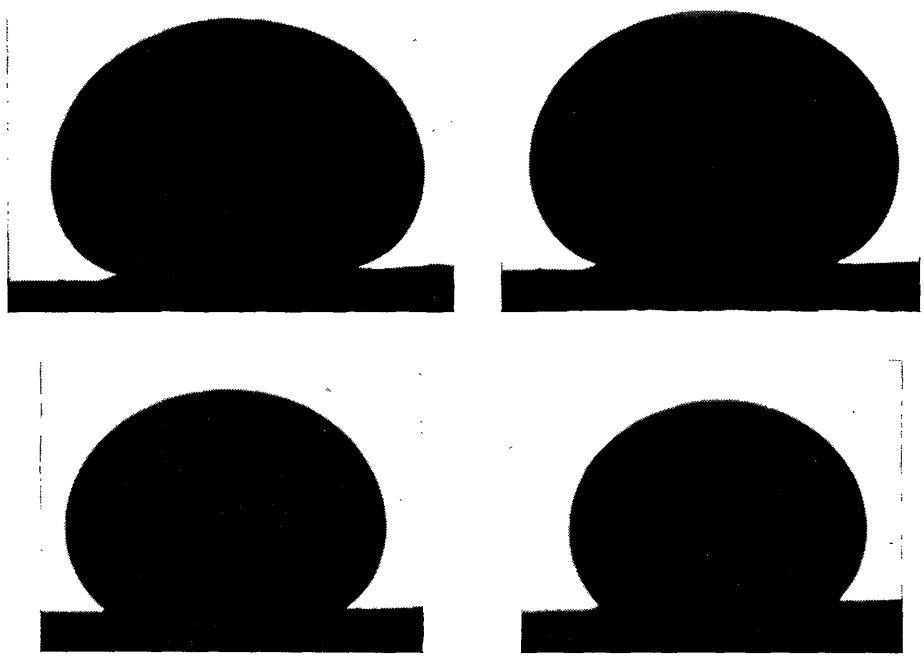

Fig. 6.—Reduction of contact angle of sodium on uranium dioxide as concentration of dissolved oxygen increases in the sodium, the concentration increasing in the drops from left to right.

The present measurements with liquid sodium offered an opportunity to test this hypothesis using MgO, CaO, and BaO as the solid phases. A reduction of contact angle should occur as a result of the increasing proportion of the surface occupied by the positively charged alkaline earth cations in this series.

The results obtained are shown in Table 2, and graphically in Figure 7. Sealed tube techniques were used and the oxygen concentration was probably small and reasonably constant as shown by the high contact angle values obtained at temperatures up to 500 °C. Assuming this was so, the results appear to lend some support to the views of Livey and Murray, although the effects are relatively small and may be open to other interpretations.

In general terms, however, it is probably true to say that, the more metallic the surface, the greater will be the wetting by a liquid metal (Taylor and Ford 1955).

TABLE 1

RELATIVE LOWERING OF SURFACE TENSIONS OF LIQUID SODIUM AND LEAD BY DISSOLVED OXYGEN

Species	Ionic Radius (Å)	Max. Lowering of Surface Tension* (%)
Pb^{++}	1·2	22
Na^{+}	0·95	36
$O^{=}$	1·4	—

* By dissolved oxygen.

(*b*) *Studies on Sodium–Potassium Alloy in Contact with* $UO_{2\cdot00}$

The sodium–potassium eutectic alloy has been used as a heat transfer medium in nuclear reactor technology, and many of its physical properties are known (USAEC 1955).

A brief study of the contact angle with uranium dioxide was carried out by Abrahams, Carlson, and Flotow (1957) and a number of less fundamental studies have been performed on sodium–potassium alloy–uranium dioxide slurries (Furman 1957 ; Bromberg and Tarpley 1958).

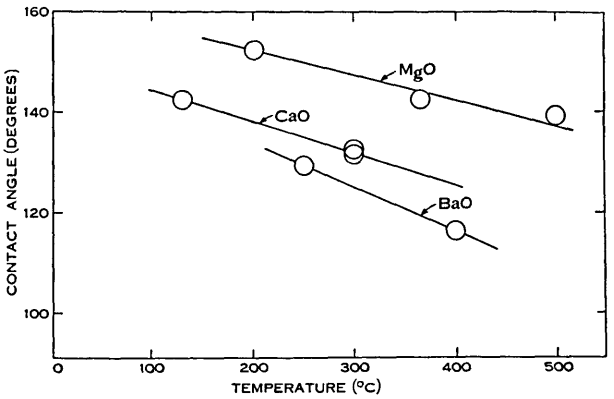

Fig. 7.—The contact angle of liquid sodium on magnesium, calcium, and barium oxides.

Sodium–potassium alloys are dangerous to handle, being pyrophoric in air to the point of explosion if vibrated. They may be handled safely under argon or *in vacuo*, however, and a series of four measurements was carried out on an alloy of approximately 60 wt. % sodium using technique (*a*) described in Section II. Throughout the determinations, which were performed with a vacuum of

better than 10^{-5} mmHg, the surface brightness of the alloy did not decrease. The oxygen concentration was not known, but as the manipulation was done at 25–30 °C, and no solid oxide was visible, it was probably not greater than the saturation concentration at 30 °C (approx. 0·001 wt. % O) (Bogard and Williams 1951).

TABLE 2

CONTACT ANGLE OF LIQUID SODIUM ON ALKALINE EARTH OXIDES

Solid Surface	Radius Ratio $M^{++} : O^{=}$	Contact Angle (degrees at 400 °C)
MgO	0·460	142±3
CaO	0·708	125±3
BaO	0·965	116±2

Figure 8 shows the decrease in the advancing contact angle obtained at a temperature of 250 °C in a vacuum. Non-wetting values were obtained at first under these conditions but showed a progressive decrease culminating in a rapid fall to a wetting value of 60°. The sudden decrease shown in Figure 8 was

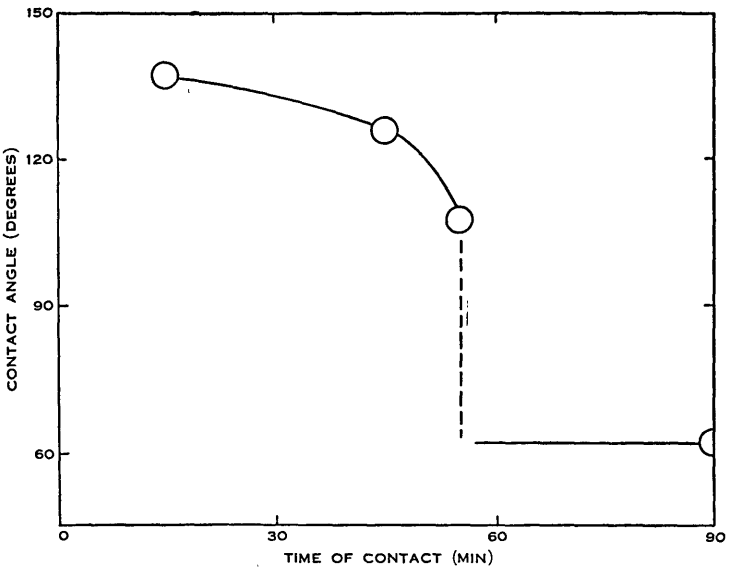

Fig. 8.—Change with time of contact angle of liquid sodium–potassium alloy on uranium dioxide.

induced by vibration. In the light of previous experience on the surface activity of dissolved oxide and bearing in mind the very strong affinity of the sodium–potassium alloy for oxygen, it is possible that this decrease in contact angle is associated with increasing concentration of dissolved oxygen, the latter possibly derived from degassing of the walls. In this connection it is interesting to note

TABLE 3

VARIATION OF WORK OF ADHESION OF LIQUID SODIUM–POTASSIUM EUTECTIC ALLOY TO UO_2 WITH TIME OF CONTACT

Temperature (°C)	Time of Contact (min)	Pressure (mmHg)	Surface Tension (dyne cm^{-1})	Contact Angle with $UO_{2\cdot00}$	Work of Adhesion (erg cm^{-2})
30	15	5×10^{-6}	133±6	137±2	42
200	45	,,	124±7	126±2	55
250	55	,,	116±7	107±2	52
≒100	90	,,	—	62±2	189

that Abrahams, Carlson, and Flotow (1957) claimed that the sodium–potassium eutectic wet $UO_{2\cdot00}$ but not $UO_{2\cdot02}$ at 25 °C. This result is difficult to interpret unless in the second case the alloy reacted with sufficient oxygen from the oxygen excess UO_2 to give an impervious skin on the surface of the metal, a condition which will give rise to non-wetting behaviour.

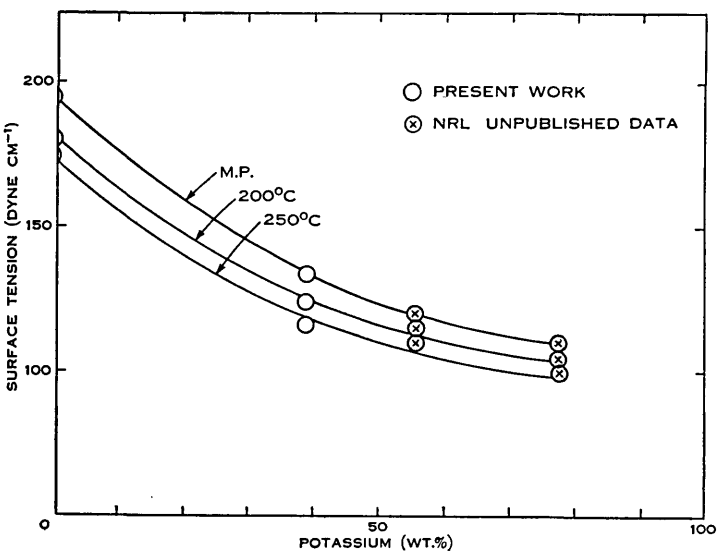

Fig. 9.—The surface tension isotherms of sodium–potassium alloys at several temperatures.

The surface tensions corresponding to the contact angles of Figure 8 are shown in Table 3.

Surface tension data from the United States Naval Research Laboratories (USAEC 1955) were given as 110–100 dyne cm^{-1} from the melting point to 250 °C for the 78 wt. % potassium alloy, and 120–110 dyne cm^{-1} over the same temperature range for the 56 wt. % potassium alloy. A summary of all these results is shown in the surface tension *v.* composition isotherms in Figure 9, and

it may be seen that the results obtained here agree well with the NRL values. The isotherms are non-linear, indicating that the surface layer in sodium–potassium alloys is potassium rich, and that the system is not ideal. This is supported by recent vapour pressure measurements (Kistiakowsky 1955) on sodium–potassium alloys where non-ideal behaviour was found and attributed to polymeric species in the vapour phase.

IV. Acknowledgment

This work was supported by a grant from the Australian Atomic Energy Commission and forms part of a programme of work on the surface chemistry of liquid metals.

V. References

Abrahams, B. M., Carlson, R. D., and Flotow, H. E. (1957).—USAEC Rep. NESC–104.
Bogard, A. D., and Williams, D. D. (1951).—USAEC Rep. NRL–3865.
Bradhurst, D. H., and Buchanan, A. S. (1959*a*).—*J. Phys. Chem.* **63**: 1486–88.
Bradhurst, D. H., and Buchanan, A. S. (1959*b*).—*Aust. J. Chem.* **12**: 523.
Bromberg, L., and Tarpley, W. B. (1958).—USAEC Rep. NYO–7929.
Dorsey, N. E. (1928).—*J. Wash. Acad. Sci.* **18**: 505.
Furman, S. C. (1957).—USAEC Rep. KAPL–1648.
Humenik, M., and Kingery, W. D. (1953).—*J. Phys. Chem.* **57**: 359.
Kistiakowsky (1955).—USAEC Rep. NRL–P–2958.
Livey, D. J., and Murray, P. (1955).—*Plansee Proc.* **1955**: 375.
Murray, P., Rodgers, E. P., and Williams, A. E. (1952).—AERE Rep. M/R 893.
Osterhoff, H. J., and Bartell, F. E. (1927).—5th Colloid Symp. Monogr.
Smythe, L. E., and de Bruin, H. J. (1958).—*Analyst* **83**: 242.
Taylor, J. W., and Ford, T. D. (1955).—UKAERE Rep. M/R 1729.
USAEC (1955).—" The Liquid Metals Handbook." Sodium and Sodium-Potassium Supplement. TID–5277, pp. 7–8, 32–44. (USAEC: Washington, D.C.)
White, J. C. (1954).—*Analyt. Chem.* **26**: 210.

J. Inorg. Nucl. Chem.,1957, Vol. 4, pp. 379 to 381. Pergamon Press Ltd., London

Radiometric titration with silver and cobalt tungstates

(*Received* 31 *December* 1956)

THE composition of tungstate solutions at different pH has still not been adequately investigated. This note reports some new facts germane to this problem. A radiometric method was used, in which labelled silver nitrate (Ag^{110}) or cobalt nitrate (Co^{60}) was titrated from a burette into a solution of

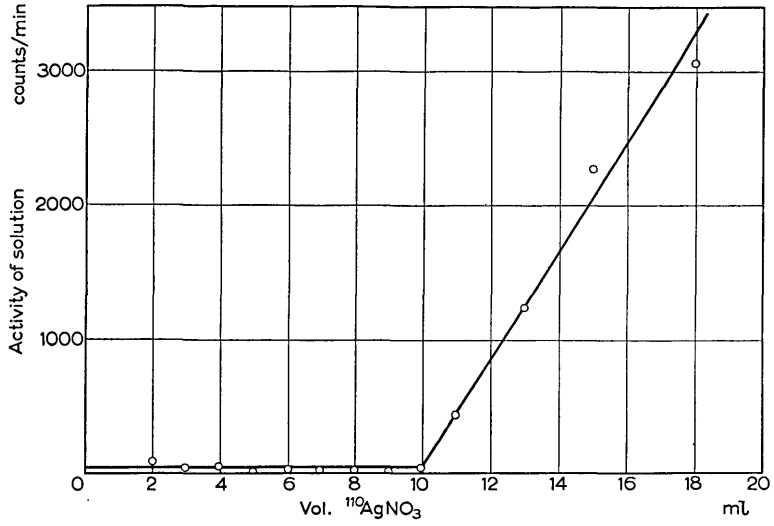

FIG. 1.—Radiometric titration of 10 ml 0·1 N sodium tungstate, with 0·1 N silver (Ag^{110}) nitrate. Unbuffered, pH 6·2–7·8.

sodium tungstate adjusted to the desired pH. Fig. 1 shows a typical titration curve with silver, from which it will be seen that the end point, and hence the Ag : W ratio, is easily calculated. The following results were obtained.

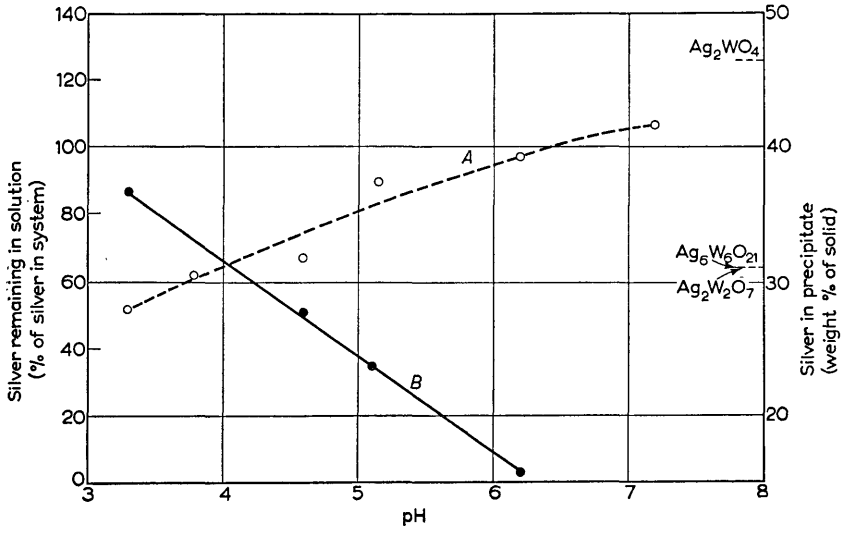

FIG. 2.—*A*: Variation of Ag : W ratio in precipitate. *B*: Per cent Ag remaining in solution at different pH.

Metal : tungstate ratio

Precipitation of cobalt tungstate occurred only at pH > 6·5, whereas silver tungstate was still being precipitated at pH = 3·5. The cobalt tungstate was analysed by the non-isotopic tracer method —that is, the cobalt content of the solid was estimated from the measured activity of a known weight and found to give 23·5 ± 1·5% cobalt, compared with 19·3% for $CoWO_4$, and 11·0 for $Co_3W_6O_{21}$. On the other hand, the silver tungstate composition varied with pH (Fig. 2). This we ascribe to

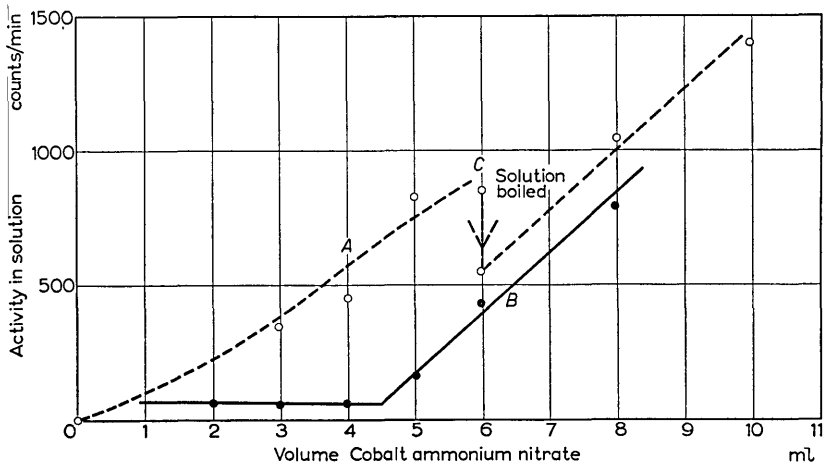

FIG. 3.—Radiometric titration of 10 ml 0·1 N sodium tungstate with 0·2 N cobalt (Co^{60}) ammonium nitrate. *A*: Points below *C* are at room temperature; others at boiling-point. *B*: Solution boiling throughout, pH 7·4.

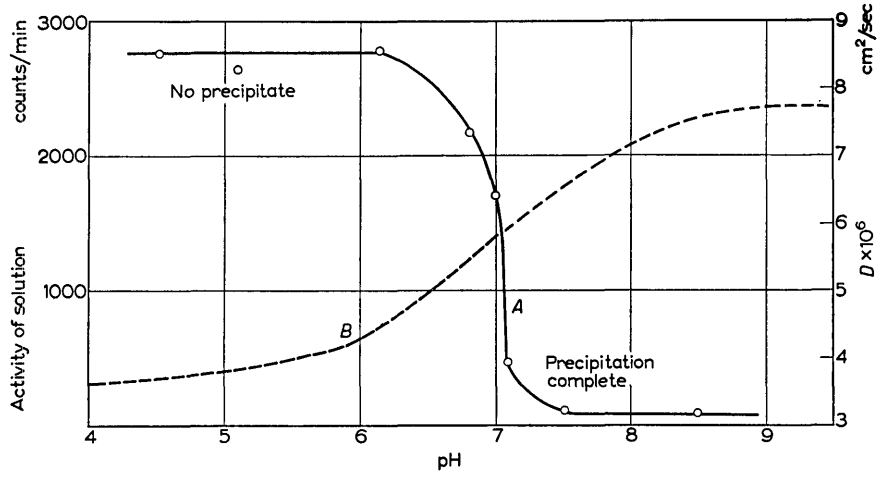

FIG. 4.—*A*: Amount of precipitated cobalt tungstate at different pH. *B*: Variation in diffusion coefficient of tungsten in tungstate solutions of different pH (after J. S. ANDERSON and K. SADDINGTON[2]).

precipitation of $Ag_6W_6O_{21}$ at low pH, whereas the corresponding cobalt paratungstate tungstate is apparently soluble, perhaps due to heteropoly acid formation (BAKER and MCCRUTCHEON[1]).

Rate of reaction

The analysis for $CoWO_4$ reported above was made on a specimen which was precipitated in the cold. It was noticed, however, that, whereas precipitation of silver was immediate, precipitation of cobalt was sluggish (especially for pH < 8), and no sharp end-point could be obtained in the cold.

[1] L. C. W. BAKER and T. P. MCCRUTCHEON *J. Amer. chem. Soc.* **78**, 4503 (1956).

Precipitation continued overnight. However, complete precipitation of cobalt tungstate occurs on boiling the solution, and a radiometric titration curve such as shown in Fig. 3 may be obtained. A Co : W ratio of 0·98 (estimated from the end-point) was obtained for pH > 8. The amount of cobalt tungstate precipitated in the cold and hot at different pH is shown in Fig. 4. Also on the same figure the diffusion coefficients measured by ANDERSON and SADDINGTON[2] are plotted. It will be seen that there is close correspondence, which suggests that the paratungstate ion plays an important role in preventing precipitation of cobalt tungstate.

Conclusions

From this work it would appear that:

(a) Precipitation of cobalt tungstate at high pH may be used to estimate the WO_4^{2-} content of tungstate solutions;

(b) The equilibrium between WO_4^{2-} and the paratungstate ion, or any complexes with cobalt, is not instantaneous.

(c) Conversion of condensed tungstate to WO_4^{2-} is complete at pH > 8.

D. H. BRADHURST
B. A. W. COLLER
J. F. DUNCAN

Chemistry Department
The University, Melbourne, Australia

[2] J. S. ANDERSON and K. SADDINGTON *J. chem. Soc.* S381 (1949).

Short Communication reprinted from the Australian Journal of Chemistry, Volume 12, Number 3, pp. 523–524, 1959

RECRYSTALLIZATION OF LEAD OXIDE FROM MOLTEN LEAD*

By D. H. BRADHURST† and A. S. BUCHANAN†

During an investigation of the surface tension of liquid lead by means of a sessile drop technique, small transparent yellow crystals were observed to form on the solidified surface after heating at 750 °C in an argon atmosphere. X-Ray crystallographic analysis, using a 9 cm Guinier camera, confirmed the tetragonal structure and lattice dimensions of yellow lead oxide. It seemed probable that the oxide had been formed from small amounts of oxygen in the cylinder argon used in these experiments. A more systematic study of this crystallization process was subsequently carried out *in vacuo*, using weighed additions of A.R. lead oxide. This note describes the recrystallization process observed.

Pure lead specimens (99·999%; supplied by the Metallurgy Department, University of Melbourne) consisting of 3·5 by 6·5 mm cylindrical pellets, were placed on specially prepared high density uranium dioxide plaques ($UO_{2\cdot00}$), and a weighed amount of A.R. lead oxide placed on the pellet. The assembly was inserted into an induction heated tube furnace which was then evacuated and heated to 750 °C. Photographs of the profile of the sessile drop were taken at different temperatures and time intervals. After each run, the plaque and lead surface were examined microscopically (×300) and photomicrographs were taken when necessary.

The process of solution of lead oxide was accompanied by random motion of the particles over the surface of the lead drop, in much the same manner as small particles of camphor move on a water surface. This effect was observed to occur for lead sulphide, lead selenide, and lead telluride also, although in these cases formation of surface crystals did not occur, a result probably associated with greater solubility in the lead. Plate 1 shows three photographs (Figs. 1–3) of the solution process with lead oxide, the motion of the particles producing a blurred image in Figure 2, for which a 60 sec exposure was used. The lowest temperature at which appreciable solution was observed lies in the range 500 to 530 °C for each of the four solutes.

The rate of cooling has some influence on the formation of the crystals. Plate 1, Figure 4, is a photomicrograph of a rapidly cooled sample, and it will be noted that the lead oxide crystal is irregular in shape and appears to have been formed by growth from a crack in the initially formed lead " crust ". Plate 1, Figure 5, on the other hand, shows some of the more regular lead oxide crystals produced by the slower cooling obtained in a furnace of larger heat capacity. These crystals were coloured red (probably an interference colour).

* Manuscript received March 4, 1959.

† Chemistry Department, University of Melbourne.

The approximate maximum solubility of lead oxide in lead at 750 °C was estimated to be 0·019 molal (0·42 wt.%), which was inferred from the surface tension *v.* concentration isotherm (Bradhurst and Buchanan 1959, unpublished data), which showed maximum depression at this concentration. The value obtained by Richardson and Webb* was somewhat smaller (saturation at an interpolated value of 0·012 molal).

This work was supported by a grant from the Australian Atomic Energy Commission and forms part of a programme of work on the surface chemistry of liquid metal systems.

* Richardson, F. D., and Webb, L. E. (1955).—*Trans. Inst. Min. Metall. Lond.* **64**: 529.

RECRYSTALLIZATION OF LEAD OXIDE FROM MOLTEN LEAD

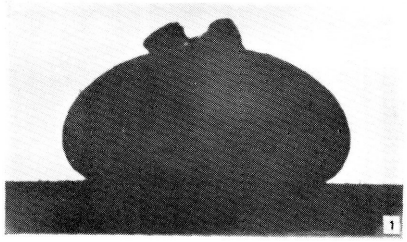

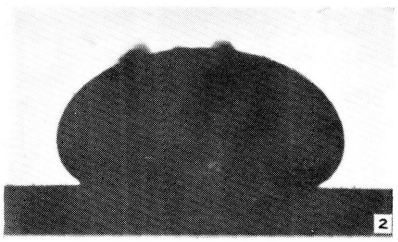

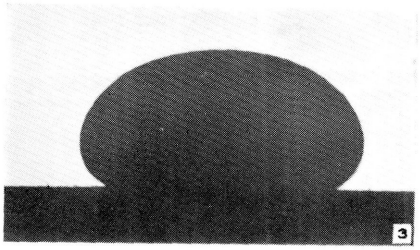

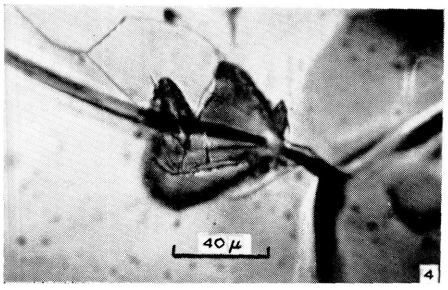

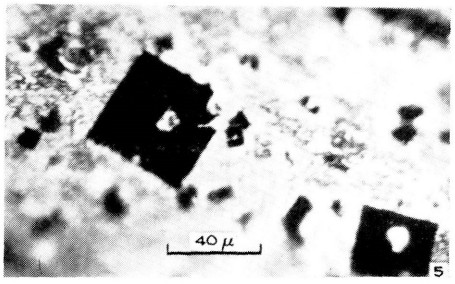

Fig. 1.—Photograph of sessile drop of liquid lead on uranium dioxide plaque at 380 °C, with sample of undissolved lead oxide at apex. ×10. Fig. 2.—The same sample at 510 °C. ×10. The blurred image was produced by motion of lead oxide particles on the lead surface. Fig. 3.—Clean profile of sessile drop at 740 °C after complete solution of lead oxide. ×10. Figs. 4 and 5.—Photomicrographs of lead oxide crystal; 4 produced by rapid cooling and 5 by slow cooling of the lead sample.

Reprinted from the
AUSTRALIAN JOURNAL OF CHEMISTRY
VOLUME 14, NUMBER 3, PAGES 417–419, 1961

SURFACE PROPERTIES OF LIQUID METALS: BISMUTH, LEAD–BISMUTH, TIN

By D. H. Bradhurst and A. S. Buchanan

SURFACE PROPERTIES OF LIQUID METALS: BISMUTH, LEAD–BISMUTH, TIN

By D. H. BRADHURST* and A. S. BUCHANAN*

[*Manuscript received February* 15, 1961]

Summary

Dissolved oxygen was shown to have inappreciable surface activity in liquid bismuth up to 700 °C. Introduction of lead as a third solute in the liquid bismuth however increased the surface activity of oxygen. The solutes oxygen, sulphur, selenium, and tellurium showed the same order of surface activity in liquid tin as in liquid lead.

I. INTRODUCTION

The preceding papers of this series have recorded the wetting behaviour of liquid metals such as lead (Bradhurst and Buchanan 1959*a*, 1959*b*), sodium and sodium–potassium mixtures (Bradhurst and Buchanan 1961*a*), and bismuth (Bradhurst and Buchanan 1961*b*) towards oxide surfaces. In general, pure liquid metals show marked non-wetting characteristics on all oxide surfaces up to quite high temperatures. On the other hand introduction of certain non-metallic solutes such as oxygen and the halogens may greatly improve the wetting even in quite low concentrations. Such surface active solutes must clearly accumulate at the surface of the liquid metal and in this way reduce its metallic character. In the present paper further studies are recorded on surface activity in bismuth, bismuth–lead mixtures, and tin.

II. EXPERIMENTAL

The sessile-drop technique for measuring surface tensions and contact angles of the liquid on a solid surface has been described previously (Bradhurst and Buchanan 1959, 1961*a*).

Pure specimens of the metals to be investigated were obtained from the Metallurgy Department, University of Melbourne. Cylindrical pellets ($3 \cdot 5 \times 6 \cdot 5$ mm) were prepared using a stainless steel punch and the weighed solutes were confined before melting in small holes drilled in the tops of the pellets. The lead–bismuth eutectic alloy was prepared in a graphite container in the evacuated furnace.

III. RESULTS

(*a*) *Surface Activity of Oxygen in Liquid Bismuth*

Weighed amounts of Bi_2O_3 were added to molten bismuth and surface tension and contact angle on UO_2 determined (Table 1).

The concentrations of oxygen shown in column 1 are in fact in excess of the saturation value of $0 \cdot 00695$ mole % Bi_2O_3 (Hansen 1958) and excess solid

* Chemistry Department, University of Melbourne.

Bi_2O_3 was present on the surface of the drop throughout the experiment. Furthermore there was no evidence, on microscopic observation, of recrystallization of the oxide from the liquid metal on cooling the drop to room temperature.

TABLE 1

SURFACE ACTIVITY OF OXYGEN IN MOLTEN BISMUTH

Bi_2O_3 (mole %)	Surface Tension at 700 °C (dyne cm^{-1})	Contact Angle (degr es)
0	350±7	156±2
0·063	346±7	149±2
0·318	345±7	150±2

TABLE 2

SURFACE ACTIVITY OF OXYGEN IN LEAD–BISMUTH EUTECTIC

PbO (mole %)	Surface Tension at 700 °C (dyne cm^{-1})	Contact Angle (degrees)	Work of Adhesion (dyne cm^{-1})
0	388±7	152	45·4
0·369	374±7	130	133
0·786	370±7	120	185

TABLE 3

COMPARISON OF SURFACE ACTIVITY IN TIN AND LEAD AT 800 °C

Solute	Maximum Reduction in Surface Tension (% at 800 °C)	
	Sn	Pb
Oxygen	20·4	22·0
Sulphur	15·8	7·0
Selenium	12·0	5·0
Tellurium	2·0	2·5

(*b*) *The Lead–Bismuth Eutectic Mixture*

Oxygen, when dissolved in the lead–bismuth eutectic, displayed significant surface activity although the effects were rather less than for pure lead (Table 2). The largest value for the work of adhesion to UO_2 corresponds approximately with that obtained for lead with oxygen as solute (198 dyne cm^{-1}).

(c) *Surface Activity in Liquid Tin*

This metal was studied over the temperature range 250–800 °C and solutes used were oxygen, sulphur, selenium, and tellurium. Saturation concentration was achieved for the first two, which are the least soluble. The results at 800 °C are compared with a similar set obtained for liquid lead (Table 3).

IV. Discussion

The surface activity of oxygen in liquid bismuth is clearly very slight (Table 1) and in fact is scarcely significant. This may be associated with the quite low solubility of oxygen in liquid bismuth, although on the other hand experience in the case of lead (Bradhurst and Buchanan 1959*a*) indicated that the least soluble and least metallic of the solutes, oxygen, was the most surface active. In this connection introduction of lead into the bismuth (to give the eutectic composition) significantly improved the surface activity of oxygen as a third solute (Table 2). The contact angle on UO_2 was decreased quite significantly although the surface tension was less definitely influenced. It is evident that the presence of lead as part of the liquid phase permits dissolved oxygen to accumulate in the surface either as oriented PbO molecules or ion pairs. Further studies on other solutes in bismuth (e.g. S, Se) would probably give some indication of the reason for the lack of surface activity (up to 700 °C) of oxygen in this metal.

Surface activity of the solutes oxygen, sulphur, selenium and tellurium in liquid tin show the same order of effectiveness as in liquid lead (Table 3). It is again evident that the important factor in determining whether a surface excess of solute will be established is the metallic character and compatibility of the solute with the liquid metal. In this connection the greater surface activity of sulphur and selenium in tin as compared with lead may be due to lower solubility and reduced compatibility of these elements with the metal.

The conclusions reached in this work may have consequences in interpreting liquid metal behaviour. Soft solder, for example, should flow and wet an oxidized metal surface more readily if the solder has already been subject to oxidizing conditions and contains a significant amount of dissolved oxygen. Naturally, flow will occur most readily on a clean non-oxidized solid metal surface. The role of a flux is probably to limit oxidation of the solid metal which is being soldered or welded. It could in certain circumstances provide non-metallic surface active solutes for the liquid metal and hence increase its ability to wet a partially oxidized solid metal surface.

V. References

Bradhurst, D. H., and Buchanan, A. S. (1959*a*).—*J. Phys. Chem.* **63**: 1486.
Bradhurst, D. H., and Buchanan, A. S. (1959*b*).—*Aust. J. Chem.* **12**: 523.
Bradhurst, D. H., and Buchanan, A. S. (1961*a*).—*Aust. J. Chem.* **14**: 397.
Bradhurst, D. H., and Buchanan, A. S. (1961*b*).—*Aust. J. Chem.* **14**: 409.
Hansen, M. (1958).—"Constitution of Binary Alloys." 2nd Ed. (McGraw-Hill Book Co.: New York.)

Printed by C.S.I.R.O., Melbourne